Contact Mechanics and Elements of Tribology

Lecture 3.
Contact and Mechanics of Materials

Vladislav A. Yastrebov

MINES Paris, PSL University, CNRS
Centre des Matériaux, Evry, France

@ Centre des Matériaux (& virtually)
February 7, 2023

Interface physics

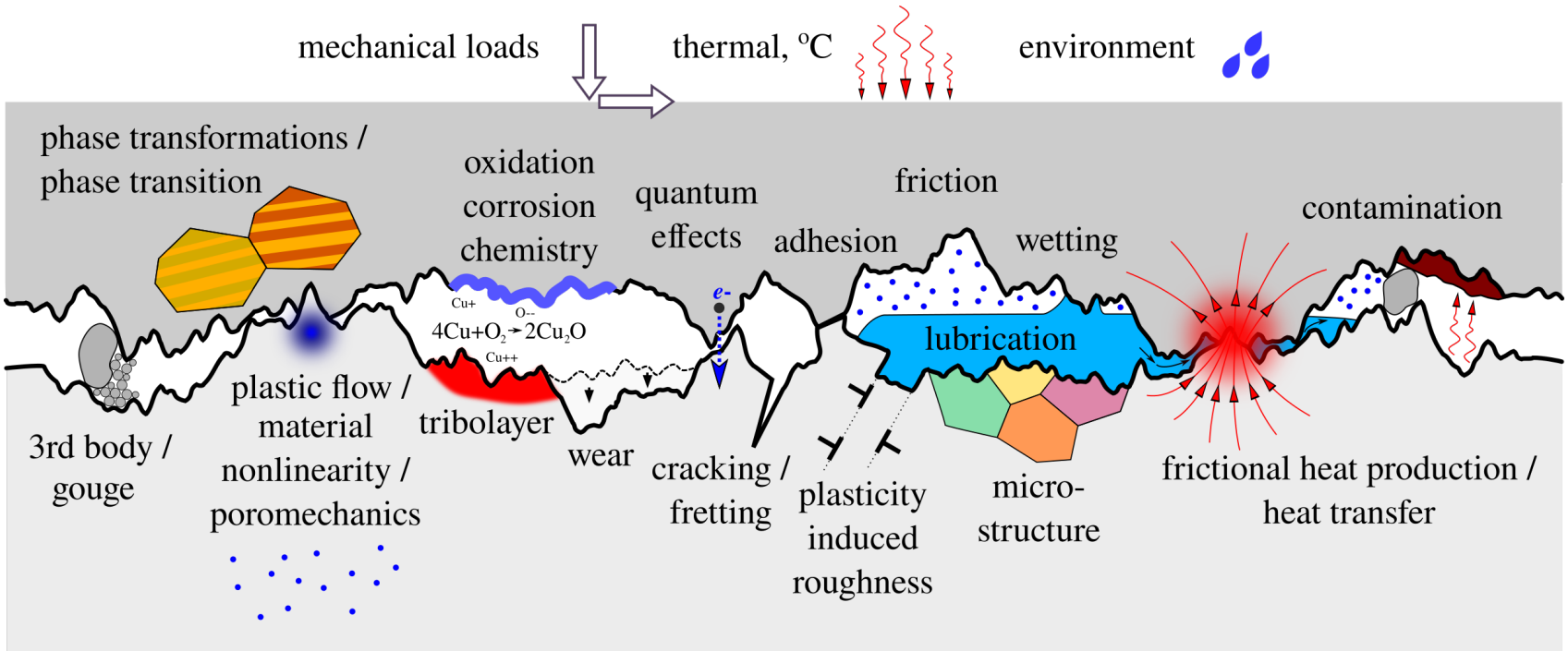

Tribological properties stem from this complex multi-scale physics of interfaces and near-surface layers[1]

[1] Vakis et al, Modeling and simulation in tribology across scales: An overview. Tribology International, 125:169-199 (2018).

Surface/near-surface properties

Surface properties:

- Friction
- Adhesion
- Wear

Surface/near-surface properties

Surface properties **are not fundamental**

- Friction ☹
- Adhesion ☹
- Wear ☹

Surface/near-surface properties

Surface properties are not fundamental

- Friction ☹
- Adhesion ☹
- Wear ☹

Fundamental properties:

- **Volume:**
  - Chemical composition
  - Microstructure
  - Elasticity/viscosity
  - Yield stress and hardening
  - Mass density
  - Thermal properties

Surface/near-surface properties

Surface properties are not fundamental

- Friction ☹
- Adhesion ☹
- Wear ☹

Fundamental properties:

- **Volume:**
  - Chemical composition
  - Microstructure
  - Elasticity/viscosity
  - Yield stress and hardening
  - Mass density
  - Thermal properties
- **Surface:**
  - Roughness
  - Oxides and films
  - Chemical reactivity
  - Absorbtion capabilities
  - Surface energy

Surface/near-surface properties

Surface properties are not fundamental

- Friction ☹
- Adhesion ☹
- Wear ☹

Fundamental properties are interdependent

- **Volume:**
  - Chemical composition
  - Microstructure
  - Elasticity/viscosity
  - Yield stress and hardening
  - Mass density
  - Thermal properties
- **Surface:**
  - Roughness
  - Oxides and films
  - Chemical reactivity
  - Absorbtion capabilities
  - Surface energy

Surface/near-surface properties

Surface properties are not fundamental

- Friction ☹
- Adhesion ☹
- Wear ☹

More fundamental properties

- solids are made of atoms
- atoms are linked by bonds
- most of the **volume** and **surface** properties are the **properties of the bonds**

Fundamental properties are interdependent

- **Volume:**
  - Chemical composition
  - Microstructure
  - Elasticity/viscosity
  - Yield stress and hardening
  - Mass density
  - Thermal properties
- **Surface:**
  - Roughness
  - Oxides and films
  - Chemical reactivity
  - Absorbtion capabilities
  - Surface energy

Let's use atoms to simulate contacts

Let's start from the bottom

- Use Molecular Dynamics
- Potential for interaction between particles
- Time integration of the system evolution
- Natural coupling between thermal and mechanical phenomena
- Inherent plaicity (dislocation movement)

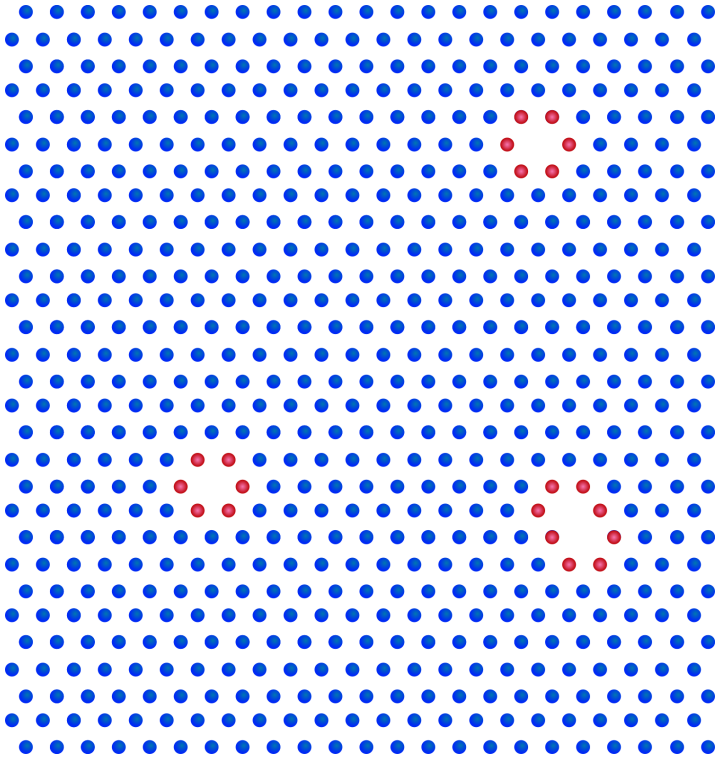

[1] Nanotribology and nanomechanics. Ed. Bhushan, B. (2008) Springer.

[2] Mo, Y., Turner, K.T. and Szlufarska, I., 2009. Friction laws at the nanoscale. Nature, 457(7233):1116-1119.

[3] Szlufarska, I., 2006. Atomistic simulations of nanoindentation. Materials Today, 9(5), pp.42-50.

[4] Spijker, P., Anciaux, G. and Molinari, J.F., 2013. Relations between roughness, temperature and dry sliding friction at the atomic scale. Tribology International, 59:222-229.

Example: high-velocity impact

Impact of a perfect crystal by a circular projectile: 20 000 particles on 20 000 time steps.

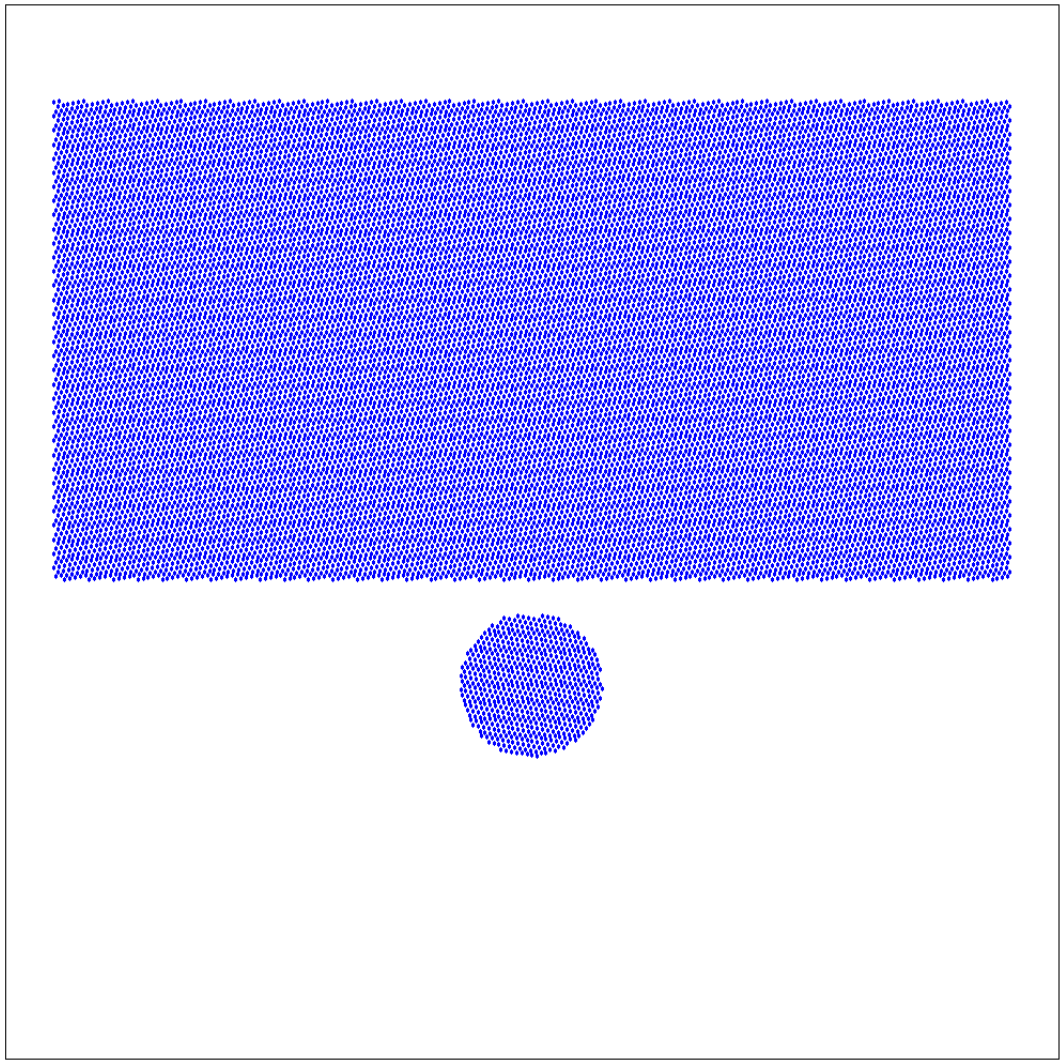

Let's use atoms to simulate contacts

Let's start from the bottom

- Use Molecular Dynamics
- Adjusted interaction potentials
- Thermal and mechanical phenomena
- Inherent plasticity (dislocations)

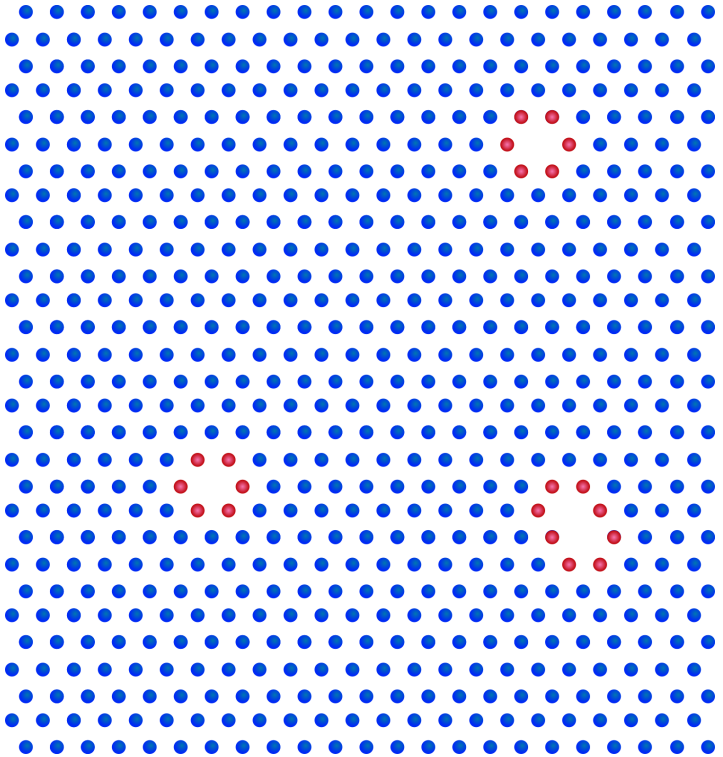

Unfortunately it is hard to obtain valuable for macroscopic scales results using MD . . .

- How to get rid of the inherent adhesion between two surfaces?
- Hard to scale roughness to representative scale
- Too huge 3D simulations even for nano-indentation

Let's use atoms to simulate contacts

Let's start from the bottom

- Use Molecular Dynamics
- Adjusted interaction potentials
- Thermal and mechanical phenomena
- Inherent plasticity (dislocations)

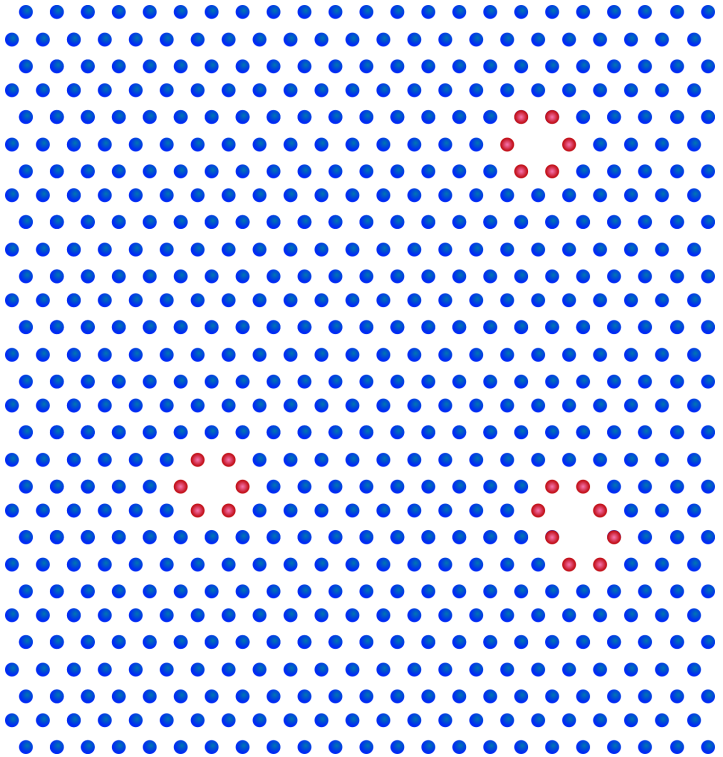

Unfortunately it is hard to obtain valuable for macroscopic scales results using MD . . .

- How to get rid of the inherent adhesion between two surfaces?
- Hard to scale roughness to representative scale
- Too huge 3D simulations even for nano-indentation

So, let's get back to a continuum description...

Plasticity

Onset of plastic yielding

Hertz contact: body of revolution

- Onset of plasticity for pressure

$$p_Y = 1.6\sigma_Y$$

- Associated force

$$F_Y = \frac{1.6^3 \pi^3 R^2}{6} \left(\frac{\sigma_Y}{E^*}\right)^2 \sigma_Y$$

- Associated contact radius

$$a_Y = \frac{1.6\pi R}{2} \frac{\sigma_Y}{E^*}$$

- Plastic flow starts at depth

$$z_Y \approx 1.21 R \frac{\sigma_Y}{E^*}$$

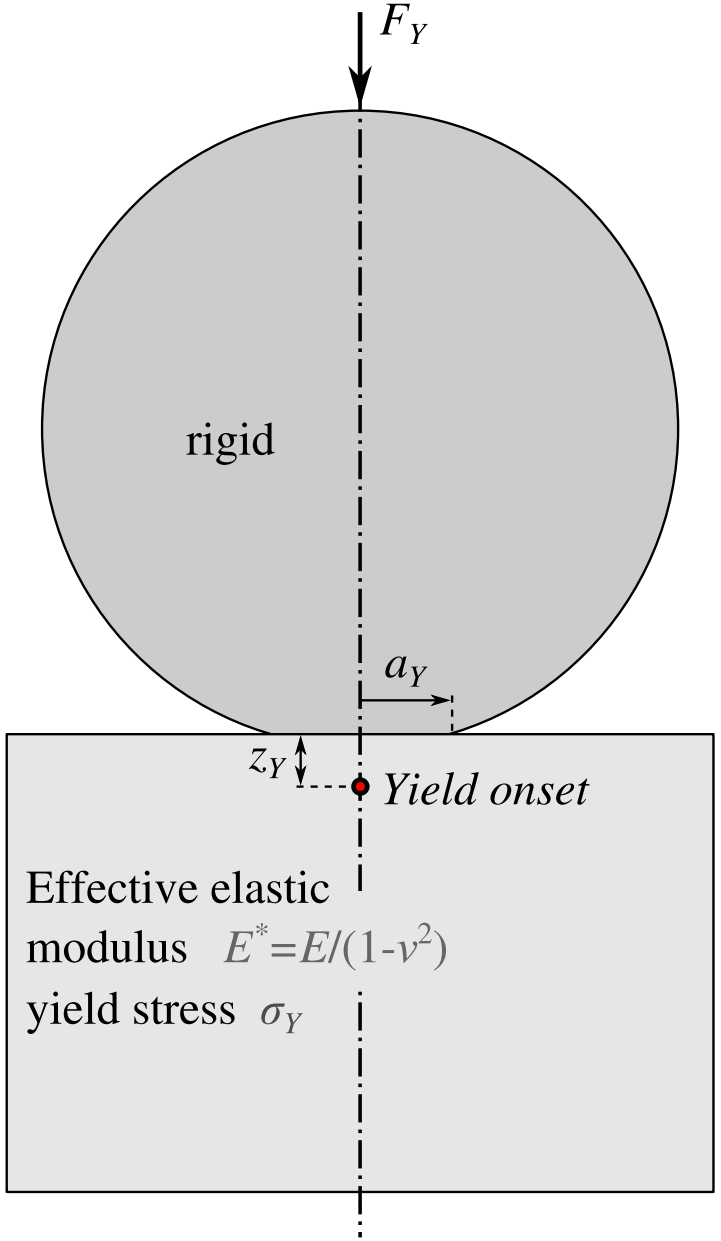

Elasto-plastic transition in contact

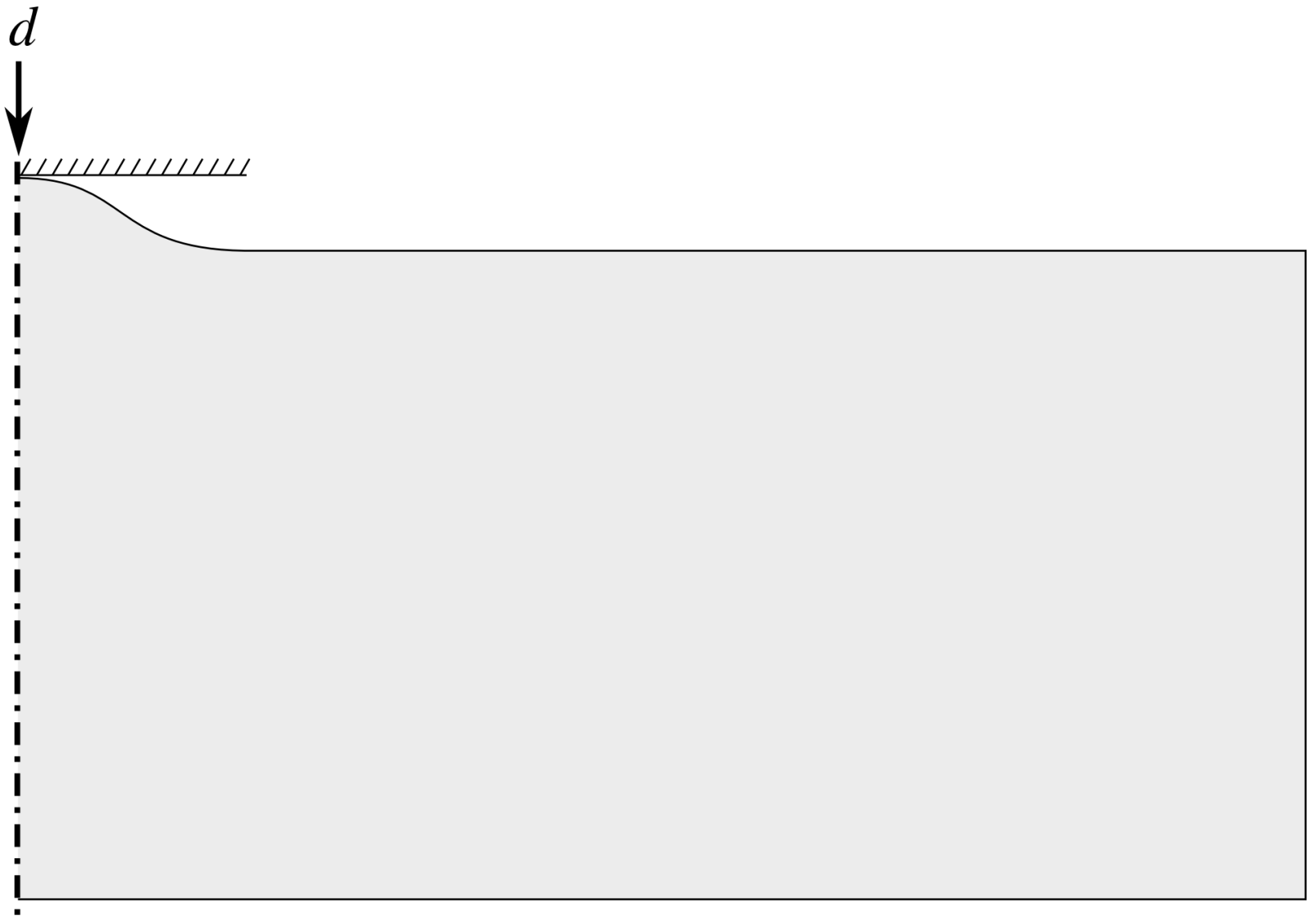

Elasto-plastic transition in contact

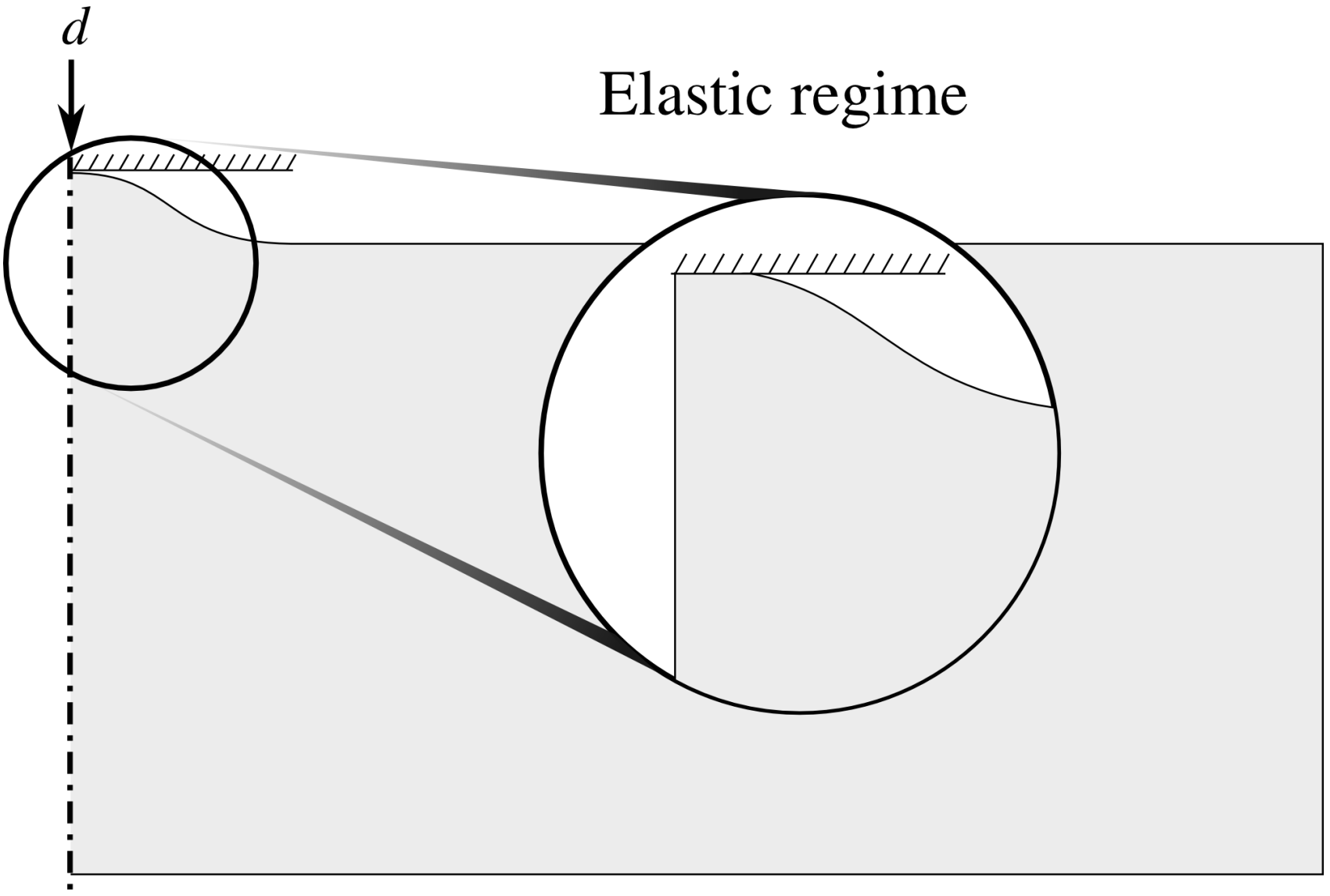

Elasto-plastic transition in contact

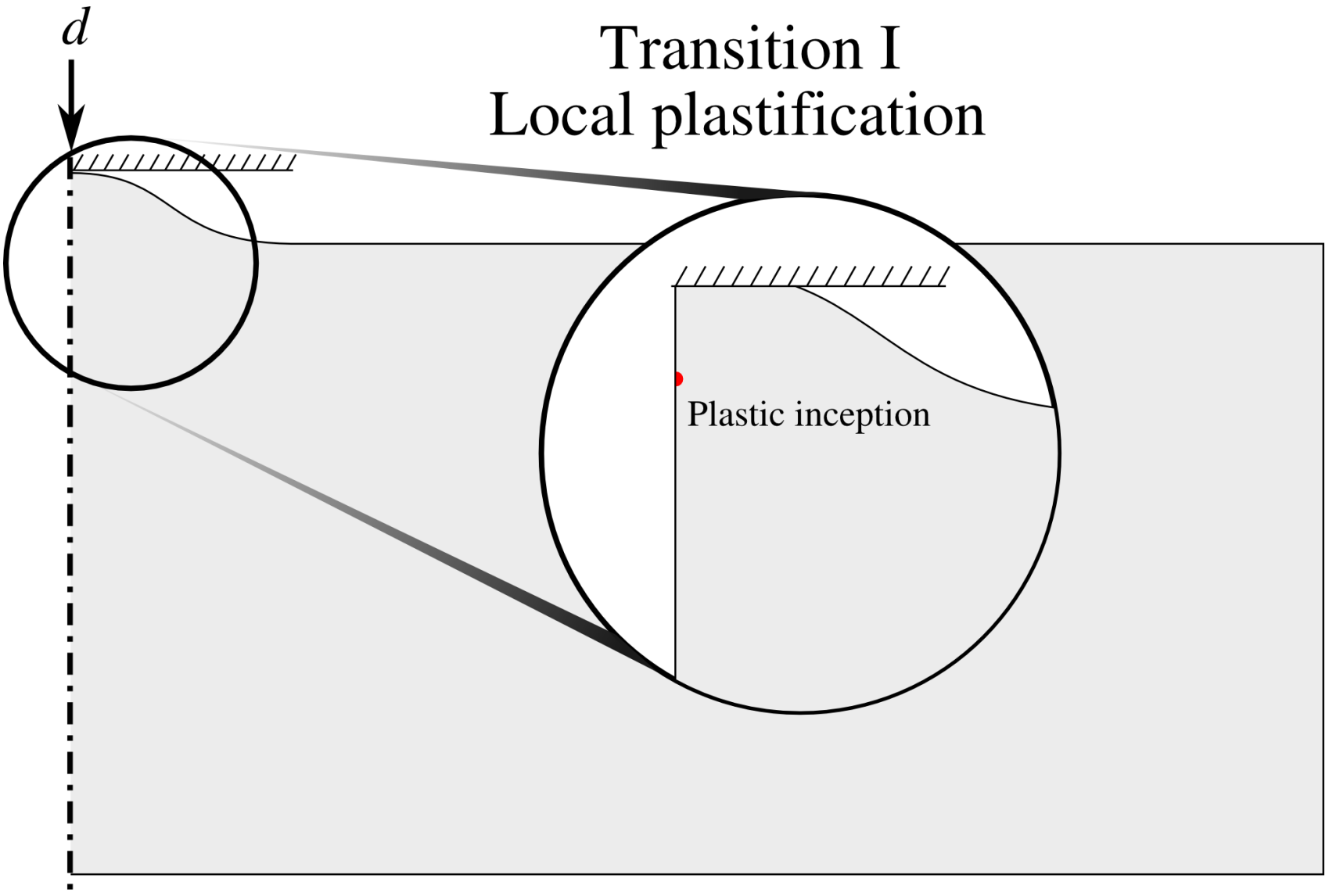

Elasto-plastic transition in contact

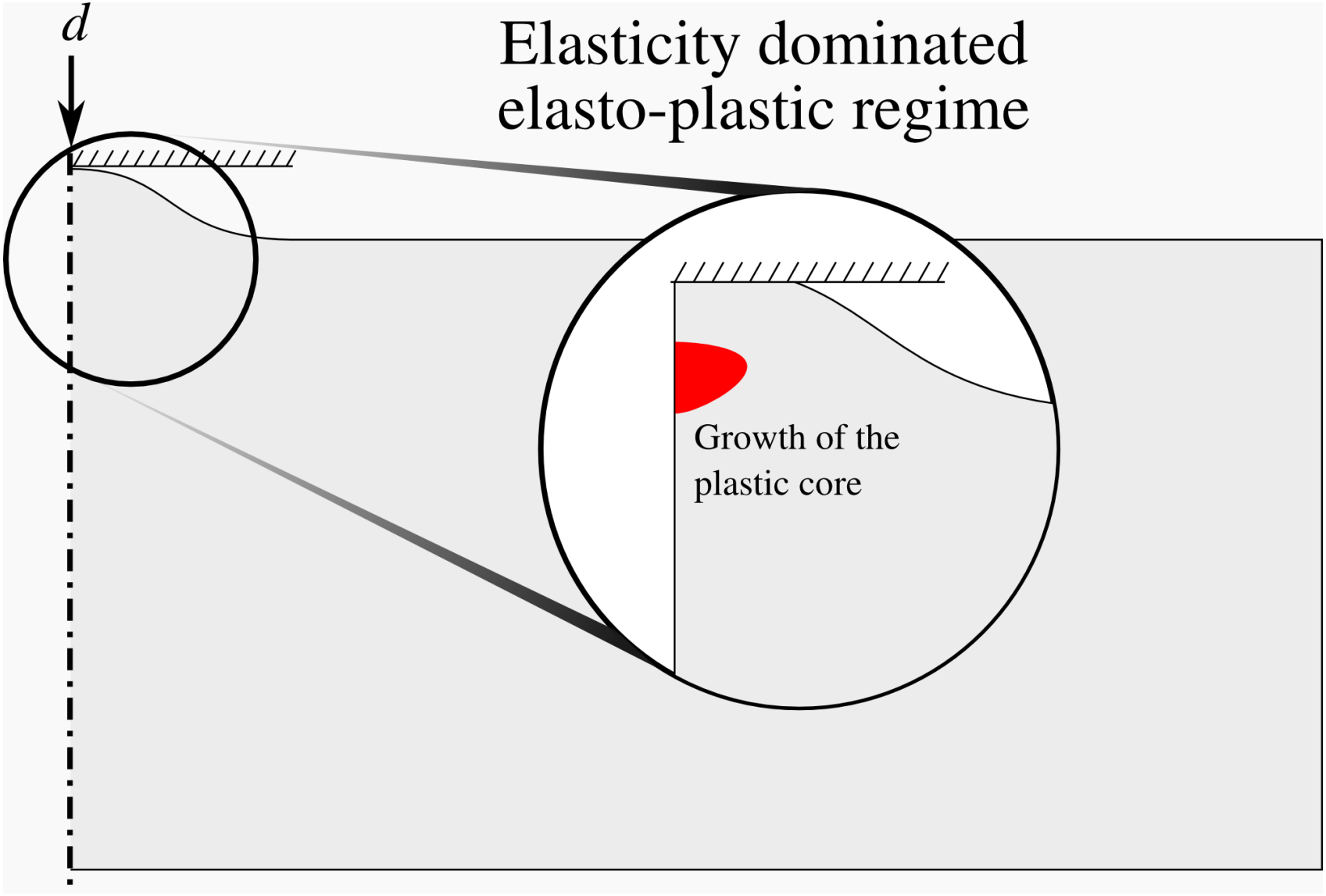

Elasto-plastic transition in contact

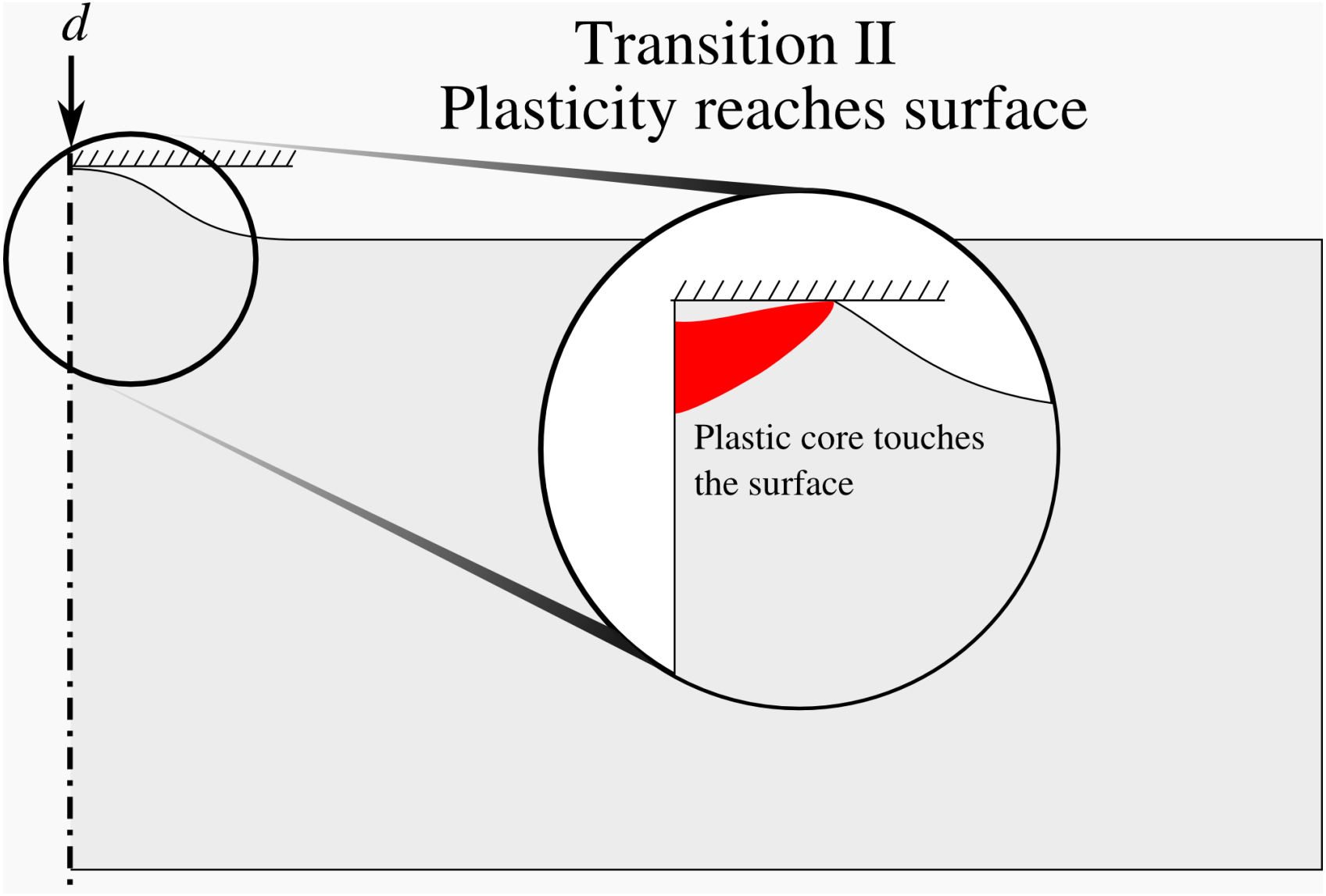

Elasto-plastic transition in contact

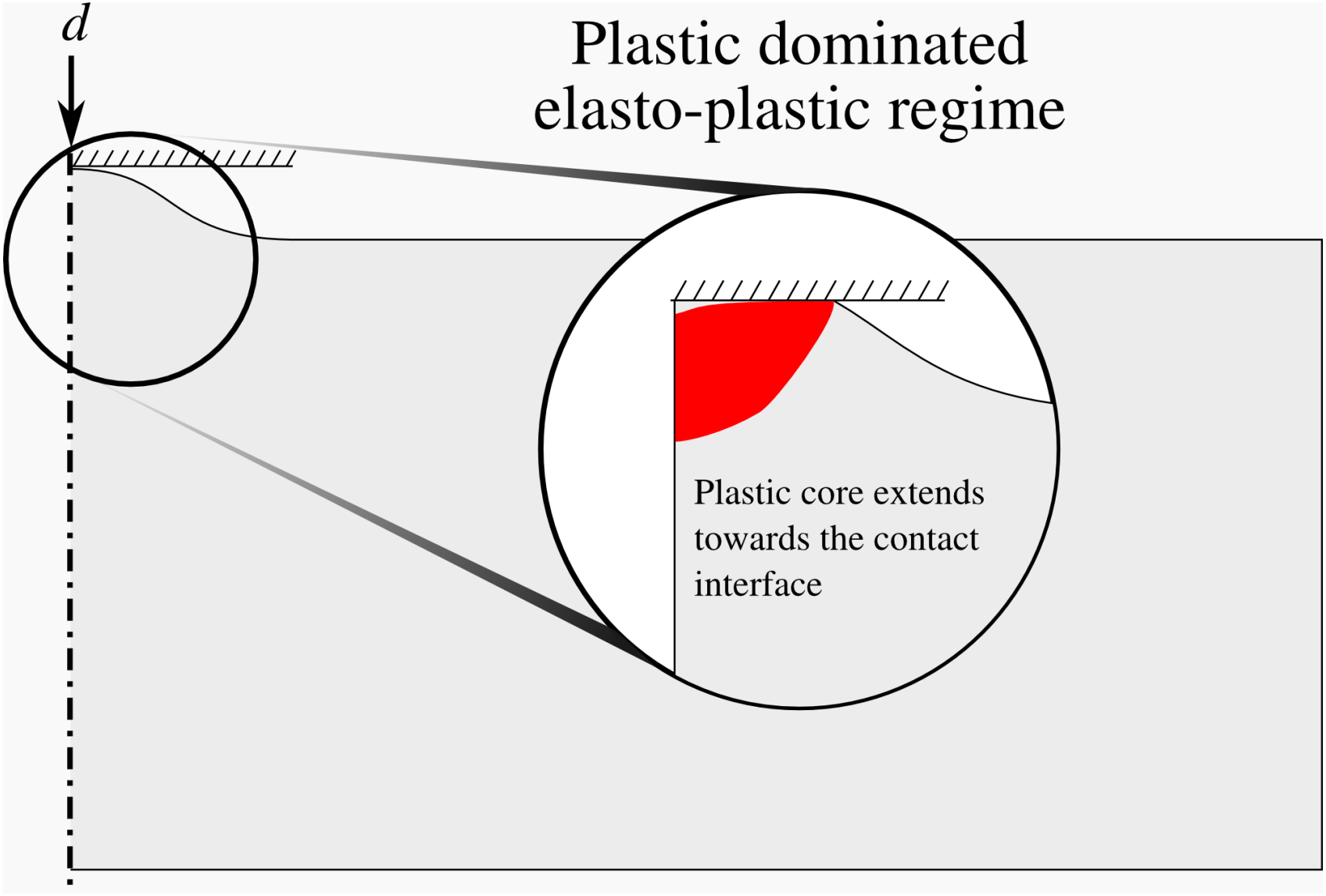

Elasto-plastic transition in contact

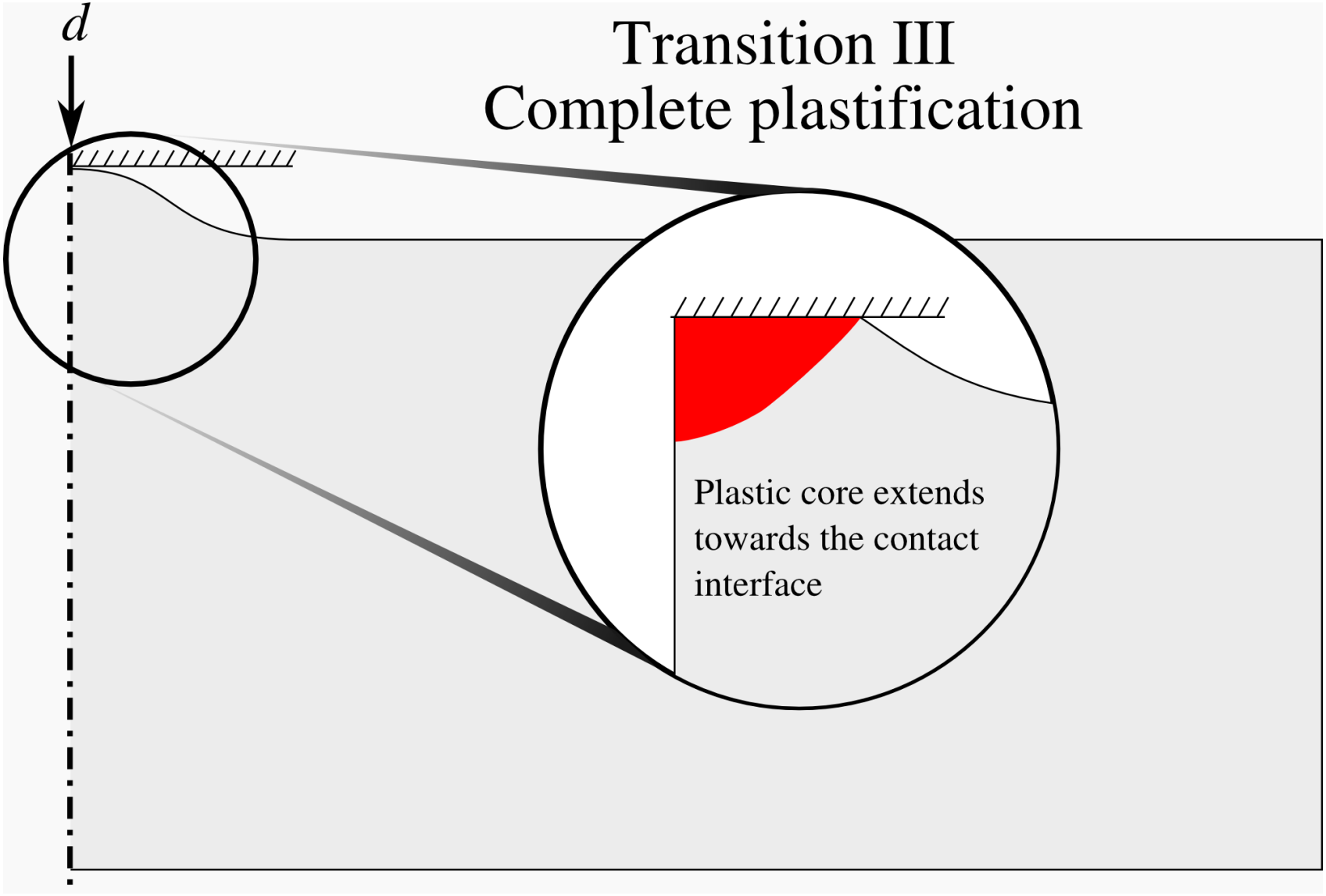

Elasto-plastic transition in contact

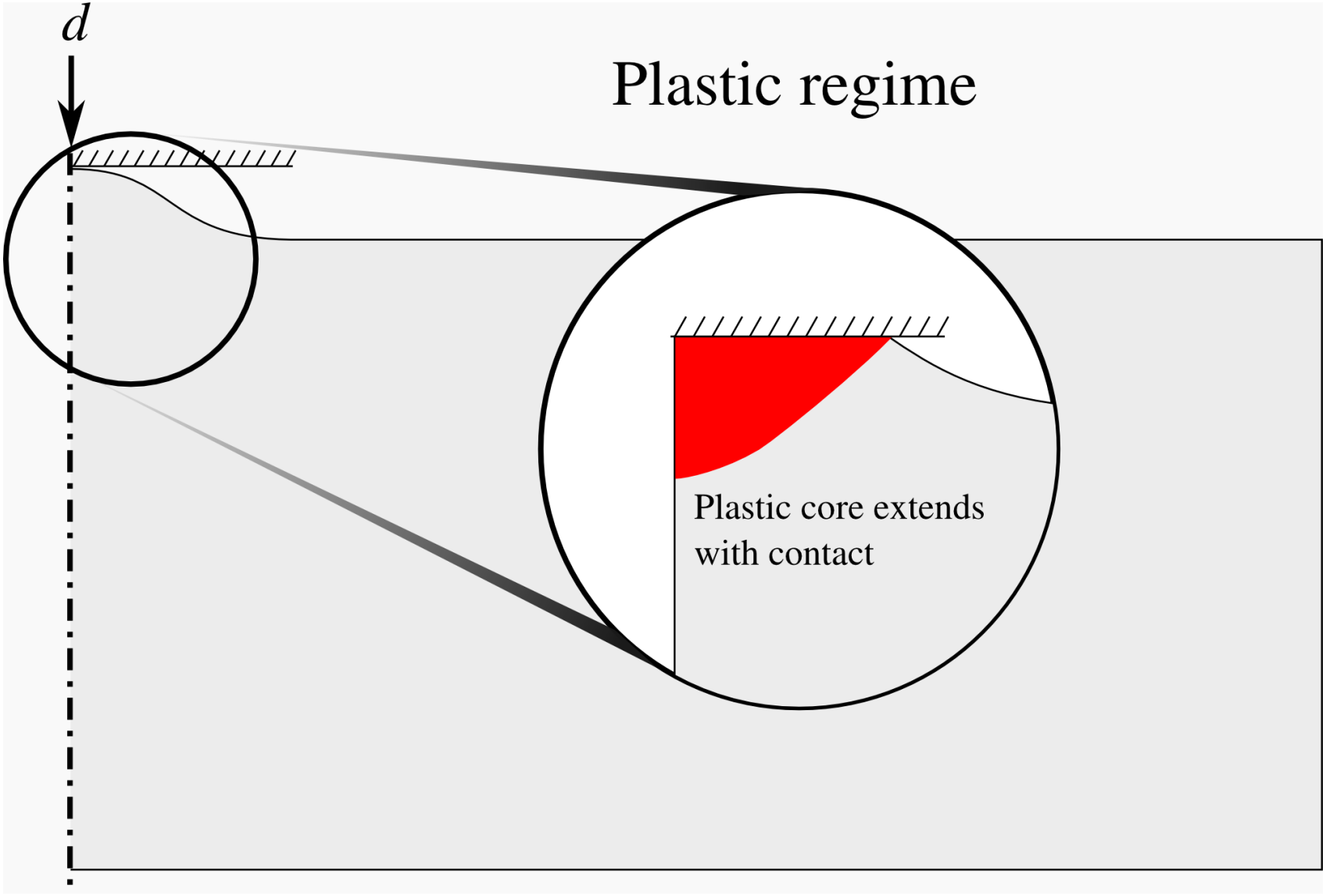

Elasto-plastic transition in contact

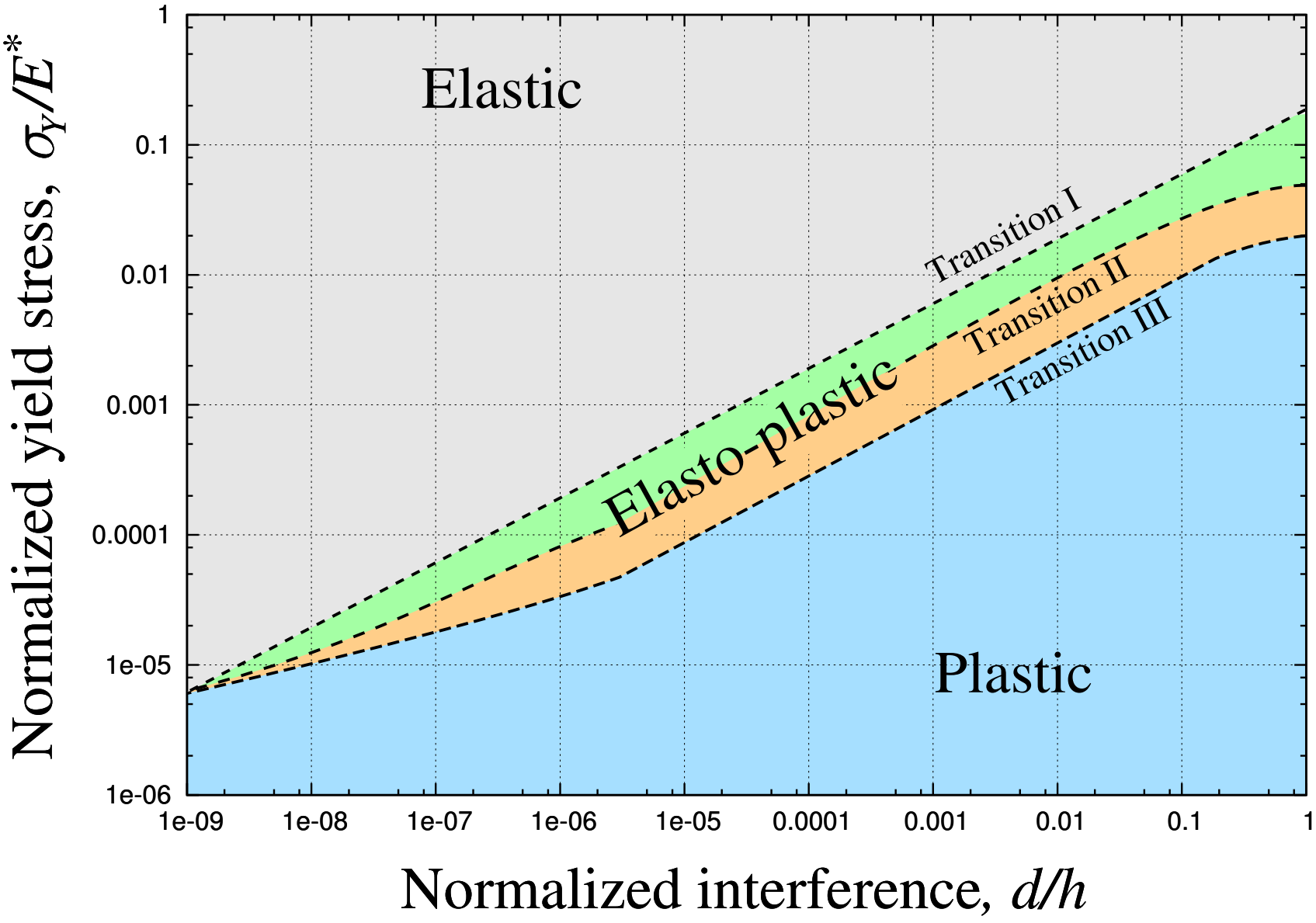

Deformation map for a sinusoidal asperity constructed with M. Liu, H. Proudhon

$h/\lambda = 0.1$

Elasto-plastic transition in contact

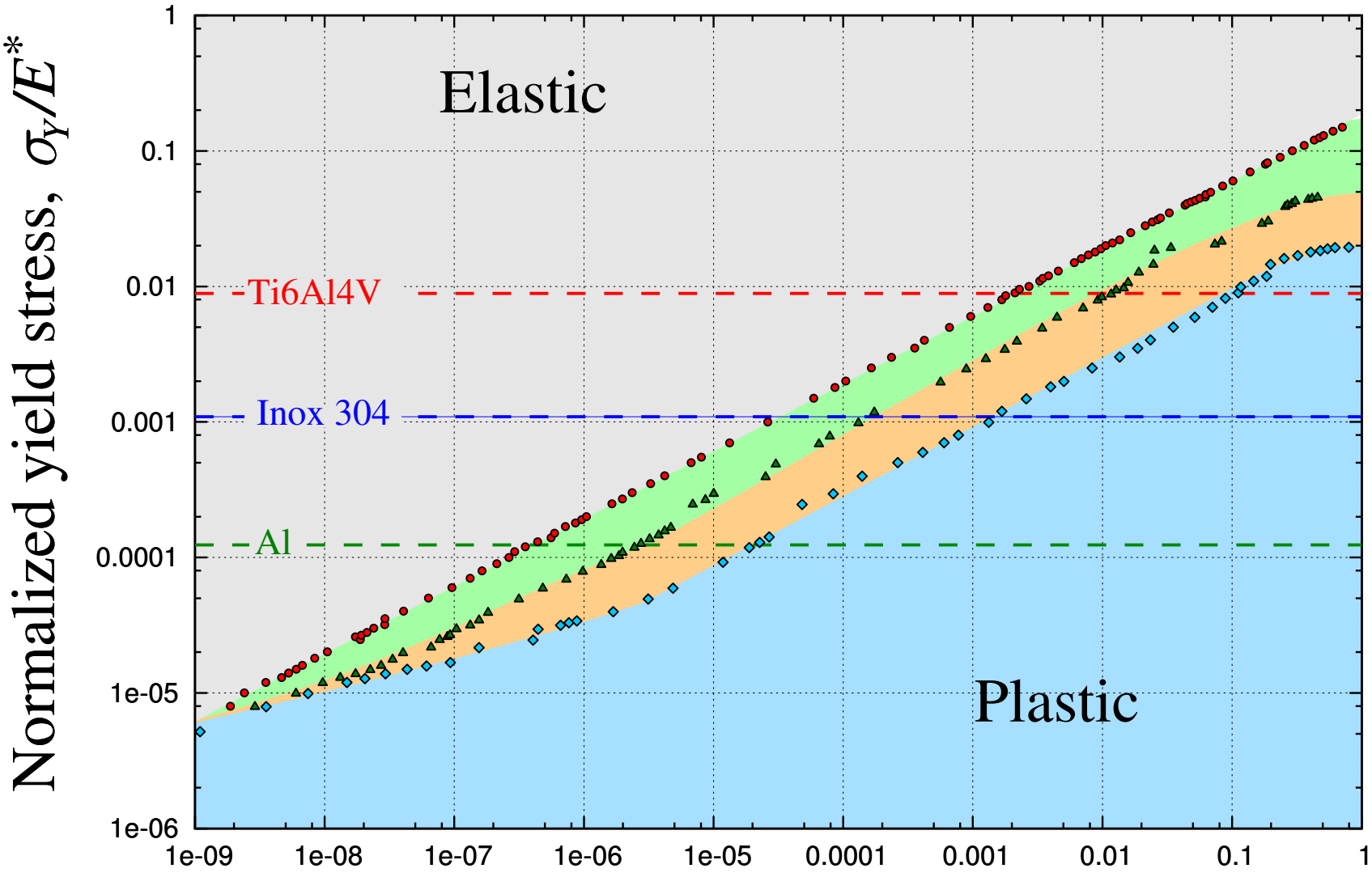

Deformation map for a sinusoidal asperity constructed with M. Liu, H. Proudhon

Elasto-plastic transition in contact

Case: $\sigma_Y/E = 0.0005$

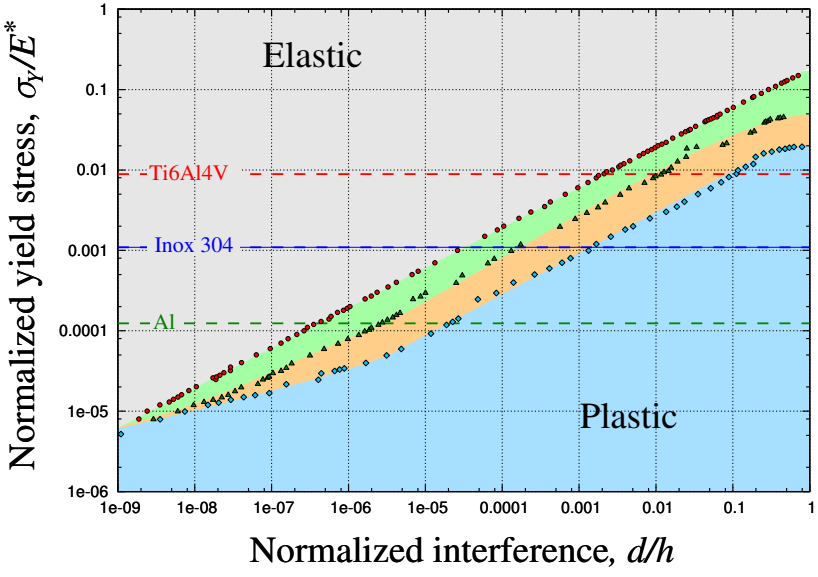

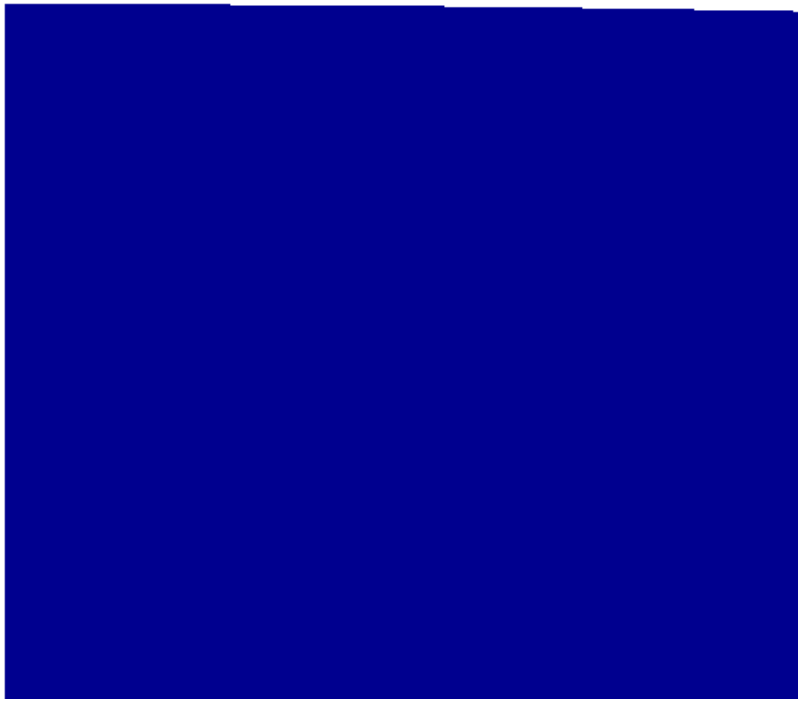

Evolution of the plastic zone in a sinusoidal asperity in contact with a rigid flat

Elasto-plastic transition in contact

Case: $\sigma_Y/E = 0.0005$

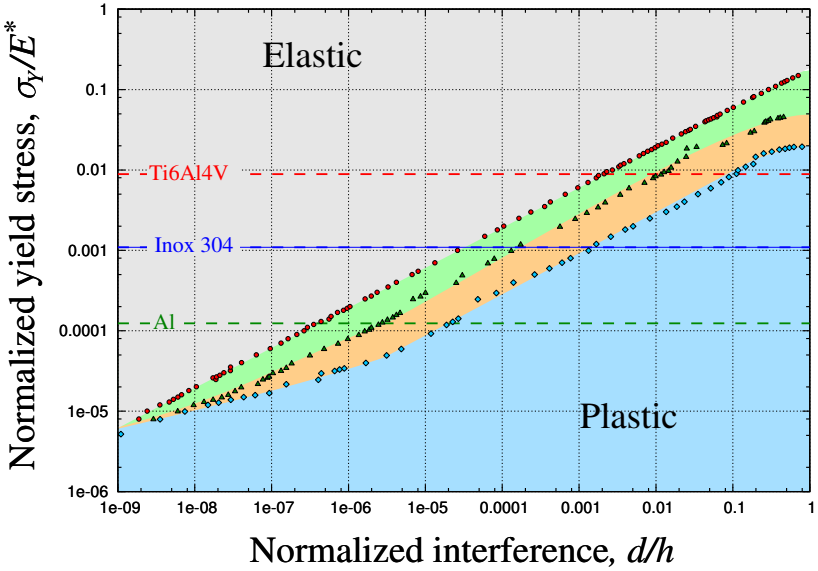

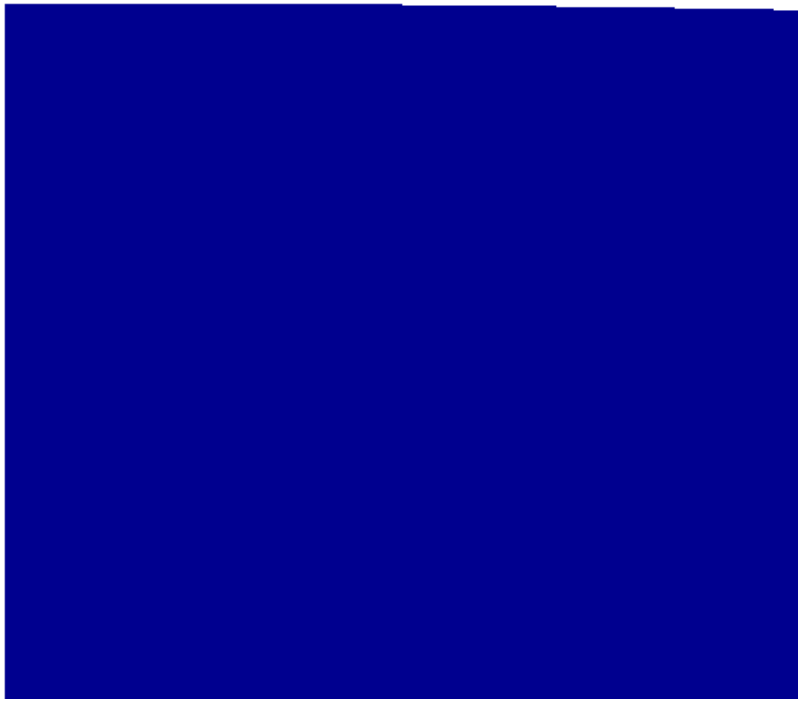

Evolution of the plastic zone in a sinusoidal asperity in contact with a rigid flat

Elasto-plastic transition in contact

Case: $\sigma_Y/E = 0.0005$

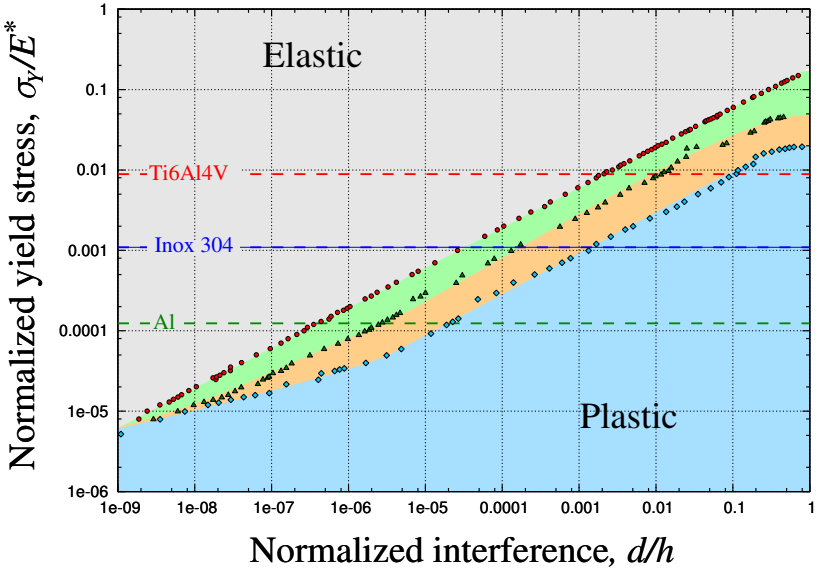

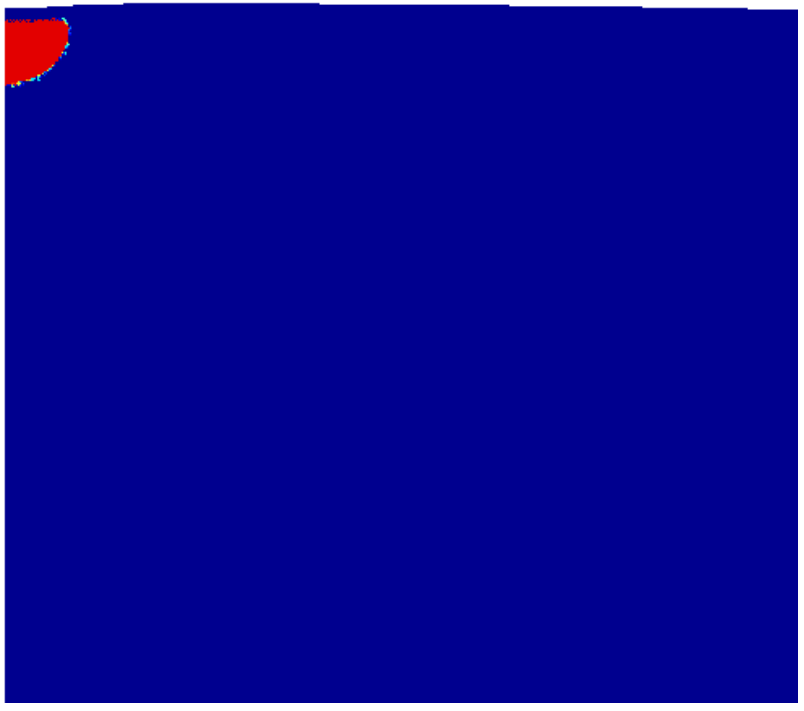

Evolution of the plastic zone in a sinusoidal asperity in contact with a rigid flat

Elasto-plastic transition in contact

Case: $\sigma_Y/E = 0.0005$

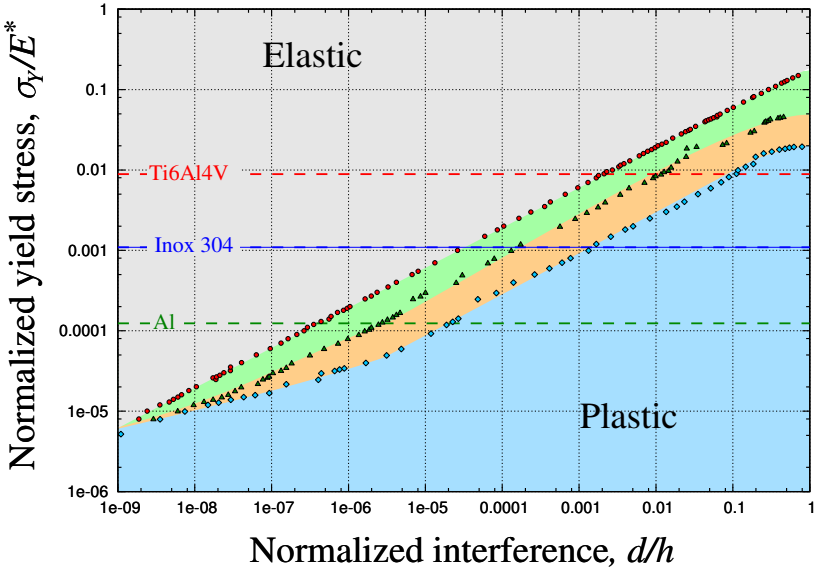

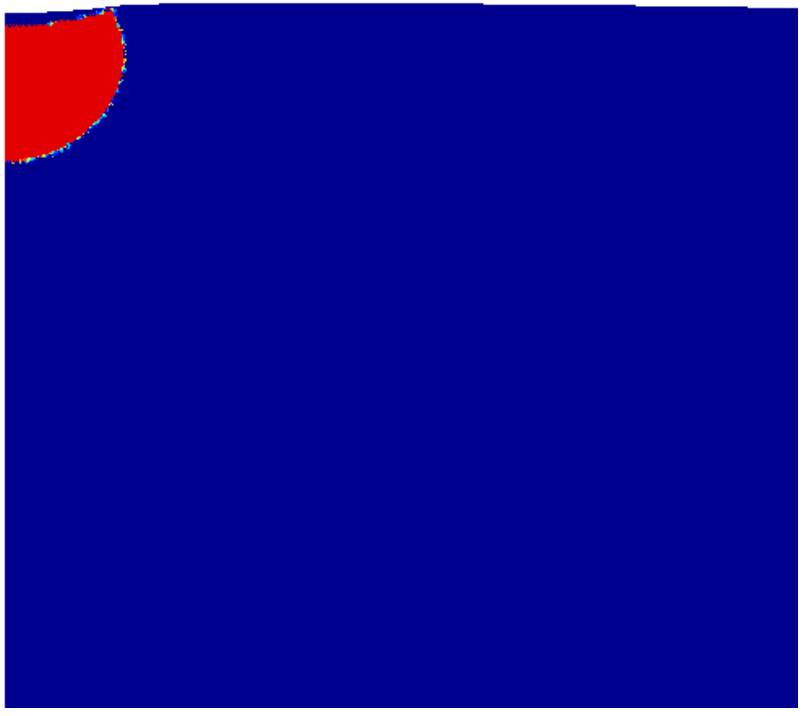

Evolution of the plastic zone in a sinusoidal asperity in contact with a rigid flat

Elasto-plastic transition in contact

Case: $\sigma_Y/E = 0.0005$

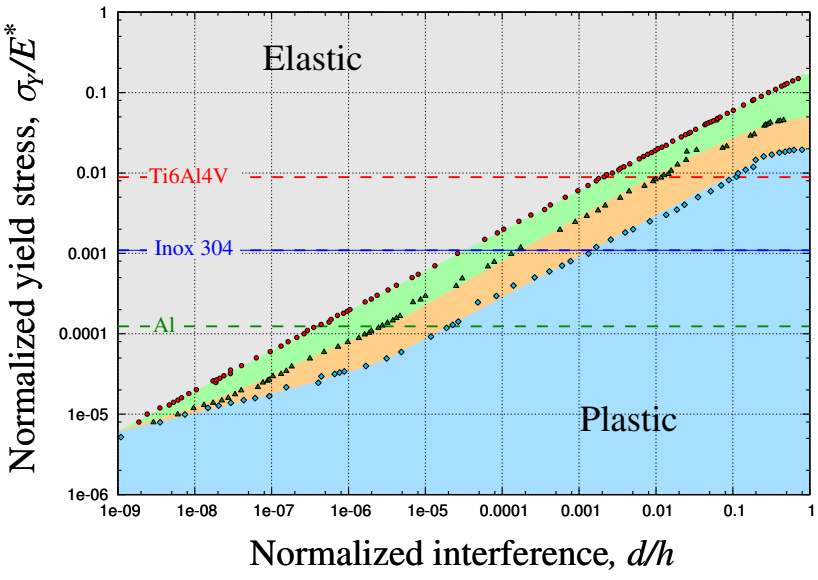

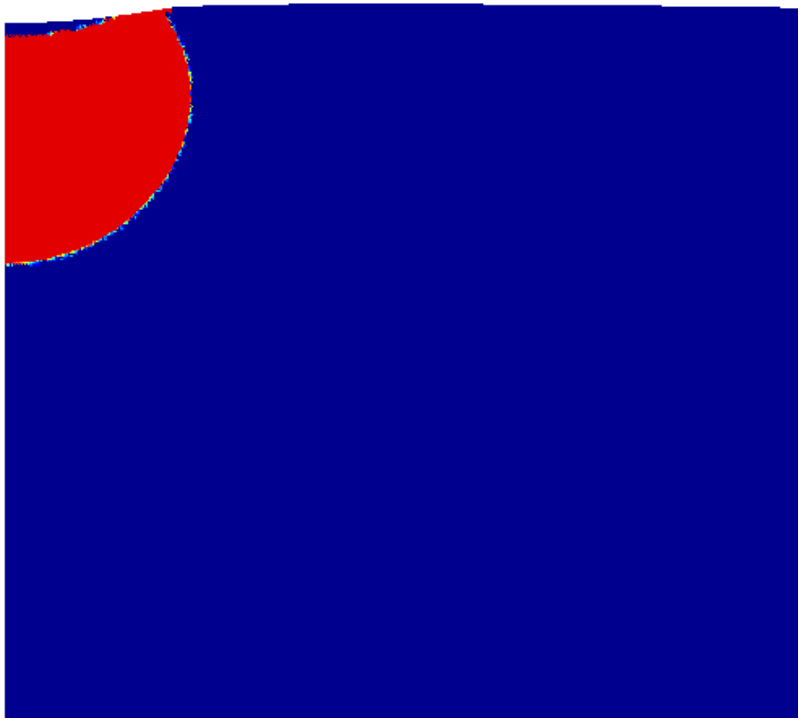

Evolution of the plastic zone in a sinusoidal asperity in contact with a rigid flat

Elasto-plastic transition in contact

Case: $\sigma_Y/E = 0.0005$

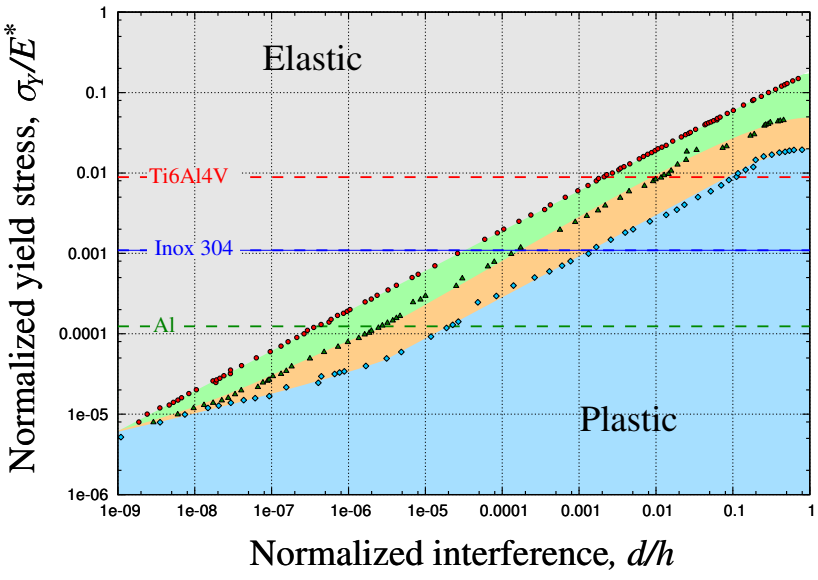

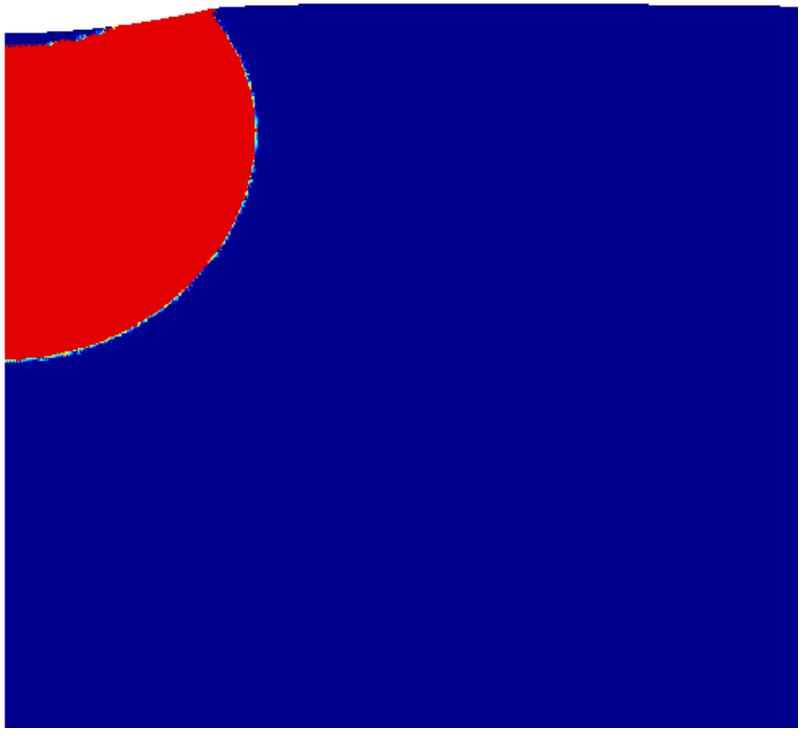

Evolution of the plastic zone in a sinusoidal asperity in contact with a rigid flat

Elasto-plastic transition in contact

Case: $\sigma_Y/E = 0.0005$

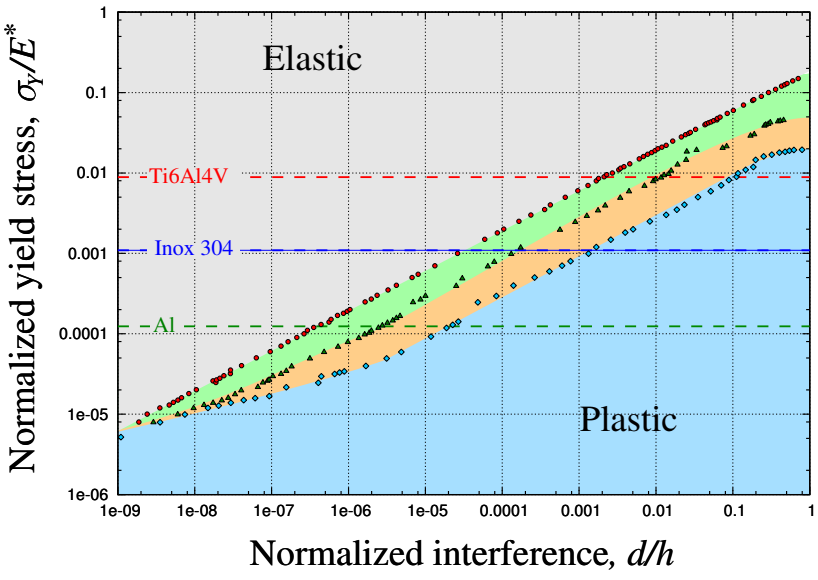

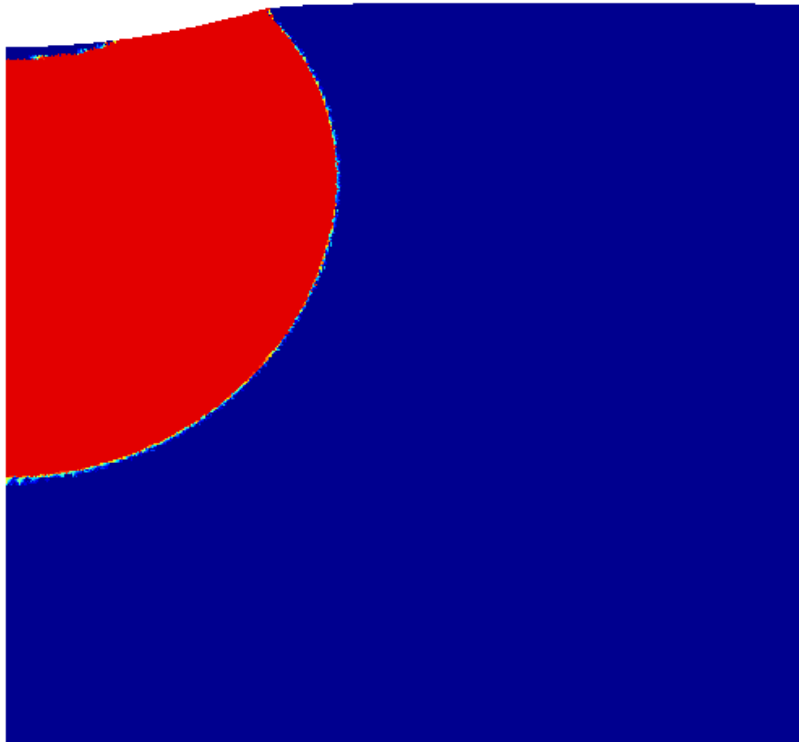

Evolution of the plastic zone in a sinusoidal asperity in contact with a rigid flat

Elasto-plastic transition in contact

Case: $\sigma_Y/E = 0.0005$

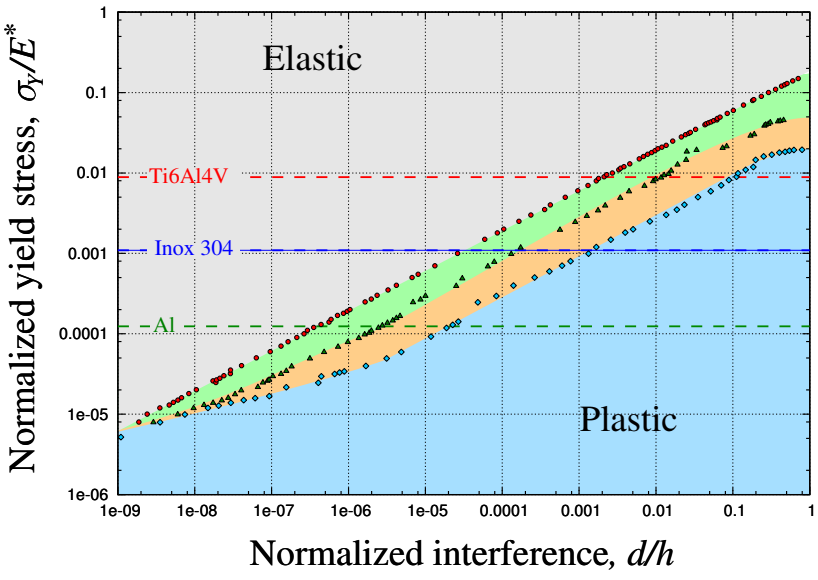

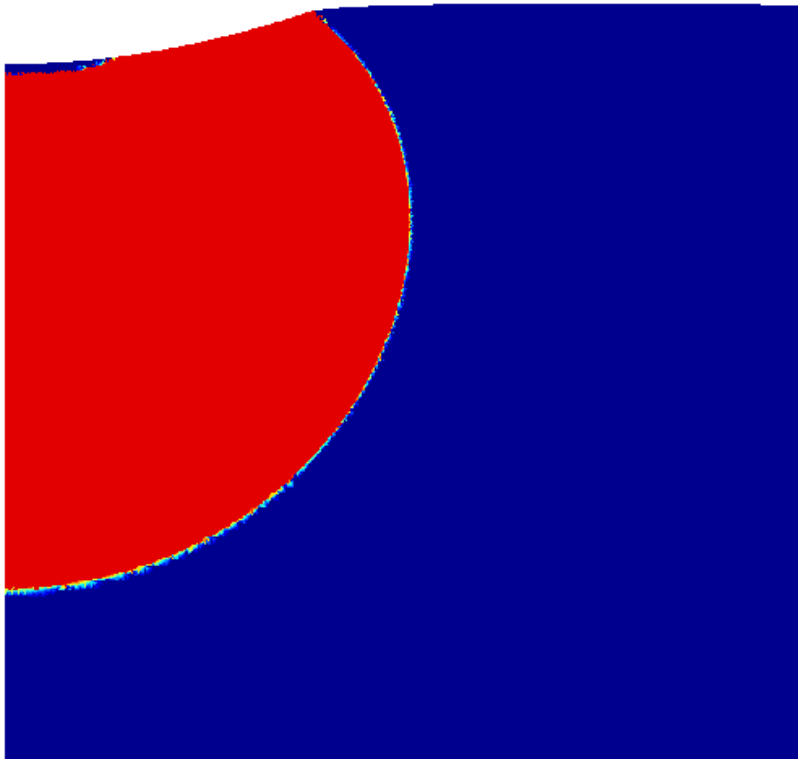

Evolution of the plastic zone in a sinusoidal asperity in contact with a rigid flat

Elastic-plastic normal contact: hardness

- Hardness ~ saturated plastic contact
- Recall: Vickers hardness $HV = N/A$
- Similarity solution[1]

$$\frac{N}{\pi a^2 \sigma_Y} = F\left(\frac{a}{R}\frac{E}{\sigma_y}\right)$$

- Hardness $H \approx 3\sigma_Y$

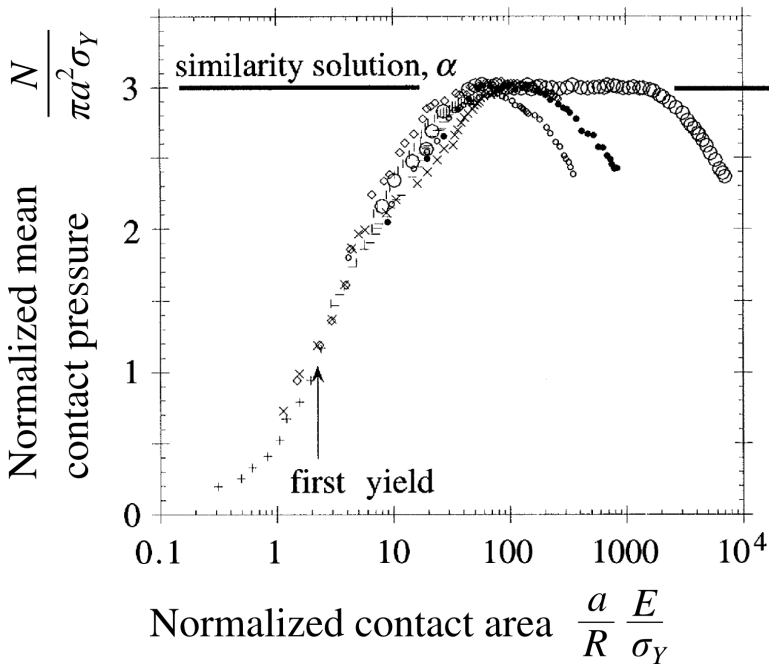

Simulation of spherical indentation of elasto-plastic solid with power-law hardening[2]

[1] Hill R., Storøakers B., Zdunek A.B. A theoretical study of the Brinell hardness test. Proc R Soc Lond A 436 (1989)

[2] Tabor, D. The Hardness of Metals. Oxford at the Clarendon Press (2000).

[3] Mesarovic S., N. Fleck, Spherical Indentation of Elastic-Plastic Solids, Proc R Soc Lond A 455 (1999)

Elasto-plastic contact under cyclic load

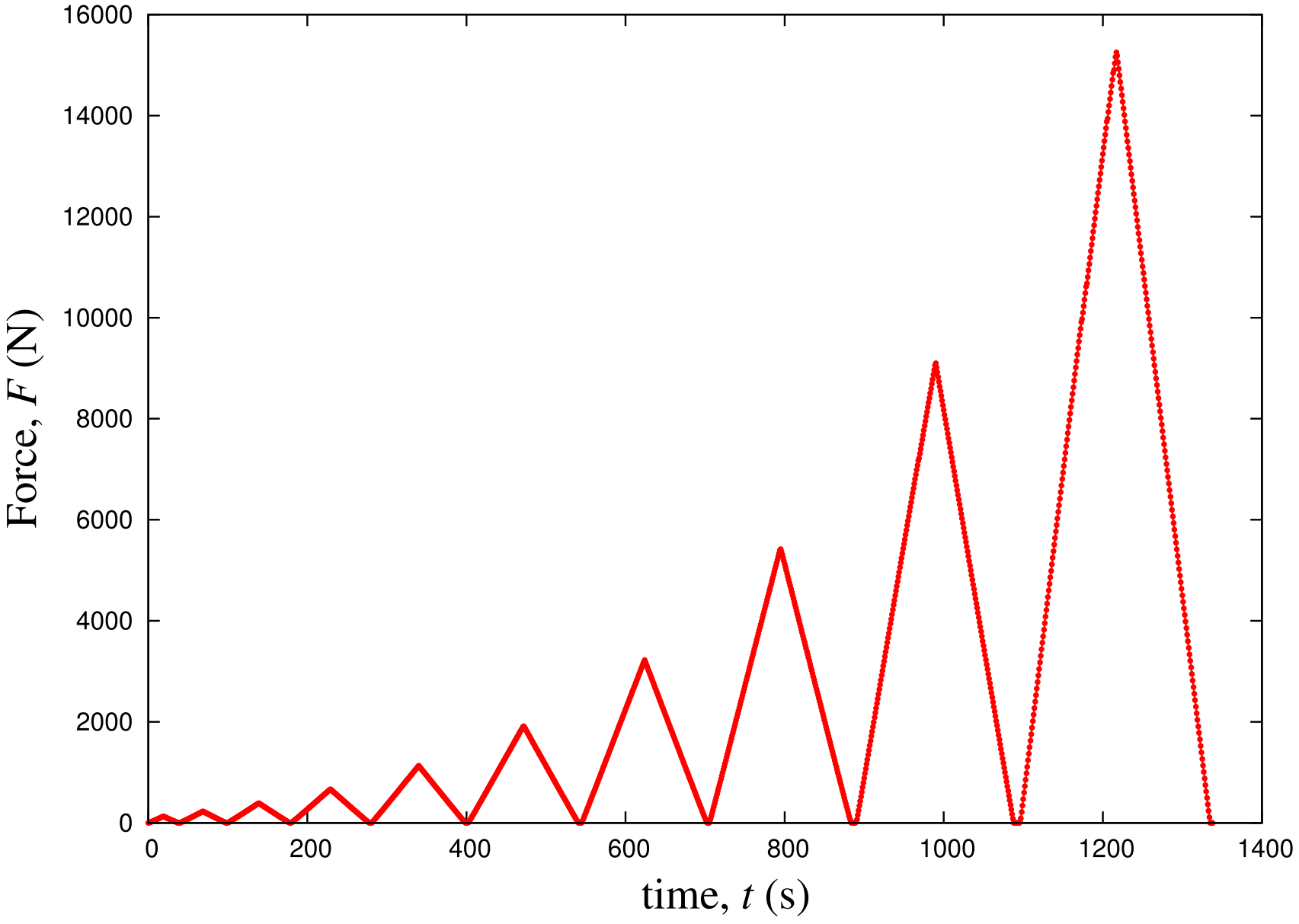

Elasto-plastic contact under cyclic load

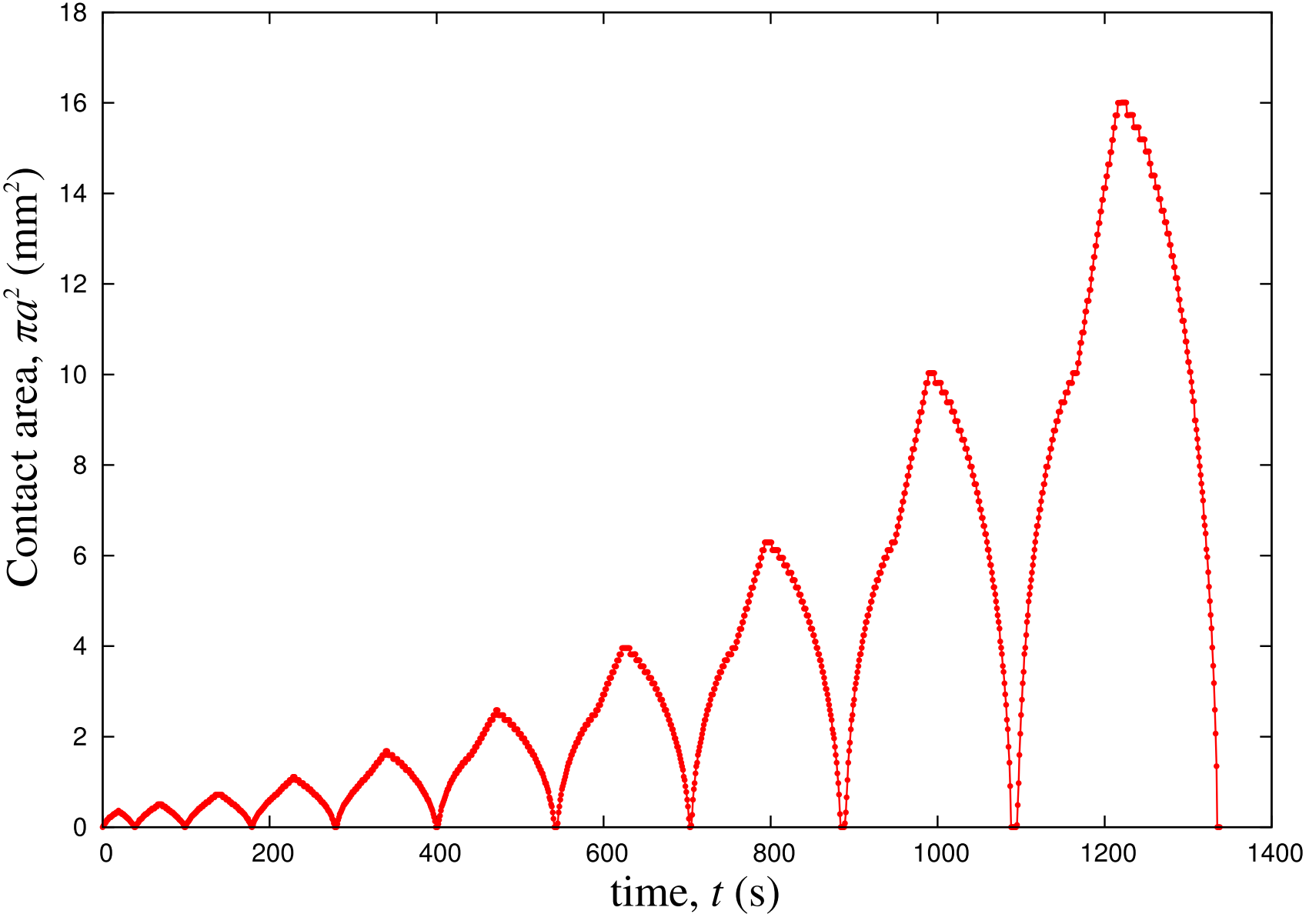

Elasto-plastic contact under cyclic load

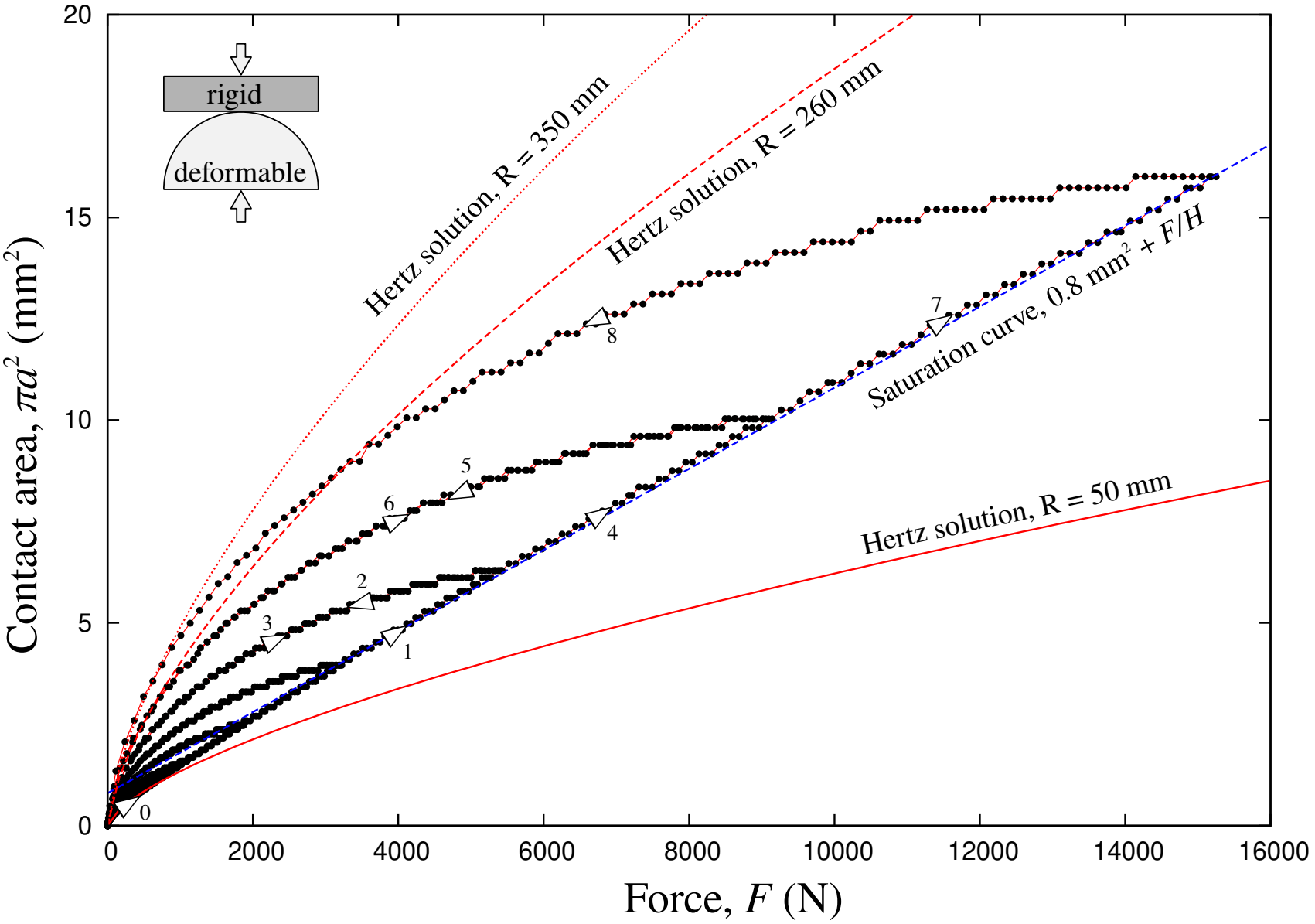

Elasto-plastic contact under cyclic load

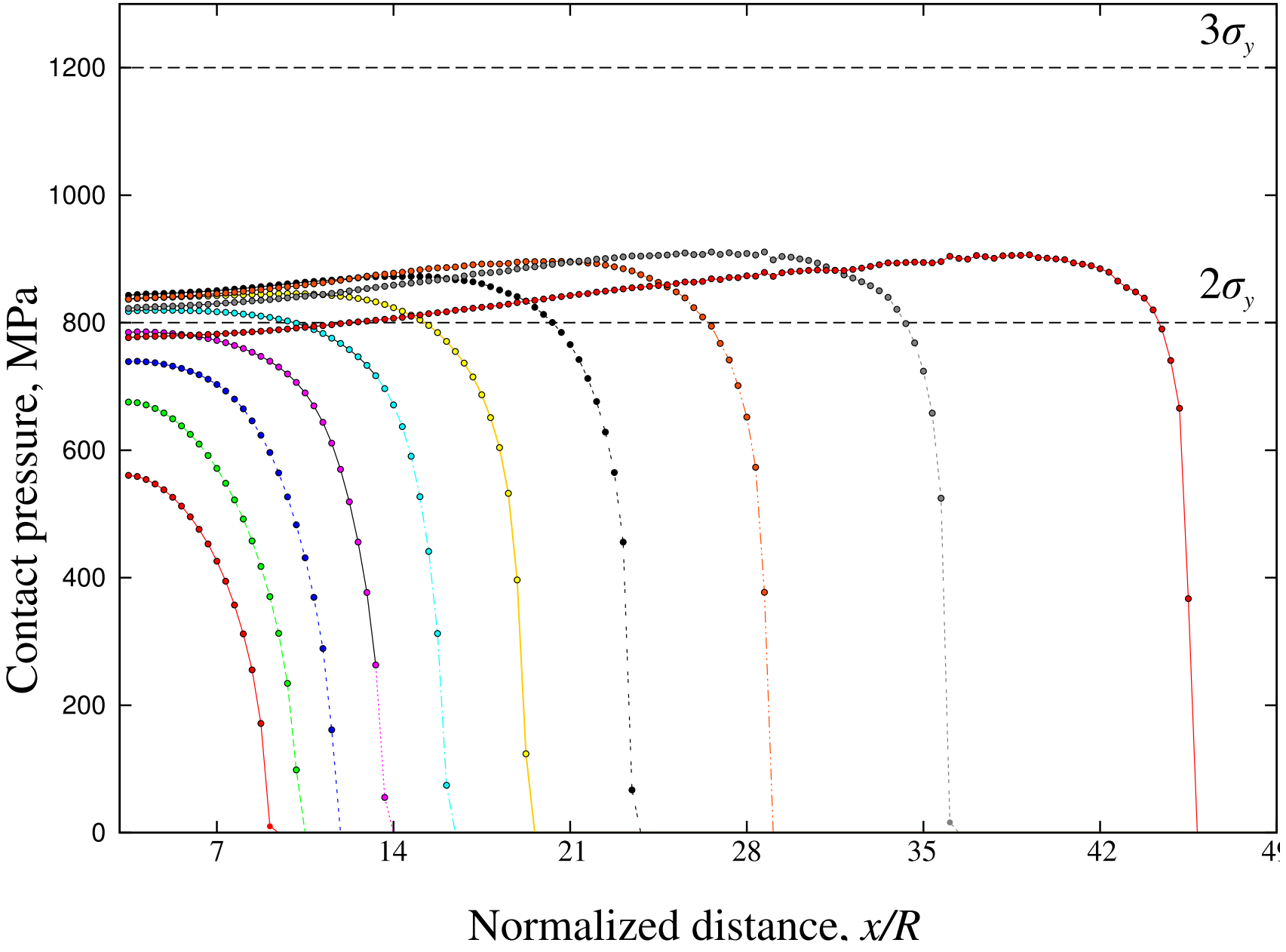

Elasto-plastic contact under cyclic load

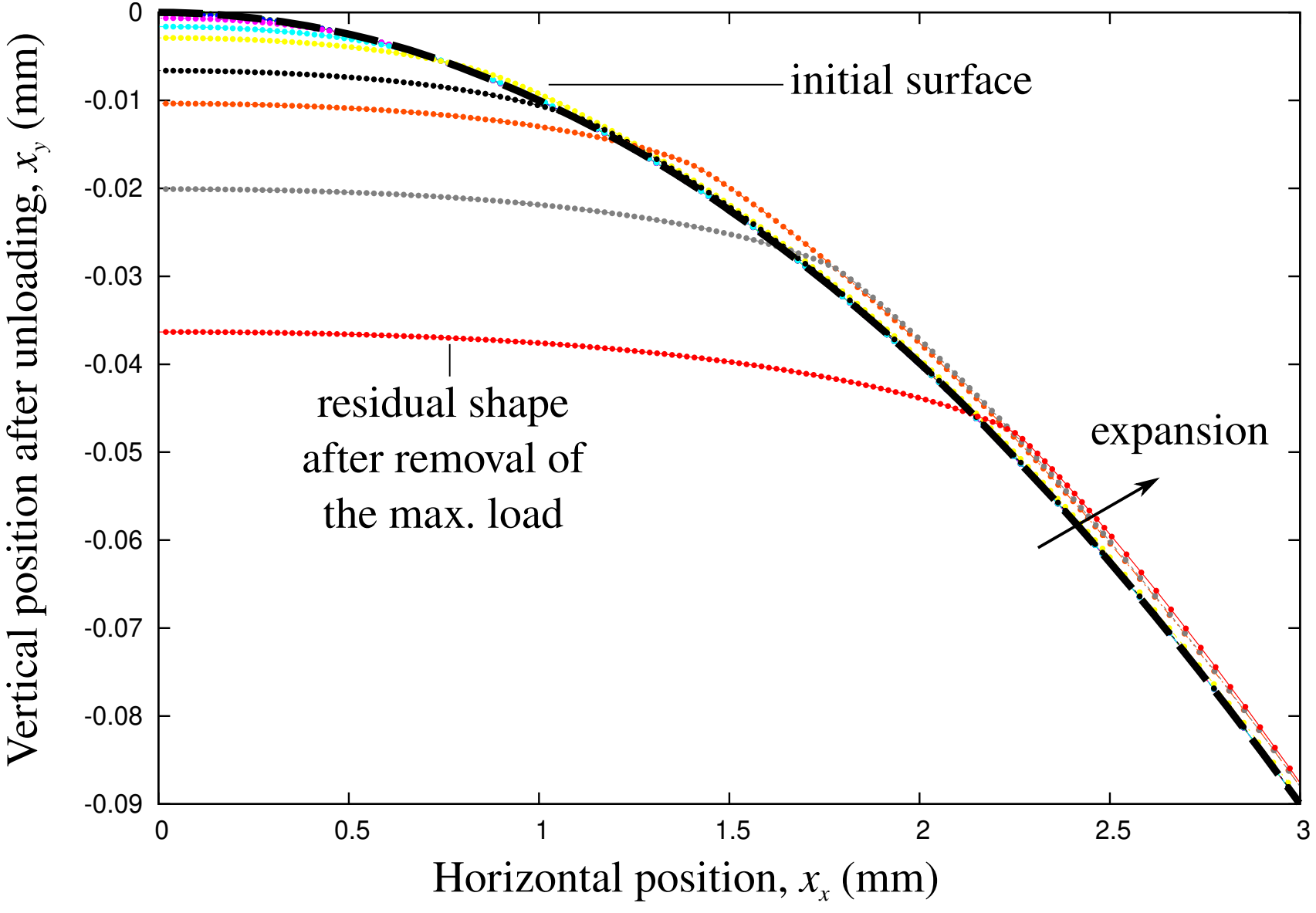

Deformation in fully plastic regime

✓ **Mesh effect**

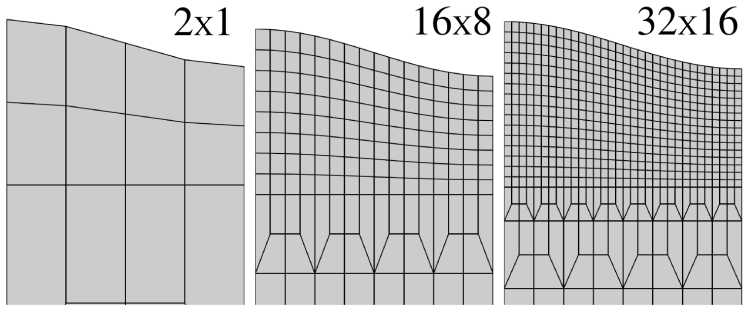

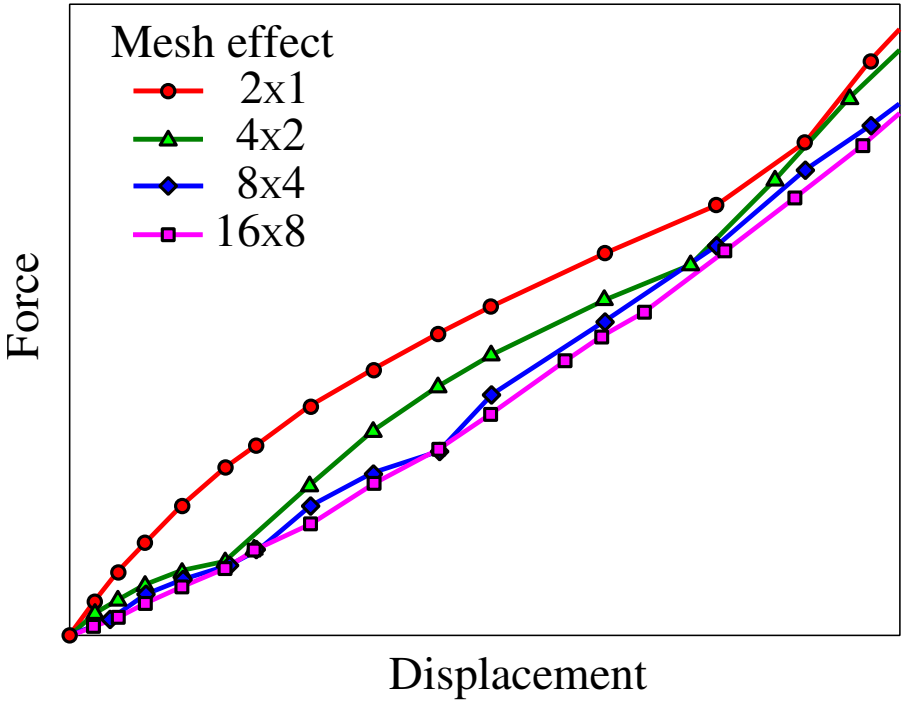

Shape effect

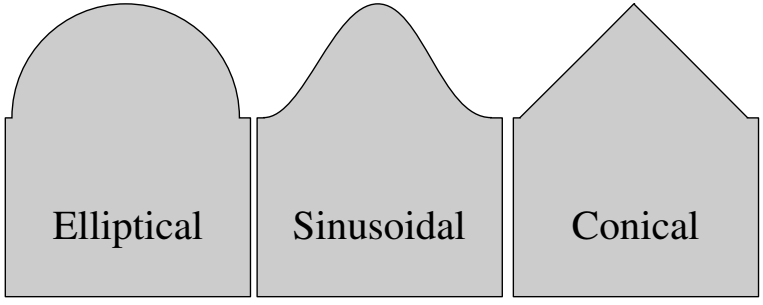

Edge effect

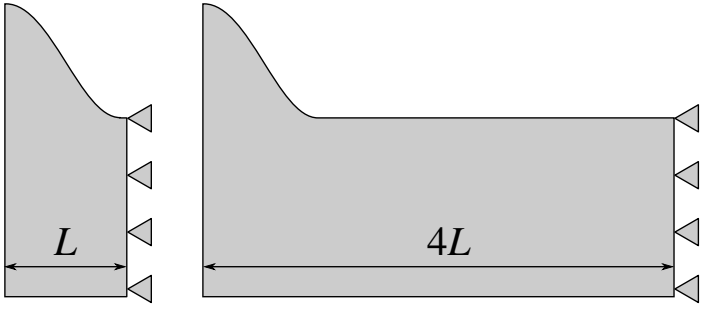

[1] V. A. Yastrebov, J. Durand, H. Proudhon, G. Cailletaud, CR Mecan, 339:473-490 (2011)

Deformation in fully plastic regime

Mesh effect

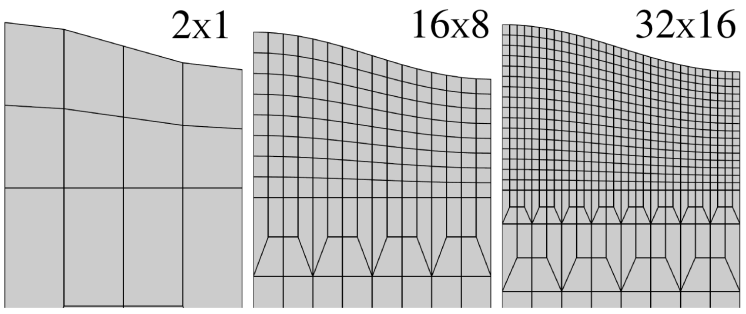

✓ **Shape effect**

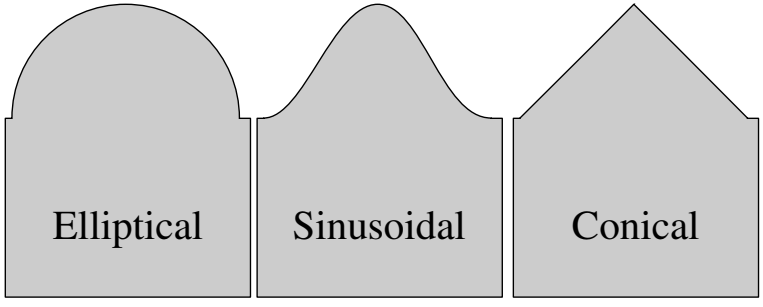

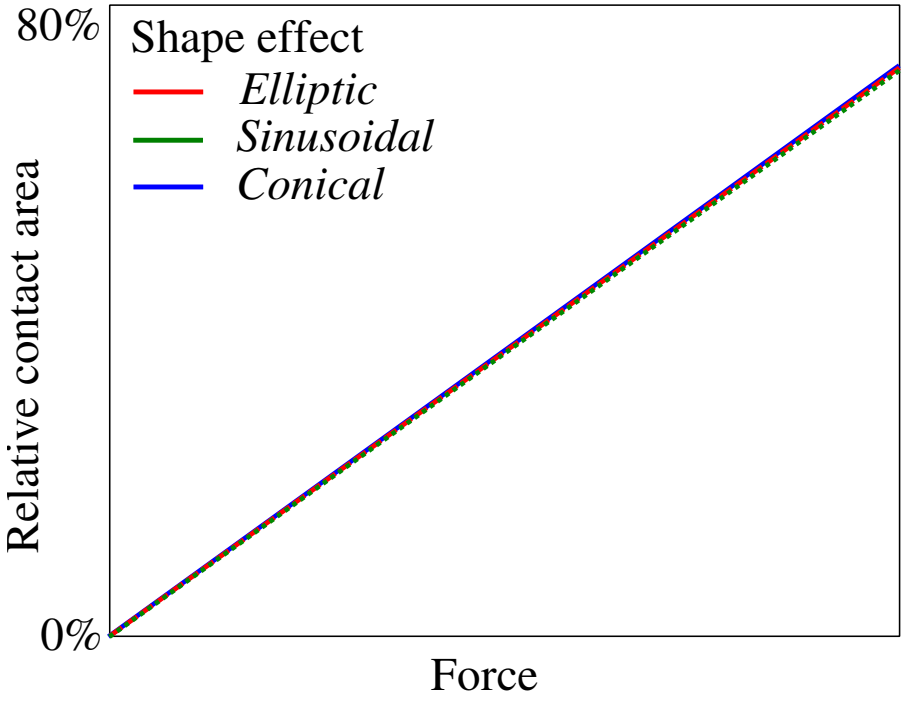

Edge effect

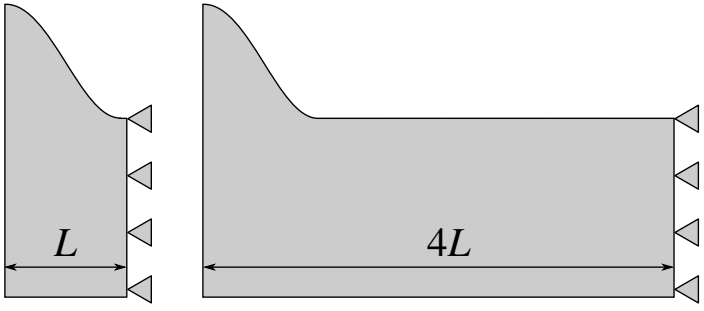

[1] V. A. Yastrebov, J. Durand, H. Proudhon, G. Cailletaud, CR Mecan, 339:473-490 (2011)

Deformation in fully plastic regime

Mesh effect

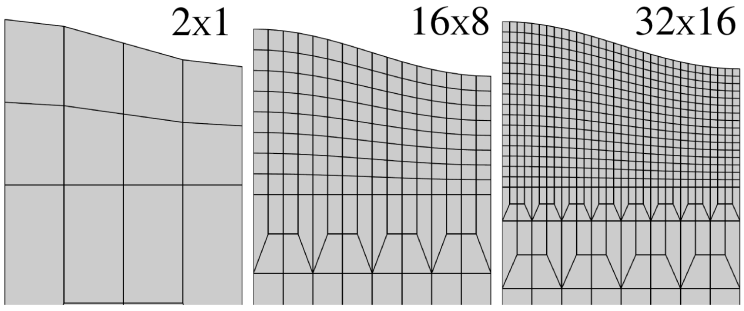

Shape effect

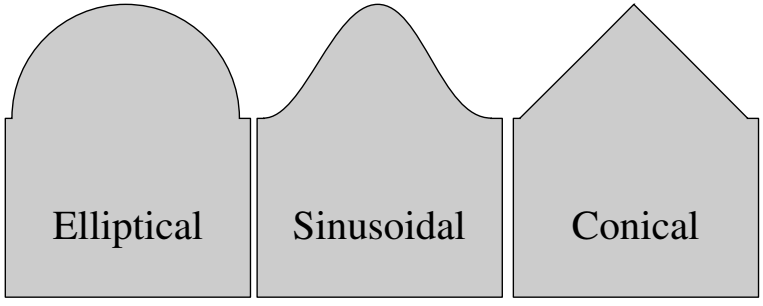

✓ **Edge effect**

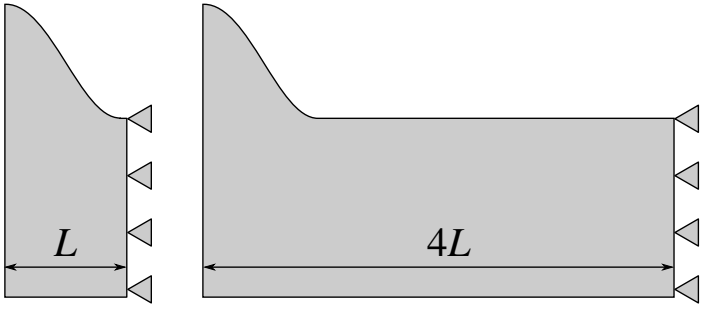

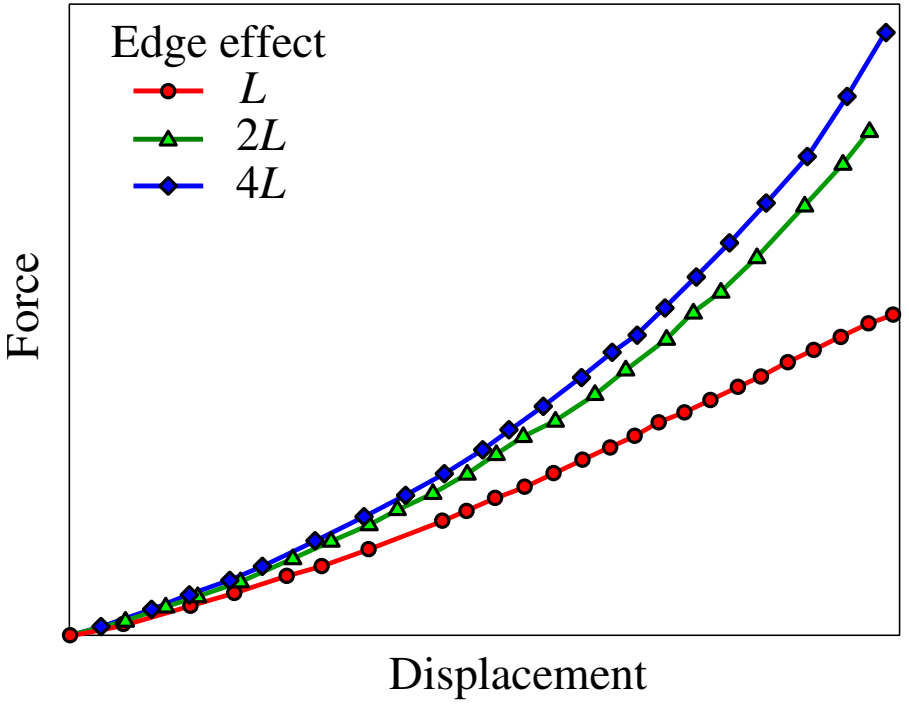

[1] V. A. Yastrebov, J. Durand, H. Proudhon, G. Cailletaud, CR Mecan, 339:473-490 (2011)

Near-surface vs bulk deformation

Material aspects

- Cold worked surface + recrystallized:
  smaller grains near the surface, Hall-Petch effect
- Thin coating films:
  nanograined, confined plasticity, Hall-Petch effect
- Oxides:
  brittle hard films

Geometrical aspects

- Roughness of all nature
- Indentation by asperities:
  confined plastic zone, high plastic strain gradients

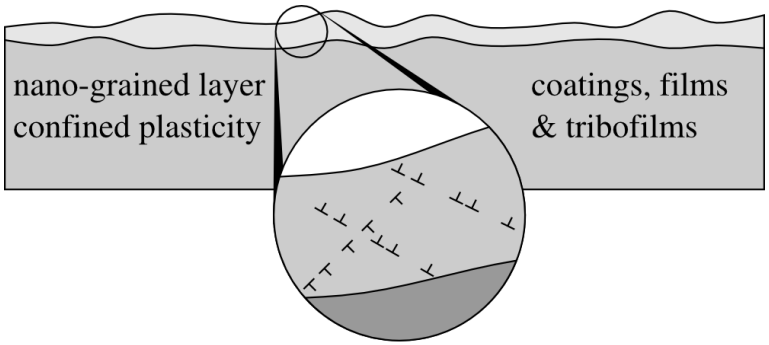

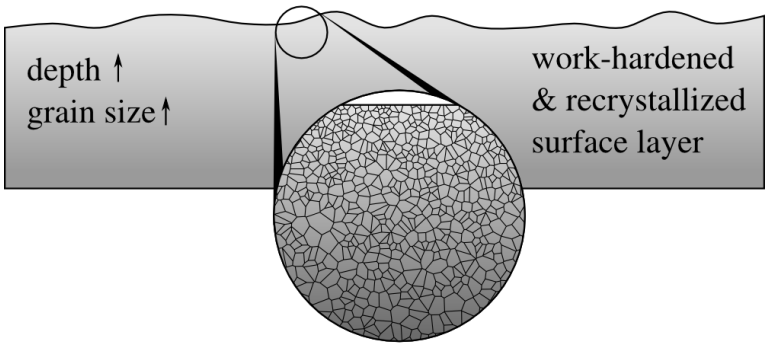

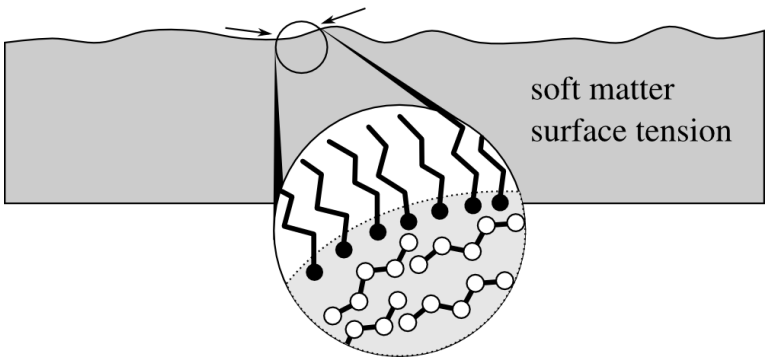

Onset of yielding at atomic scale

Hertz contact: body of revolution

- Onset of plasticity for pressure

$$p_Y = 1.6\sigma_Y$$

- Associated force

$$F_Y = \frac{1.6^3\pi^3R^2}{6}\left(\frac{\sigma_Y}{E^*}\right)^2\sigma_Y$$

- Associated contact radius

$$a_Y = \frac{1.6\pi R}{2}\frac{\sigma_Y}{E^*}$$

- Plastic flow starts at depth

$$z_Y \approx 1.21R\frac{\sigma_Y}{E^*}$$

- Example: golden asperity $R = 10\ \mu$m

$E^* \approx 96$ GPa, $\sigma_y \approx 140$ MPa, $d \approx 4.1$Å

$$F_Y \approx 3.8\ \mu\text{N}, \quad z_Y \approx 18\ \text{nm}, \quad a_Y \approx 36\ \text{nm}$$

$$z_Y \approx 45d, \quad a_Y \approx 115d$$

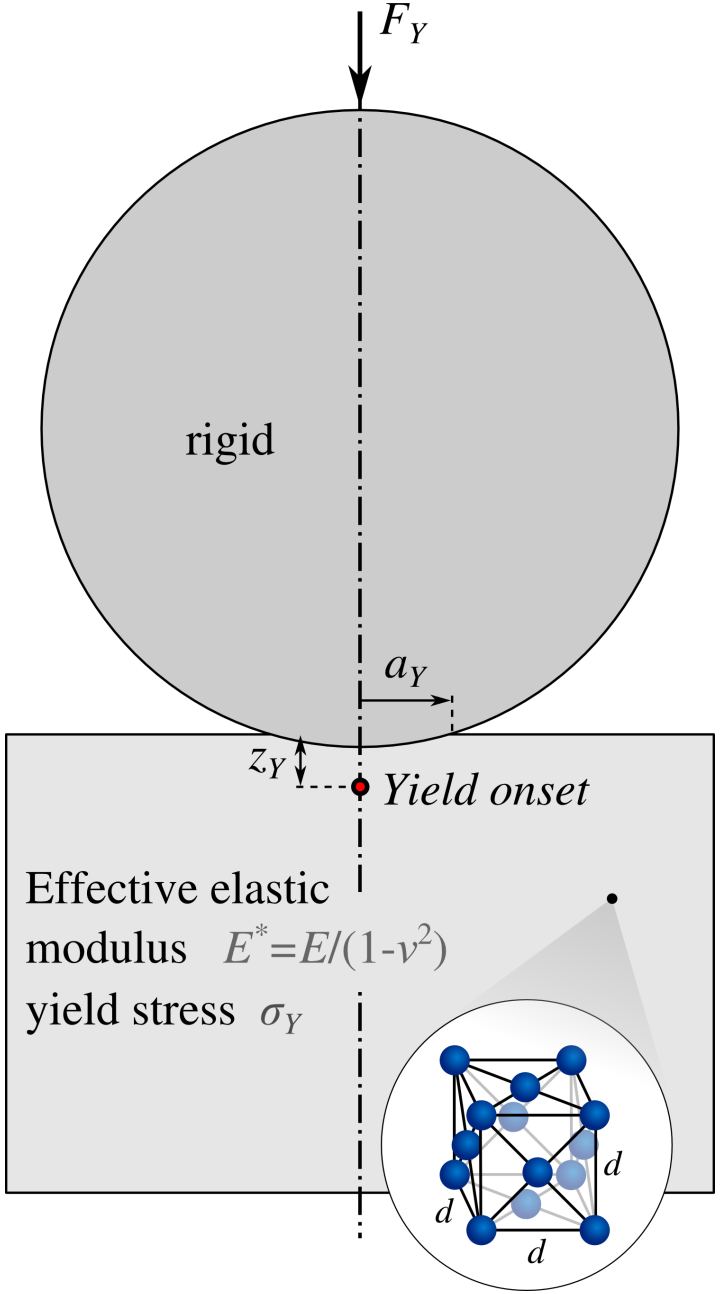

Indentation and hardness

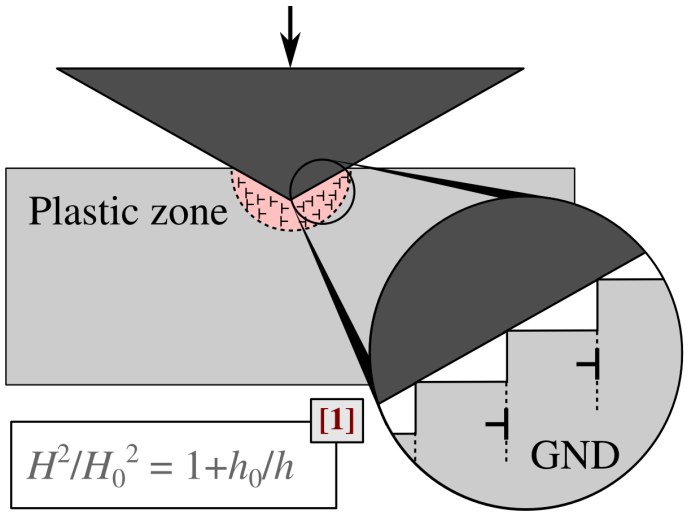

[1] Nix, Gao. *J Mech Phys Solids* (1998).

Indentation and hardness

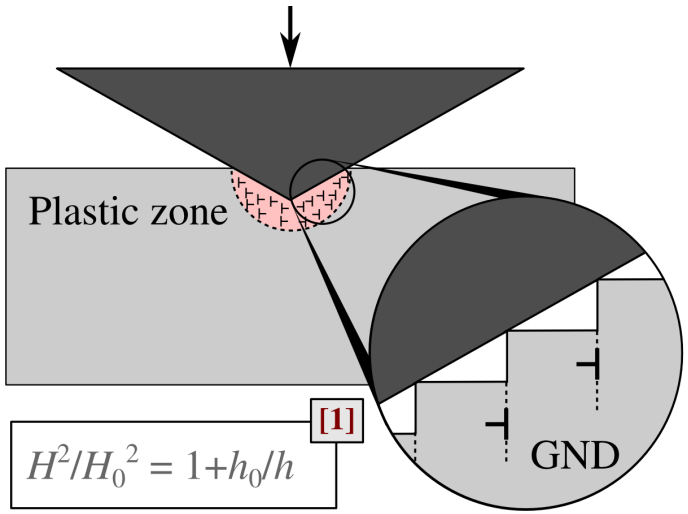

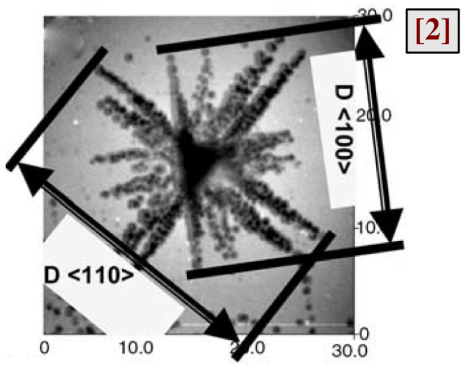

[1] Nix, Gao. *J Mech Phys Solids* (1998).
[2] Feng, Nix. *Scripta Mater* (2004).

Indentation and hardness

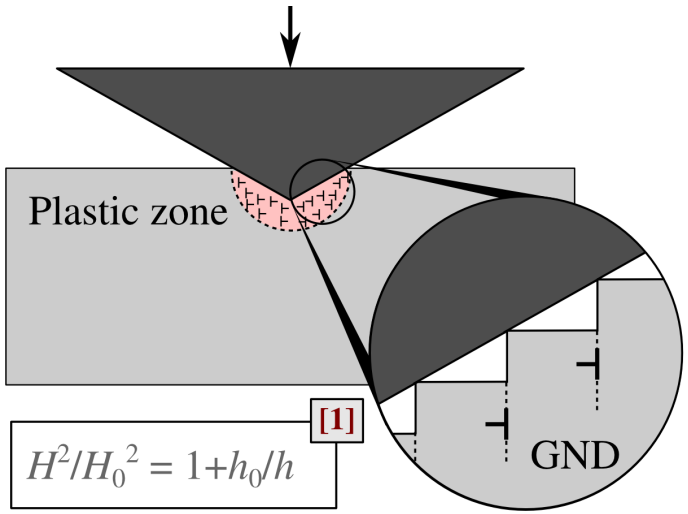

[1] $H^2/H_0^2 = 1+h_0/h$

$$\frac{\text{Plastic zone } r}{\text{Contact radius } a} \sim 1 + b\exp(-h/h_1)$$

[2] $H^2/H_0^2 = 1+[1+b\exp(-h/h_1)]^{-3}h_0/h$

[2,3] $(H-H_P)^2/(H_0-H_P)^2 = 1+[1+b\exp(-h/h_1)]^{-3}h_0/h$

[1] Nix, Gao. *J Mech Phys Solids* (1998).
[2] Feng, Nix. *Scripta Mater* (2004).
[3] Qui, Huang, Nix, Hwang, Gao. *Acta Mater* (2001).

Indentation and hardness

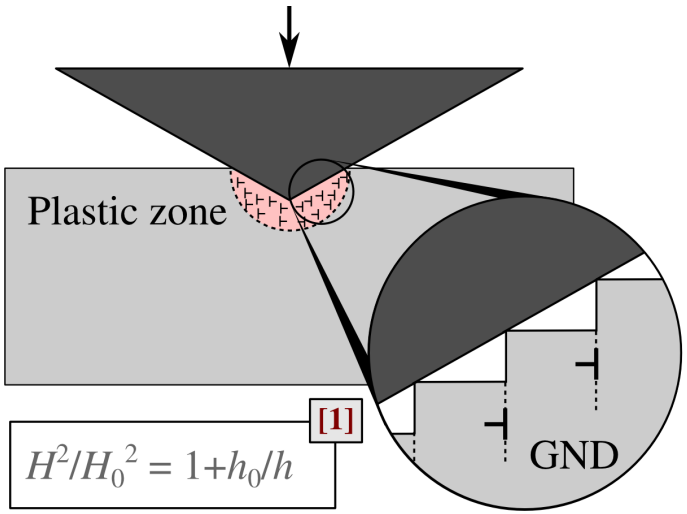

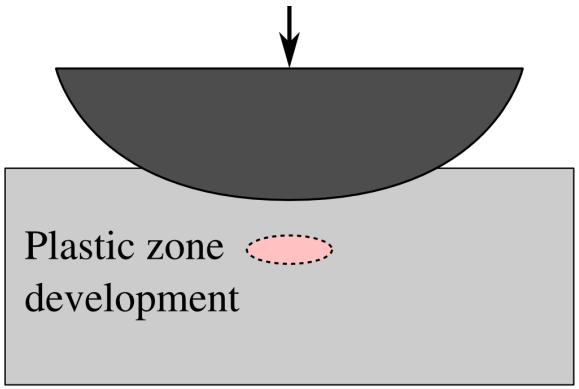

$$H^2/H_0^2 = 1+h_0/h \quad [1]$$

$$\frac{\text{Plastic zone } r}{\text{Contact radius } a} \sim 1 + b\exp(-h/h_1)$$

$$H^2/H_0^2 = 1+[1+b\exp(-h/h_1)]^{-3}h_0/h \quad [2]$$

$$(H-H_P)^2/(H_0-H_P)^2 = 1+[1+b\exp(-h/h_1)]^{-3}h_0/h \quad [2,3]$$

[1] Nix, Gao. *J Mech Phys Solids* (1998).
[2] Feng, Nix. *Scripta Mater* (2004).
[3] Qui, Huang, Nix, Hwang, Gao. *Acta Mater* (2001).

Indentation and hardness

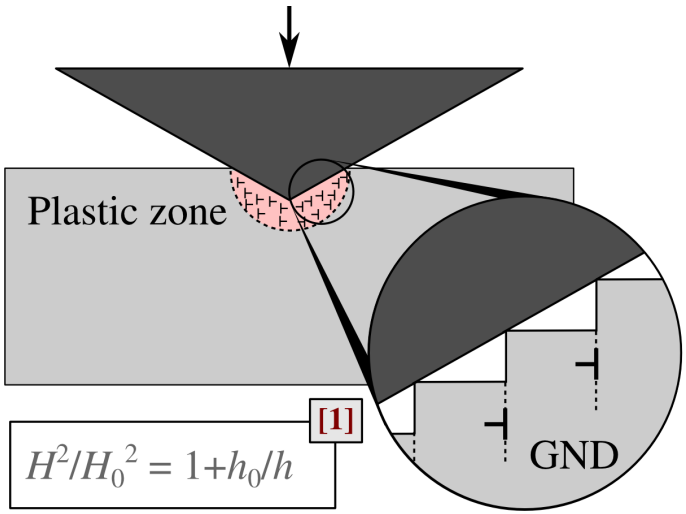

$$H^2/H_0^2 = 1+h_0/h \quad [1]$$

$$\frac{\text{Plastic zone } r}{\text{Contact radius } a} \sim 1 + b\exp(-h/h_1)$$

$$H^2/H_0^2 = 1+[1+b\exp(-h/h_1)]^{-3}h_0/h \quad [2]$$

$$(H-H_P)^2/(H_0-H_P)^2 = 1+[1+b\exp(-h/h_1)]^{-3}h_0/h \quad [2,3]$$

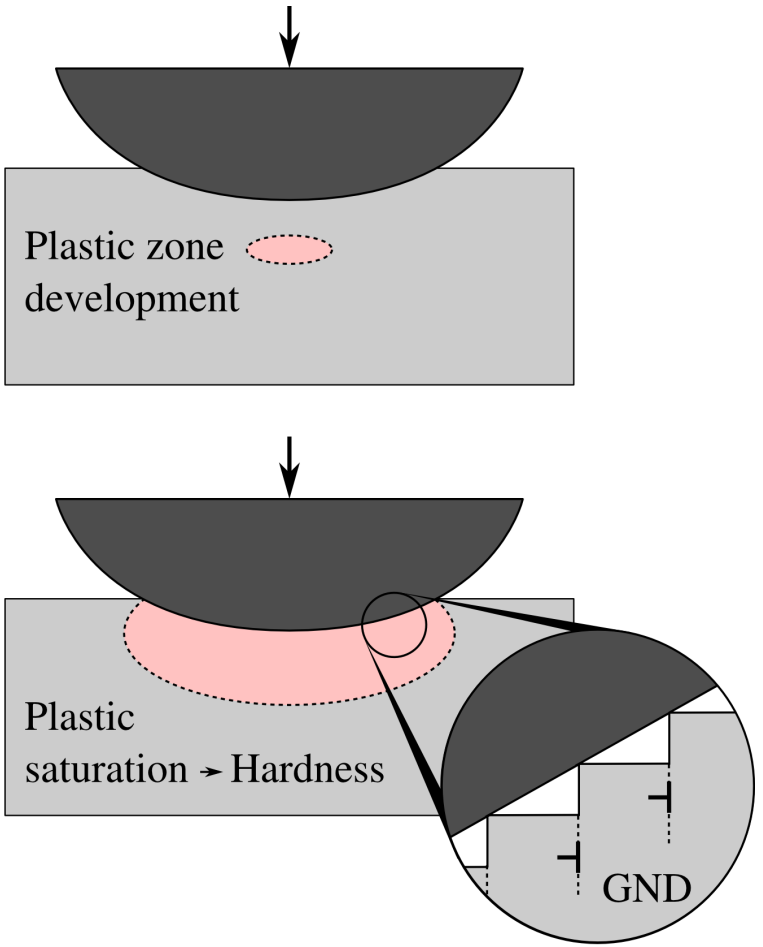

[1] Nix, Gao. *J Mech Phys Solids* (1998).
[2] Feng, Nix. *Scripta Mater* (2004).
[3] Qui, Huang, Nix, Hwang, Gao. *Acta Mater* (2001).

Indentation and hardness

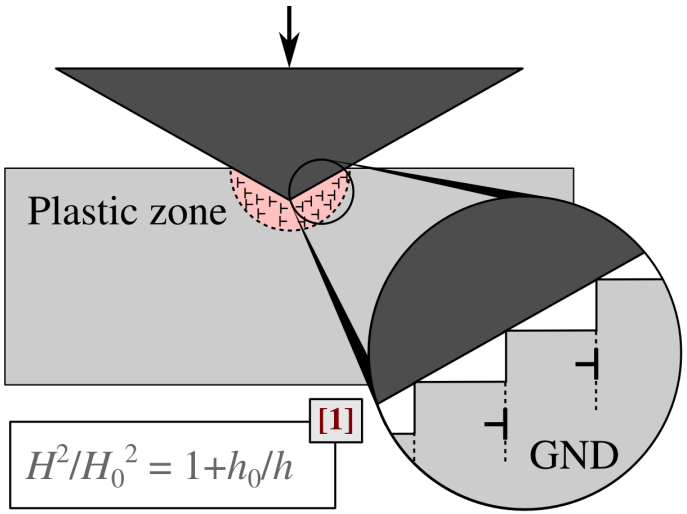

[1] $H^2/H_0^2 = 1+h_0/h$

$$\frac{\text{Plastic zone } r}{\text{Contact radius } a} \sim 1 + b\exp(-h/h_1)$$

[2] $H^2/H_0^2 = 1+[1+b\exp(-h/h_1)]^{-3}h_0/h$

[2,3] $(H-H_P)^2/(H_0-H_P)^2 = 1+[1+b\exp(-h/h_1)]^{-3}h_0/h$

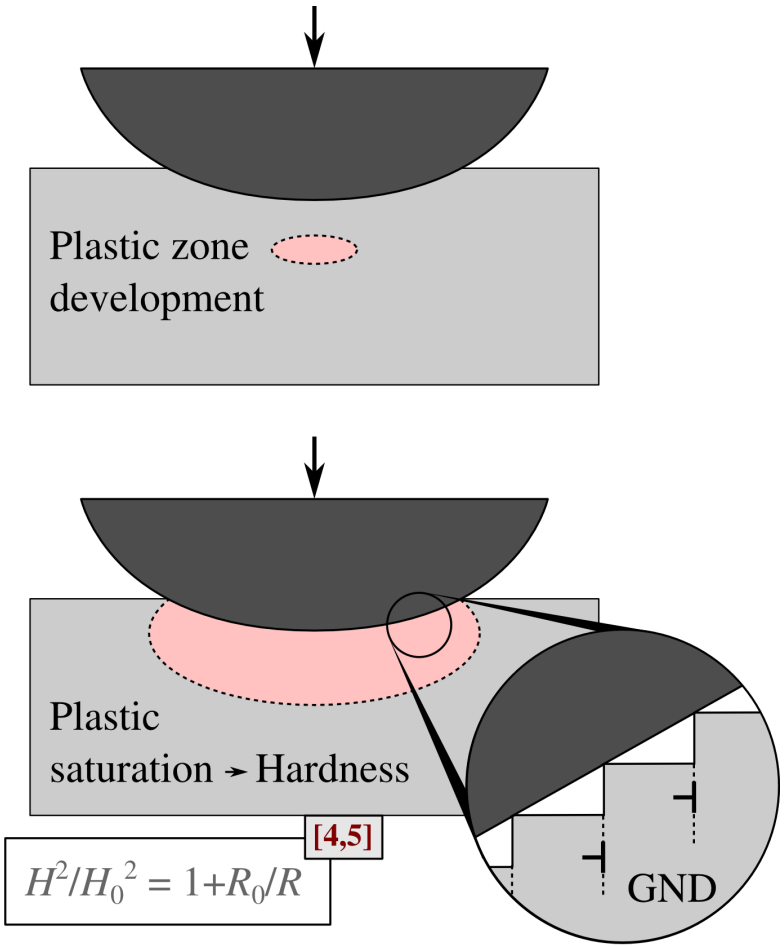

[4,5] $H^2/H_0^2 = 1+R_0/R$

[1] Nix, Gao. *J Mech Phys Solids* (1998).
[2] Feng, Nix. *Scripta Mater* (2004).
[3] Qui, Huang, Nix, Hwang, Gao. *Acta Mater* (2001).
[4] Swadener, George, Pharr. *J Mech Phys Solids* (2002).
[5] Gao, Larson, Lee, Nicola, Tischler, Pharr. *J Appl Mech* (2015).

Enhanced material behavior: beyond *J2* plasticity

- Crystal plasticity models
  in indentation all slip systems are activated
  Difference with isotropic plasticity is small
- Discrete models with inherent characteristic length
  - *Molecular Dynamics*
  -*Dislocation Dynamics*
- Continuum models with characteristic length
  - *Cosserat continuum*[1]
  - *Second-gradient plasticity*[2]

[1] Forest S., Sievert R. Elastoviscoplastic constitutive frameworks for generalized continua. Acta Mech 160 (2003)

[2] Cordero N.M., Forest S. et al. Grain size effects on plastic strain and dislocation density tensor fields in metal polycrystals, Comp Mater Sci 52 (2012)

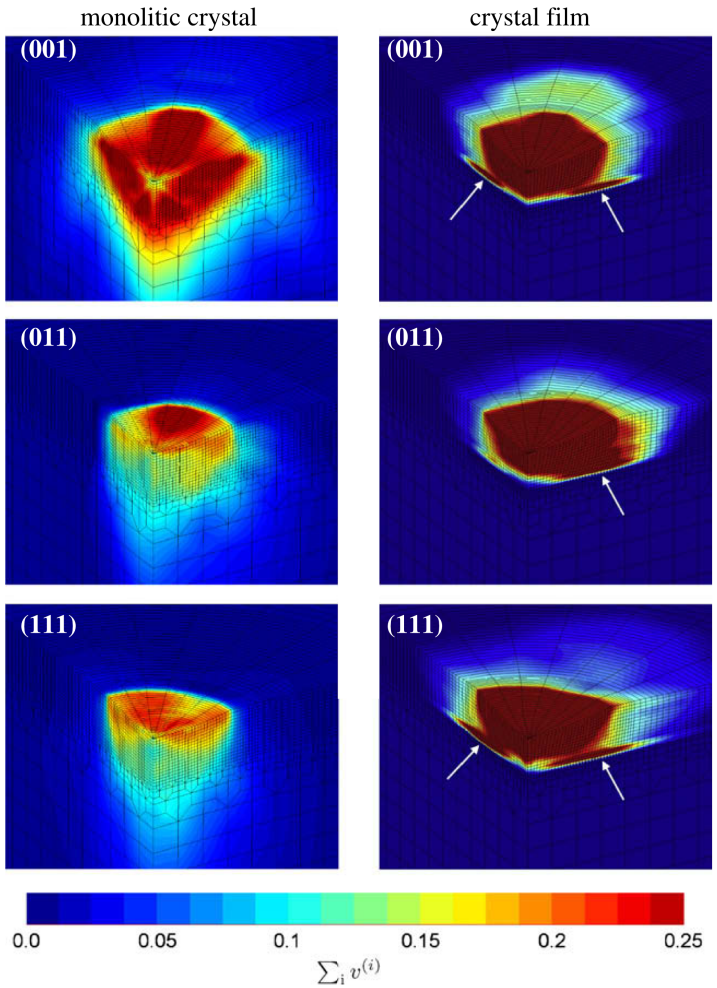

Spherical indentation of FCC copper crystal using crystal plasticity model in Zset

[3] Casals O., Forest S. Finite element crystal plasticity analysis of spherical indentation in bulk single crystals and coatings. Comp Mater Sci 45 (2009)

Enhanced material behavior: beyond *J2* plasticity

- Crystal plasticity models
  in indentation all slip systems are activated
  Difference with isotropic plasticity is small
- Discrete models with inherent characteristic length
  - *Molecular Dynamics*
  -*Dislocation Dynamics*
- Continuum models with characteristic length
  - *Cosserat continuum*[1]
  - *Second-gradient plasticity*[2]

[1] Forest S., Sievert R. Elastoviscoplastic constitutive frameworks for generalized continua. Acta Mech 160 (2003)

[2] Cordero N.M., Forest S. et al. Grain size effects on plastic strain and dislocation density tensor fields in metal polycrystals, Comp Mater Sci 52 (2012)

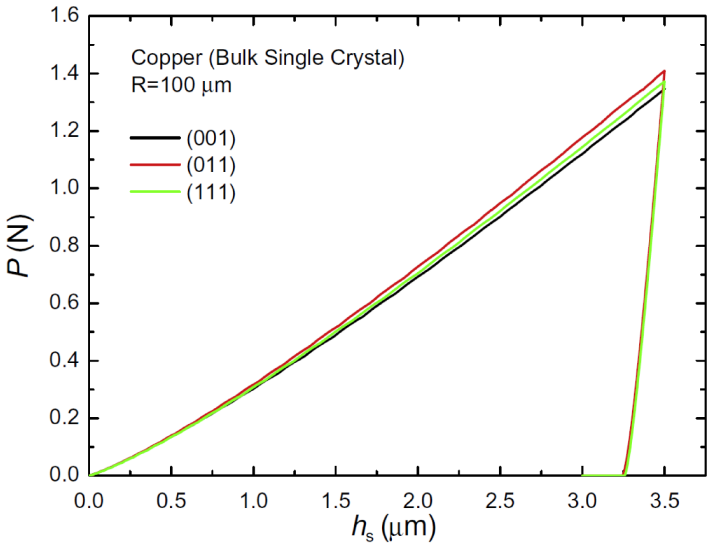

Spherical indentation of FCC copper crystal using crystal plasticity model in Zset

[3] Casals O., Forest S. Finite element crystal plasticity analysis of spherical indentation in bulk single crystals and coatings. Comp Mater Sci 45 (2009)

Enhanced material behavior: beyond *J2* plasticity

- Crystal plasticity models
  in indentation all slip systems are activated
  Difference with isotropic plasticity is small
- Discrete models with inherent characteristic length
  - *Molecular Dynamics*
  -*Dislocation Dynamics*
- Continuum models with characteristic length
  - *Cosserat continuum*[1]
  - *Second-gradient plasticity*[2]

[1] Forest S., Sievert R. Elastoviscoplastic constitutive frameworks for generalized continua. Acta Mech 160 (2003)

[2] Cordero N.M., Forest S. et al. Grain size effects on plastic strain and dislocation density tensor fields in metal polycrystals, Comp Mater Sci 52 (2012)

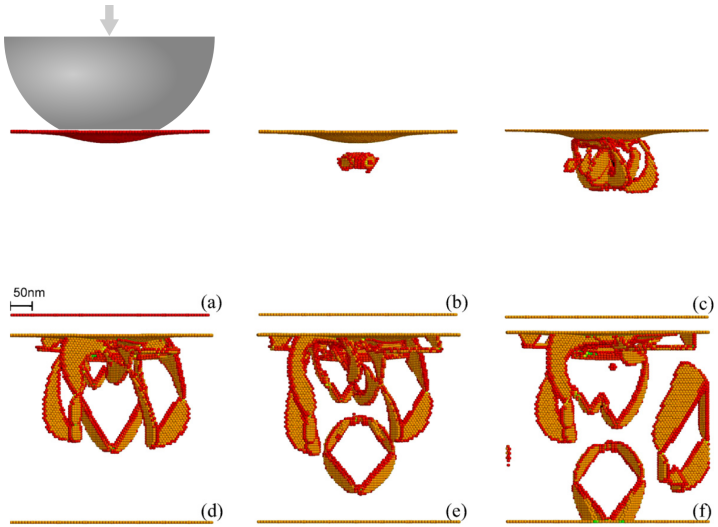

MD simulation of a spherical indentation on (111) FCC cube

[4] H.J. Chang, M. Fivel, D. Rodney, M. Verdier. Multiscale modelling of indentation in FCC metals: From atomic to continuum, CR Physique 11 (2010)

Enhanced material behavior: beyond *J2* plasticity

- Crystal plasticity models
  in indentation all slip systems are activated
  Difference with isotropic plasticity is small
- Discrete models with inherent characteristic length
  - *Molecular Dynamics*
  -*Dislocation Dynamics*
- Continuum models with characteristic length
  - *Cosserat continuum*[1]
  - *Second-gradient plasticity*[2]

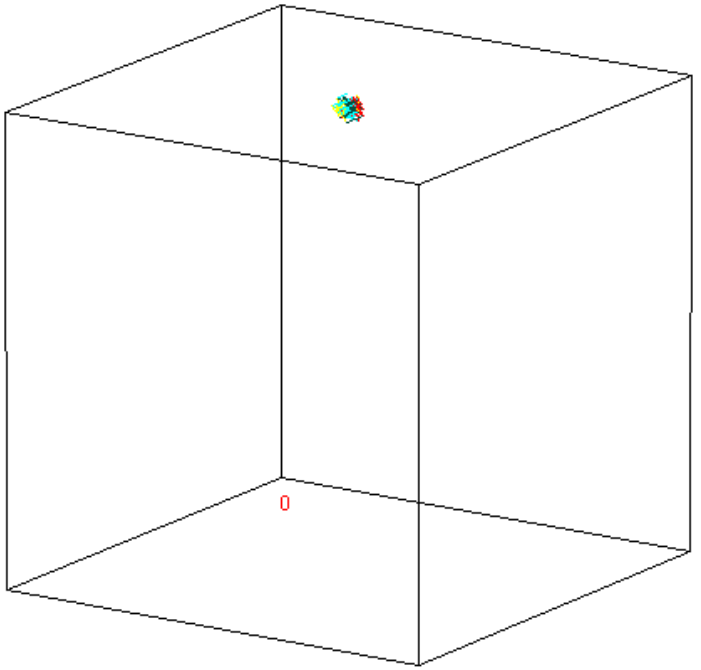

Resulting DD simulation of a spherical indentation on (111) FCC cube

[1] Forest S., Sievert R. Elastoviscoplastic constitutive frameworks for generalized continua. Acta Mech 160 (2003)

[2] Cordero N.M., Forest S. et al. Grain size effects on plastic strain and dislocation density tensor fields in metal polycrystals, Comp Mater Sci 52 (2012)

[4] H.J. Chang, M. Fivel, D. Rodney, M. Verdier. Multiscale modelling of indentation in FCC metals: From atomic to continuum, CR Physique 11 (2010)
www.numodis.com

Enhanced material behavior: beyond *J2* plasticity

- Crystal plasticity models
  in indentation all slip systems are activated
  Difference with isotropic plasticity is small
- Discrete models with inherent characteristic length
  - *Molecular Dynamics*
  -*Dislocation Dynamics*
- Continuum models with characteristic length
  - *Cosserat continuum*[1]
  - *Second-gradient plasticity*[2]

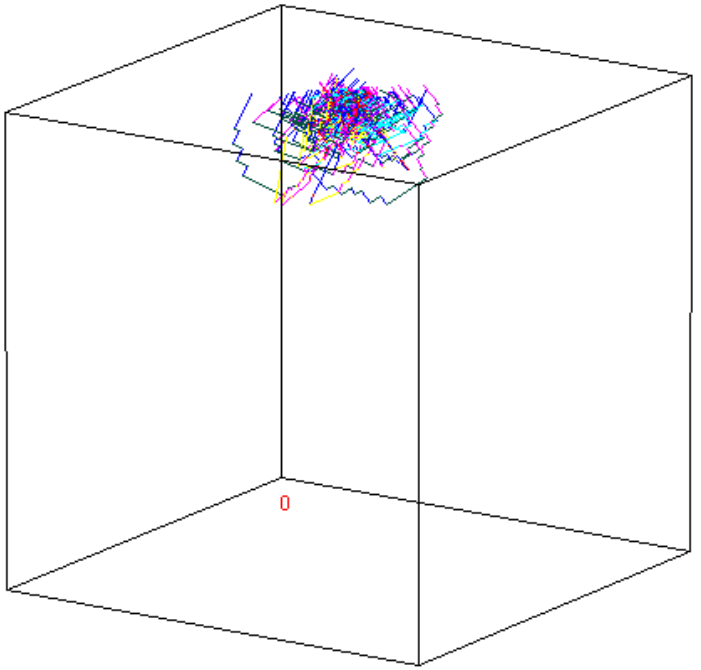

Resulting DD simulation of a spherical indentation on (111) FCC cube

[4] H.J. Chang, M. Fivel, D. Rodney, M. Verdier. Multiscale modelling of indentation in FCC metals: From atomic to continuum, CR Physique 11 (2010)
www.numodis.com

[1] Forest S., Sievert R. Elastoviscoplastic constitutive frameworks for generalized continua. Acta Mech 160 (2003)

[2] Cordero N.M., Forest S. et al. Grain size effects on plastic strain and dislocation density tensor fields in metal polycrystals, Comp Mater Sci 52 (2012)

Enhanced material behavior: beyond *J2* plasticity

- Crystal plasticity models
  in indentation all slip systems are activated
  Difference with isotropic plasticity is small
- Discrete models with inherent characteristic length
  - *Molecular Dynamics*
  -*Dislocation Dynamics*
- Continuum models with characteristic length
  - *Cosserat continuum*[1]
  - *Second-gradient plasticity*[2]

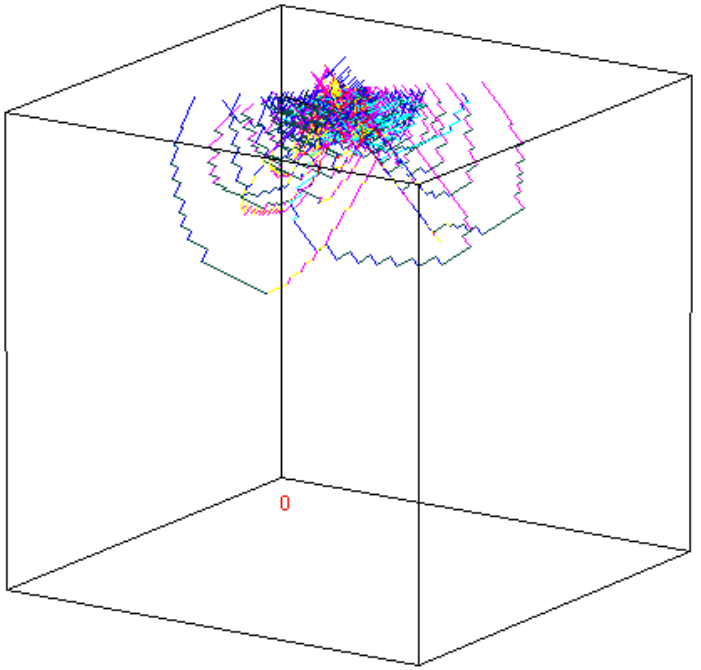

Resulting DD simulation of a spherical indentation on (111) FCC cube

[4] H.J. Chang, M. Fivel, D. Rodney, M. Verdier. Multiscale modelling of indentation in FCC metals: From atomic to continuum, CR Physique 11 (2010)
www.numodis.com

[1] Forest S., Sievert R. Elastoviscoplastic constitutive frameworks for generalized continua. Acta Mech 160 (2003)

[2] Cordero N.M., Forest S. et al. Grain size effects on plastic strain and dislocation density tensor fields in metal polycrystals, Comp Mater Sci 52 (2012)

Enhanced material behavior: beyond *J2* plasticity

- Crystal plasticity models
  in indentation all slip systems are activated
  Difference with isotropic plasticity is small
- Discrete models with inherent characteristic length
  - *Molecular Dynamics*
  -*Dislocation Dynamics*
- Continuum models with characteristic length
  - *Cosserat continuum*[1]
  - *Second-gradient plasticity*[2]

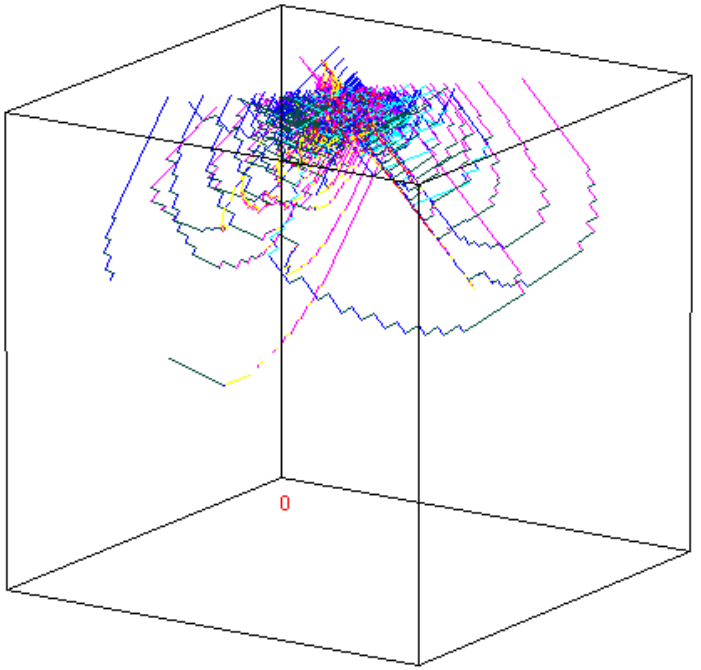

Resulting DD simulation of a spherical indentation on (111) FCC cube

[4] H.J. Chang, M. Fivel, D. Rodney, M. Verdier. Multiscale modelling of indentation in FCC metals: From atomic to continuum, CR Physique 11 (2010)
www.numodis.com

[1] Forest S., Sievert R. Elastoviscoplastic constitutive frameworks for generalized continua. Acta Mech 160 (2003)

[2] Cordero N.M., Forest S. et al. Grain size effects on plastic strain and dislocation density tensor fields in metal polycrystals, Comp Mater Sci 52 (2012)

Enhanced material behavior: beyond *J2* plasticity

- Crystal plasticity models
  in indentation all slip systems are activated
  Difference with isotropic plasticity is small
- Discrete models with inherent characteristic length
  - *Molecular Dynamics*
  -*Dislocation Dynamics*
- Continuum models with characteristic length
  - *Cosserat continuum*[1]
  - *Second-gradient plasticity*[2]

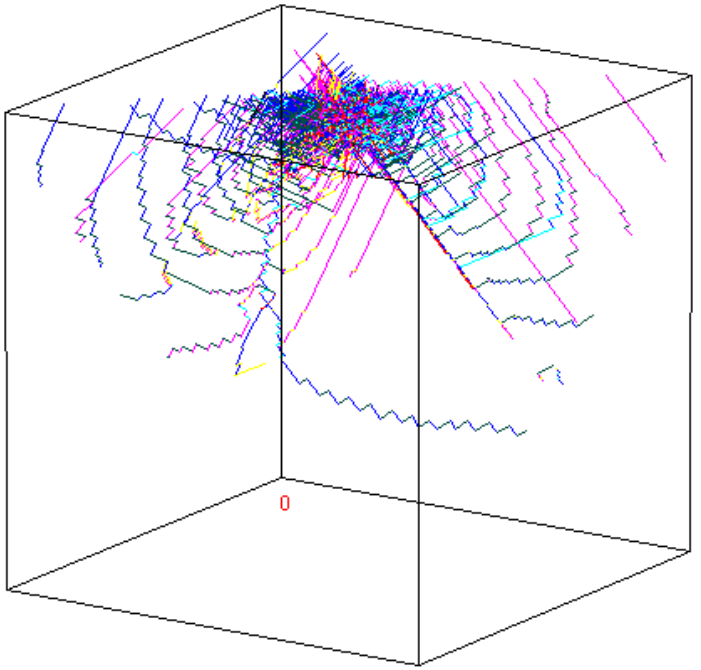

Resulting DD simulation of a spherical indentation on (111) FCC cube

[4] H.J. Chang, M. Fivel, D. Rodney, M. Verdier. Multiscale modelling of indentation in FCC metals: From atomic to continuum, CR Physique 11 (2010)
www.numodis.com

[1] Forest S., Sievert R. Elastoviscoplastic constitutive frameworks for generalized continua. Acta Mech 160 (2003)

[2] Cordero N.M., Forest S. et al. Grain size effects on plastic strain and dislocation density tensor fields in metal polycrystals, Comp Mater Sci 52 (2012)

Enhanced material behavior: beyond *J2* plasticity

- Crystal plasticity models
  in indentation all slip systems are activated
  Difference with isotropic plasticity is small
- Discrete models with inherent characteristic length
  - *Molecular Dynamics*
  -*Dislocation Dynamics*
- Continuum models with characteristic length
  - *Cosserat continuum*[1]
  - *Second-gradient plasticity*[2]

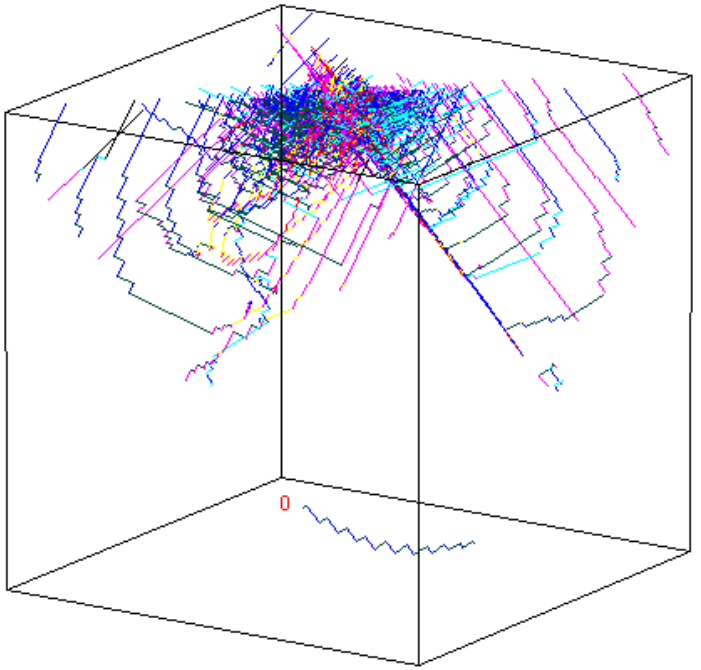

Resulting DD simulation of a spherical indentation on (111) FCC cube

[4] H.J. Chang, M. Fivel, D. Rodney, M. Verdier. Multiscale modelling of indentation in FCC metals: From atomic to continuum, CR Physique 11 (2010)
www.numodis.com

[1] Forest S., Sievert R. Elastoviscoplastic constitutive frameworks for generalized continua. Acta Mech 160 (2003)

[2] Cordero N.M., Forest S. et al. Grain size effects on plastic strain and dislocation density tensor fields in metal polycrystals, Comp Mater Sci 52 (2012)

Enhanced material behavior: beyond *J2* plasticity

- Crystal plasticity models
  in indentation all slip systems are activated
  Difference with isotropic plasticity is small
- Discrete models with inherent characteristic length
  - *Molecular Dynamics*
  -*Dislocation Dynamics*
- Continuum models with characteristic length
  - *Cosserat continuum*[1]
  - *Second-gradient plasticity*[2]

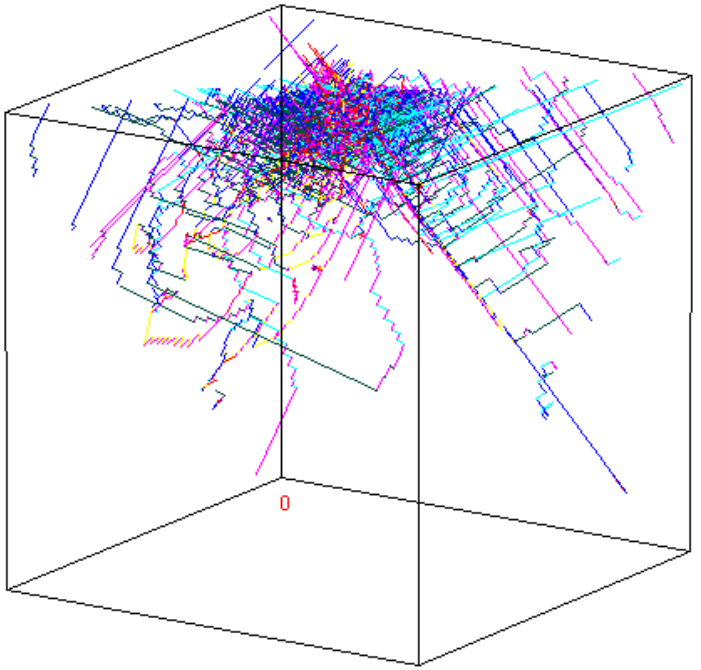

Resulting DD simulation of a spherical indentation on (111) FCC cube

[4] H.J. Chang, M. Fivel, D. Rodney, M. Verdier. Multiscale modelling of indentation in FCC metals: From atomic to continuum, CR Physique 11 (2010)
www.numodis.com

[1] Forest S., Sievert R. Elastoviscoplastic constitutive frameworks for generalized continua. Acta Mech 160 (2003)

[2] Cordero N.M., Forest S. et al. Grain size effects on plastic strain and dislocation density tensor fields in metal polycrystals, Comp Mater Sci 52 (2012)

Enhanced material behavior: beyond *J2* plasticity

- Crystal plasticity models
  in indentation all slip systems are activated
  Difference with isotropic plasticity is small
- Discrete models with inherent characteristic length
  - *Molecular Dynamics*
  -*Dislocation Dynamics*
- Continuum models with characteristic length
  - *Cosserat continuum*[1]
  - *Second-gradient plasticity*[2]

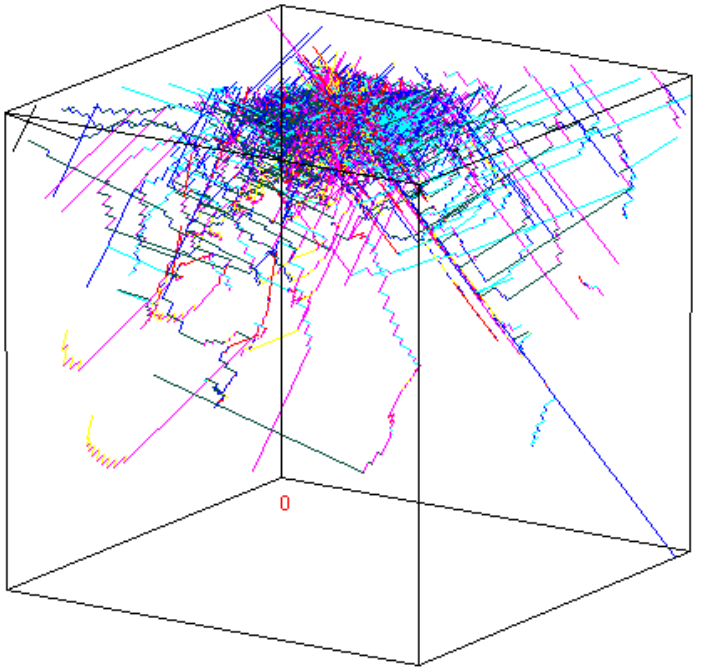

Resulting DD simulation of a spherical indentation on (111) FCC cube

[4] H.J. Chang, M. Fivel, D. Rodney, M. Verdier. Multiscale modelling of indentation in FCC metals: From atomic to continuum, CR Physique 11 (2010)
www.numodis.com

[1] Forest S., Sievert R. Elastoviscoplastic constitutive frameworks for generalized continua. Acta Mech 160 (2003)

[2] Cordero N.M., Forest S. et al. Grain size effects on plastic strain and dislocation density tensor fields in metal polycrystals, Comp Mater Sci 52 (2012)

Enhanced material behavior: beyond *J2* plasticity

- Crystal plasticity models
  in indentation all slip systems are activated
  Difference with isotropic plasticity is small
- Discrete models with inherent characteristic length
  - *Molecular Dynamics*
  -*Dislocation Dynamics*
- Continuum models with characteristic length
  - *Cosserat continuum*[1]
  - *Second-gradient plasticity*[2]

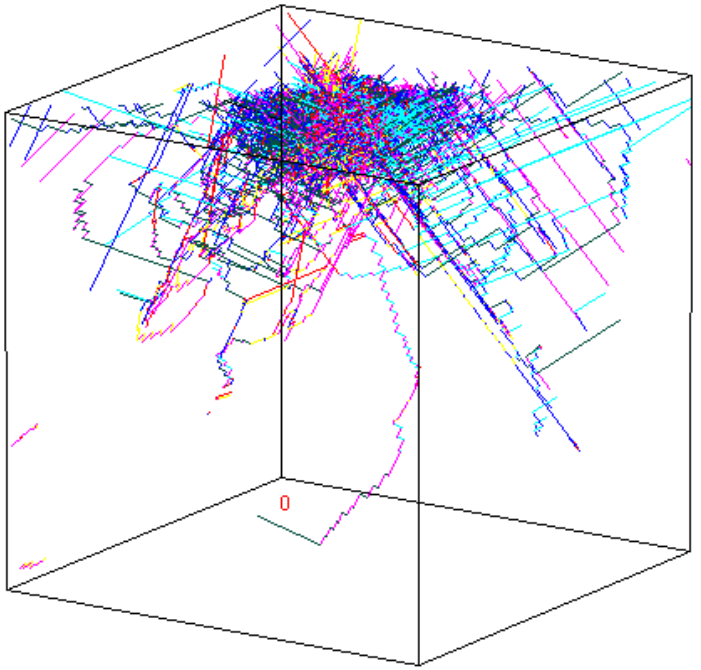

Resulting DD simulation of a spherical indentation on (111) FCC cube

[4] H.J. Chang, M. Fivel, D. Rodney, M. Verdier. Multiscale modelling of indentation in FCC metals: From atomic to continuum, CR Physique 11 (2010)
www.numodis.com

[1] Forest S., Sievert R. Elastoviscoplastic constitutive frameworks for generalized continua. Acta Mech 160 (2003)

[2] Cordero N.M., Forest S. et al. Grain size effects on plastic strain and dislocation density tensor fields in metal polycrystals, Comp Mater Sci 52 (2012)

Enhanced material behavior: beyond *J2* plasticity

- Crystal plasticity models
  in indentation all slip systems are activated
  Difference with isotropic plasticity is small
- Discrete models with inherent characteristic length
  - *Molecular Dynamics*
  -*Dislocation Dynamics*
- Continuum models with characteristic length
  - *Cosserat continuum*[1]
  - *Second-gradient plasticity*[2]

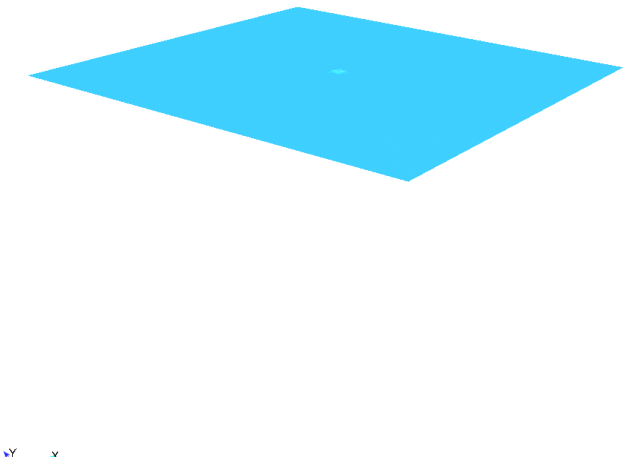

DD simulation of Berkovich nanoindentation

www.numodis.com

[1] Forest S., Sievert R. Elastoviscoplastic constitutive frameworks for generalized continua. Acta Mech 160 (2003)

[2] Cordero N.M., Forest S. et al. Grain size effects on plastic strain and dislocation density tensor fields in metal polycrystals, Comp Mater Sci 52 (2012)

Enhanced material behavior: beyond *J2* plasticity

- Crystal plasticity models
  in indentation all slip systems are activated
  Difference with isotropic plasticity is small
- Discrete models with inherent characteristic length
  - *Molecular Dynamics*
  -*Dislocation Dynamics*
- Continuum models with characteristic length
  - *Cosserat continuum*[1]
  - *Second-gradient plasticity*[2]

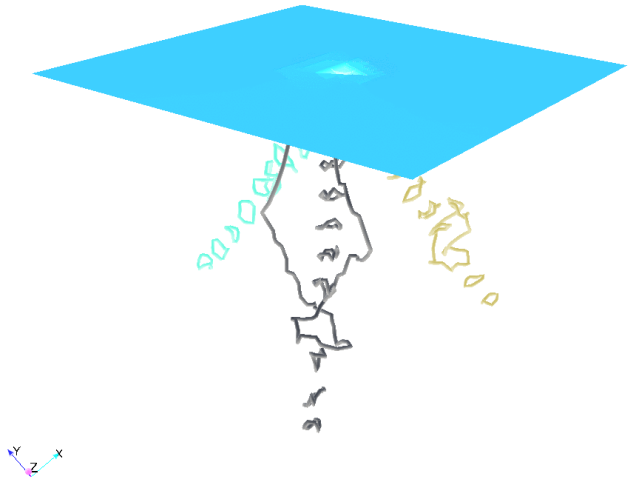

DD simulation of Berkovich nanoindentation

www.numodis.com

[1] Forest S., Sievert R. Elastoviscoplastic constitutive frameworks for generalized continua. Acta Mech 160 (2003)

[2] Cordero N.M., Forest S. et al. Grain size effects on plastic strain and dislocation density tensor fields in metal polycrystals, Comp Mater Sci 52 (2012)

Enhanced material behavior: beyond *J2* plasticity

- Crystal plasticity models
  in indentation all slip systems are activated
  Difference with isotropic plasticity is small
- Discrete models with inherent characteristic length
  - *Molecular Dynamics*
  -*Dislocation Dynamics*
- Continuum models with characteristic length
  - *Cosserat continuum*[1]
  - *Second-gradient plasticity*[2]

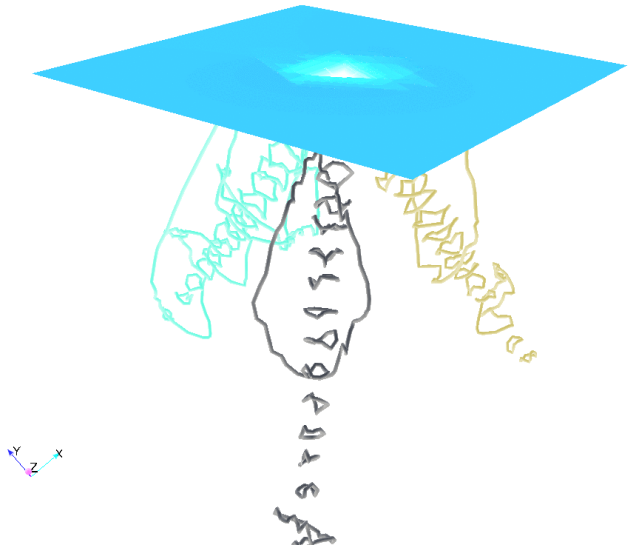

DD simulation of Berkovich nanoindentation

www.numodis.com

[1] Forest S., Sievert R. Elastoviscoplastic constitutive frameworks for generalized continua. Acta Mech 160 (2003)

[2] Cordero N.M., Forest S. et al. Grain size effects on plastic strain and dislocation density tensor fields in metal polycrystals, Comp Mater Sci 52 (2012)

Enhanced material behavior: beyond *J2* plasticity

- Crystal plasticity models
  in indentation all slip systems are activated
  Difference with isotropic plasticity is small
- Discrete models with inherent characteristic length
  - *Molecular Dynamics*
  -*Dislocation Dynamics*
- Continuum models with characteristic length
  - *Cosserat continuum*[1]
  - *Second-gradient plasticity*[2]

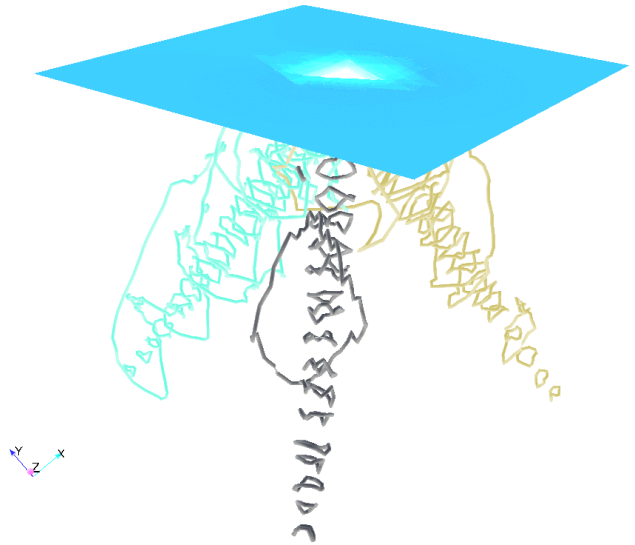

DD simulation of Berkovich nanoindentation

www.numodis.com

[1] Forest S., Sievert R. Elastoviscoplastic constitutive frameworks for generalized continua. Acta Mech 160 (2003)

[2] Cordero N.M., Forest S. et al. Grain size effects on plastic strain and dislocation density tensor fields in metal polycrystals, Comp Mater Sci 52 (2012)

Enhanced material behavior: beyond *J2* plasticity

- Crystal plasticity models
  in indentation all slip systems are activated
  Difference with isotropic plasticity is small
- Discrete models with inherent characteristic length
  - *Molecular Dynamics*
  -*Dislocation Dynamics*
- Continuum models with characteristic length
  - *Cosserat continuum*[1]
  - *Second-gradient plasticity*[2]

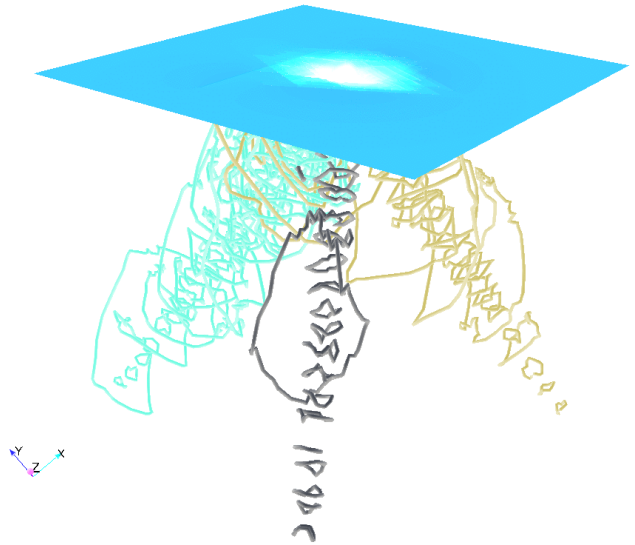

DD simulation of Berkovich nanoindentation

www.numodis.com

[1] Forest S., Sievert R. Elastoviscoplastic constitutive frameworks for generalized continua. Acta Mech 160 (2003)

[2] Cordero N.M., Forest S. et al. Grain size effects on plastic strain and dislocation density tensor fields in metal polycrystals, Comp Mater Sci 52 (2012)

Enhanced material behavior: beyond *J2* plasticity

- Crystal plasticity models
  in indentation all slip systems are activated
  Difference with isotropic plasticity is small
- Discrete models with inherent characteristic length
  - *Molecular Dynamics*
  -*Dislocation Dynamics*
- Continuum models with characteristic length
  - *Cosserat continuum*[1]
  - *Second-gradient plasticity*[2]

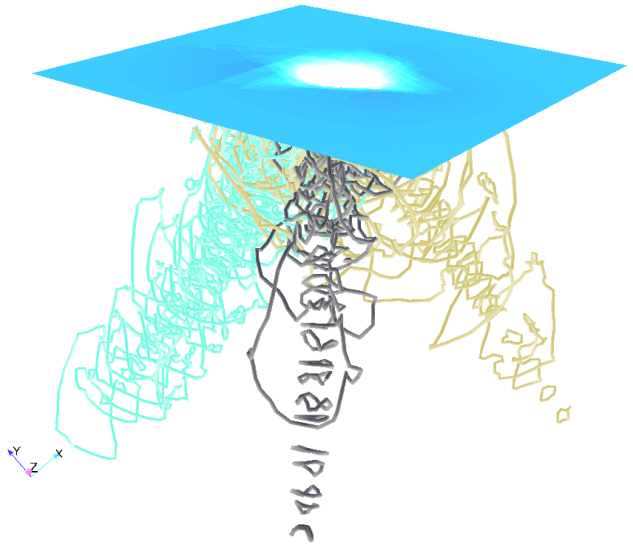

DD simulation of Berkovich nanoindentation

www.numodis.com

[1] Forest S., Sievert R. Elastoviscoplastic constitutive frameworks for generalized continua. Acta Mech 160 (2003)

[2] Cordero N.M., Forest S. et al. Grain size effects on plastic strain and dislocation density tensor fields in metal polycrystals, Comp Mater Sci 52 (2012)

Enhanced material behavior: beyond *J2* plasticity

- Crystal plasticity models
  in indentation all slip systems are activated
  Difference with isotropic plasticity is small
- Discrete models with inherent characteristic length
  - *Molecular Dynamics*
  -*Dislocation Dynamics*
- Continuum models with characteristic length
  - *Cosserat continuum*[1]
  - *Second-gradient plasticity*[2]

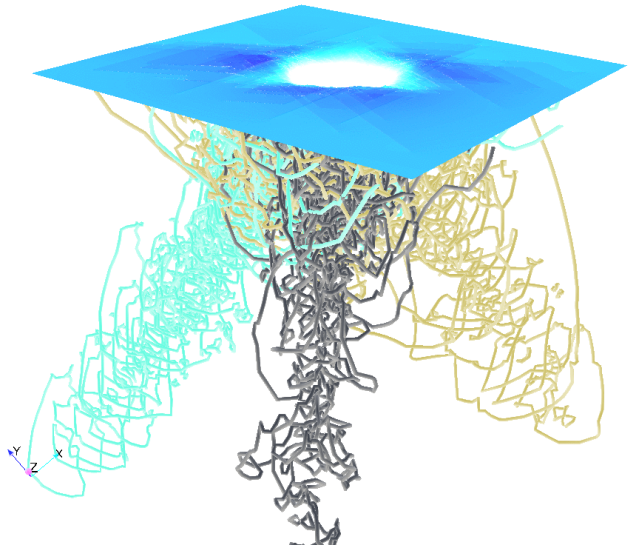

DD simulation of Berkovich nanoindentation

www.numodis.com

[1] Forest S., Sievert R. Elastoviscoplastic constitutive frameworks for generalized continua. Acta Mech 160 (2003)

[2] Cordero N.M., Forest S. et al. Grain size effects on plastic strain and dislocation density tensor fields in metal polycrystals, Comp Mater Sci 52 (2012)

Enhanced material behavior: beyond *J2* plasticity

- Crystal plasticity models
  in indentation all slip systems are activated
  Difference with isotropic plasticity is small
- Discrete models with inherent characteristic length
  - *Molecular Dynamics*
  -*Dislocation Dynamics*
- Continuum models with characteristic length
  - *Cosserat continuum*[1]
  - *Second-gradient plasticity*[2]

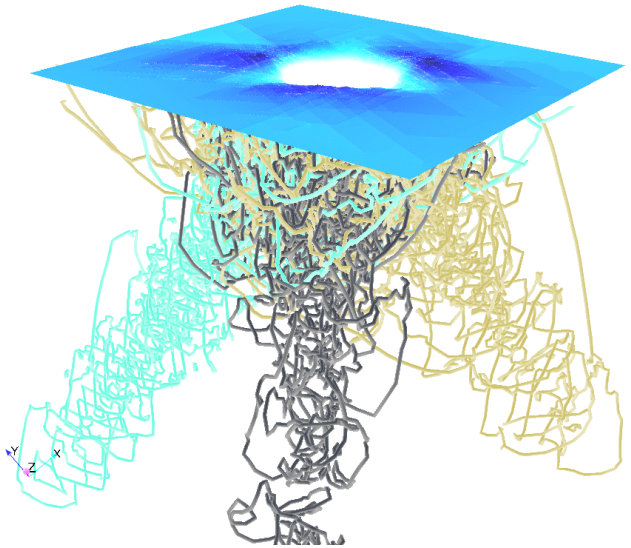

DD simulation of Berkovich nanoindentation

www.numodis.com

[1] Forest S., Sievert R. Elastoviscoplastic constitutive frameworks for generalized continua. Acta Mech 160 (2003)

[2] Cordero N.M., Forest S. et al. Grain size effects on plastic strain and dislocation density tensor fields in metal polycrystals, Comp Mater Sci 52 (2012)

Enhanced material behavior: beyond *J2* plasticity

- Crystal plasticity models
  in indentation all slip systems are activated
  Difference with isotropic plasticity is small
- Discrete models with inherent characteristic length
  - *Molecular Dynamics*
  -*Dislocation Dynamics*
- Continuum models with characteristic length
  - *Cosserat continuum*[1]
  - *Second-gradient plasticity*[2]

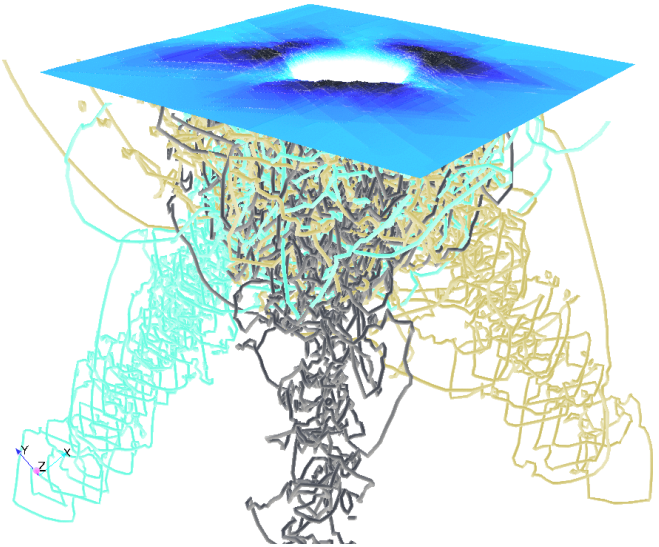

DD simulation of Berkovich nanoindentation

www.numodis.com

[1] Forest S., Sievert R. Elastoviscoplastic constitutive frameworks for generalized continua. Acta Mech 160 (2003)

[2] Cordero N.M., Forest S. et al. Grain size effects on plastic strain and dislocation density tensor fields in metal polycrystals, Comp Mater Sci 52 (2012)

Cosserat continuum

- Field variables (displacement & rotation): $\underline{u}, \underline{\omega}$
- Small deformation tensor: $\underline{\underline{\varepsilon}} = \nabla \underline{u} + {}^3\underline{\epsilon} \cdot \underline{\omega}$
- Torsion-curvature tensor: $\underline{\kappa} = \nabla \underline{\omega}$
- Elasticity: $\underline{\sigma} = \lambda \mathrm{tr}\left(\underline{\underline{\varepsilon}}_e\right) \underline{\underline{I}} + \mu(\underline{\underline{\varepsilon}}_e + \underline{\underline{\varepsilon}}_e^\top) + \mu_c(\underline{\underline{\varepsilon}}_e - \underline{\underline{\varepsilon}}_e^\top), \quad \underline{m} = \alpha \mathrm{tr}\left(\underline{\kappa}_e\right) \underline{\underline{I}} + 2\beta \underline{\kappa}_e$

  $$\boxed{l_e = \sqrt{\beta/\mu}}$$

  Note: $\underline{\underline{\varepsilon}}^\top \neq \underline{\underline{\varepsilon}}, \underline{\kappa}^\top \neq \underline{\kappa}, \underline{\sigma}^\top \neq \underline{\sigma}, \underline{m}^\top \neq \underline{m}$
- In non-inertial problems without volume forces and couple-forces, balance of momentum and of moment of momentum:

  $$\nabla \cdot \underline{\sigma} = 0, \quad \nabla \cdot \underline{m} - {}^3\underline{\epsilon} : \underline{\sigma} = 0$$
- Plasticity: equivalent stress[1,2] $Y = \sqrt{\frac{3}{2}\left(a_1 \underline{s} : \underline{s} + a_2 \underline{s} : \underline{s}^\top + \boxed{\frac{1}{l_p^2}} \underline{m} : \underline{m}\right)}$
- Internal lengths: elastic l_e, plastic l_p

[1] R. de Borst, L.J. Sluys, *Comp Meth Appl Mech Engin* (1991)
[2] S. Forest, R. Sievert, *Acta Mech* (2003)

---

where permutation tensor ${}^3\underline{\epsilon} \sim \epsilon_{ijk} = \begin{cases} 1, & \text{if } \{ijk\} = \{123\} \text{ or } \{231\} \text{ or } \{312\} \\ -1, & \text{if } \{ijk\} = \{321\} \text{ or } \{213\} \text{ or } \{132\} \\ 0, & \text{otherwise} \end{cases}$

Single asperity analysis

Assumptions

- Rigid spherical asperity
- Axisymmetric FE problem
- Generalized Cosserat continuum

Parameters

- Au: $E = 96$ GPa, $\nu = 0.42$, $\sigma_y = 140$ MPa
- $\mu_c = 10\mu, l_e = 100$ nm, $a_1 = 1$
- Indenter radius $R \in [0.002, 2000]$ μm

Objectives

- Study size effect
- Enhance asperity based models for rough contact

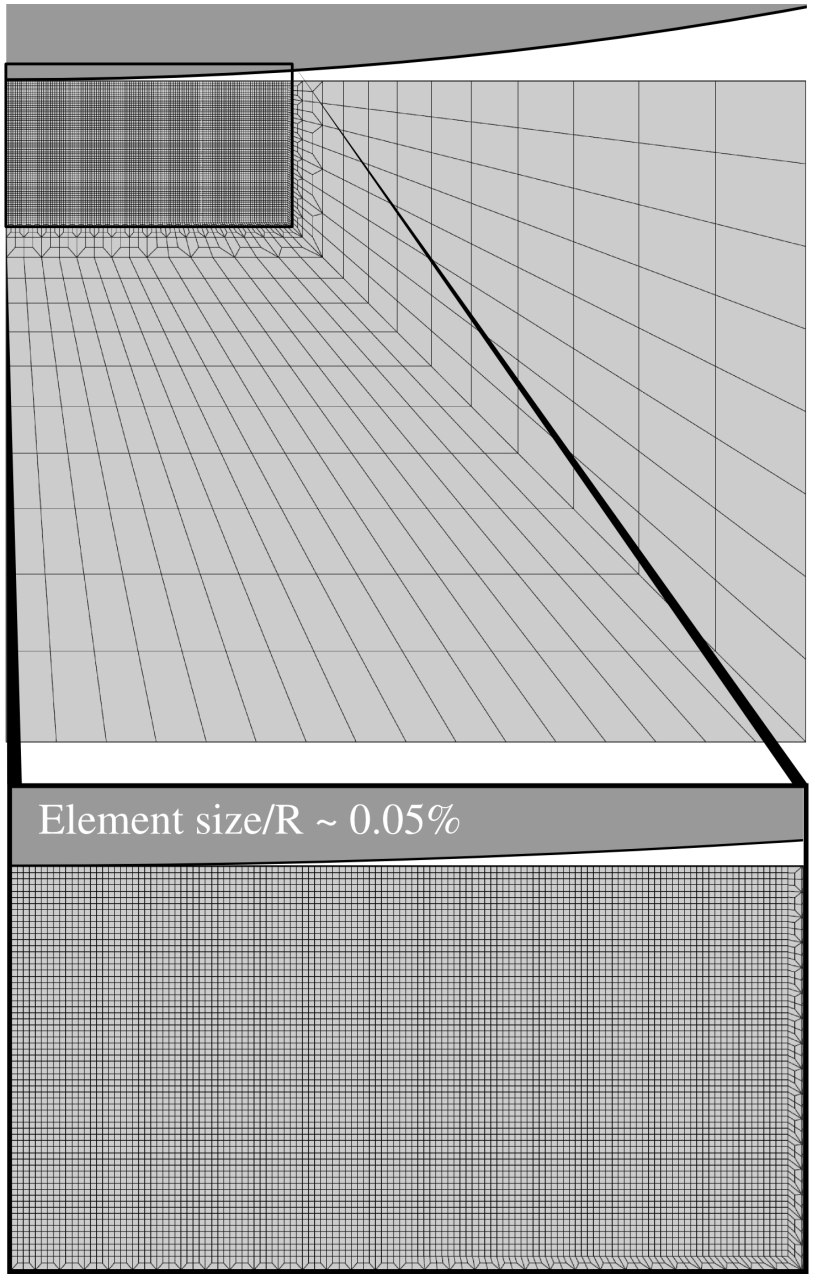

Accumulated plasticity

- Different plastic distribution

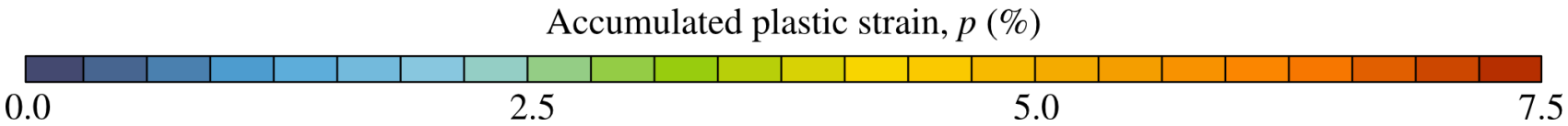

Displacement × 5

Indenter radius $R = 20\mu$m
Max plastic strain $p_{\max} \approx 7.5\%$

Displacement × 5

Indenter radius $R = 2\mu$m
Max plastic strain $p_{\max} \approx 11\%$

Accumulated plasticity

- Different plastic distribution

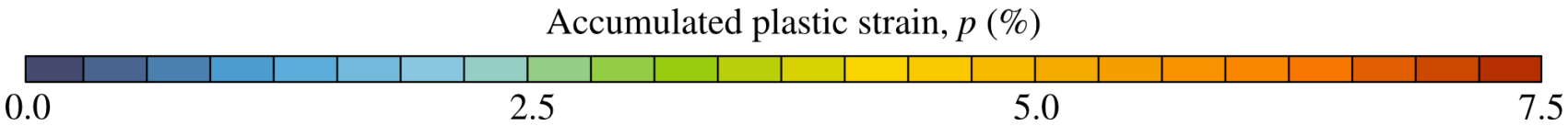

Displacement × 5

Indenter radius $R = 20\mu$m
Max plastic strain $p_{\max} \approx 7.5\%$

Displacement × 5

Indenter radius $R = 2\mu$m
Max plastic strain $p_{\max} \approx 11\%$

Accumulated plasticity

- Different plastic distribution

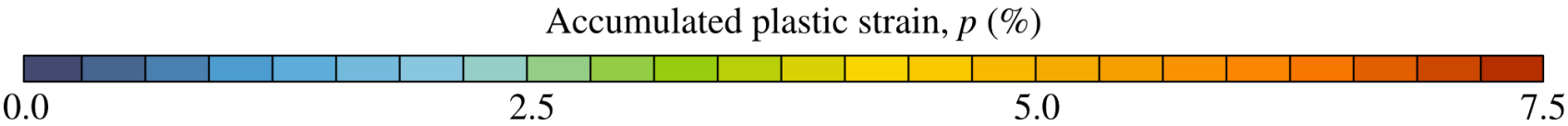

Displacement × 5

Indenter radius $R = 20\mu$m
Max plastic strain $p_{\max} \approx 7.5\%$

Displacement × 5

Indenter radius $R = 2\mu$m
Max plastic strain $p_{\max} \approx 11\%$

Accumulated plasticity

- Different plastic distribution

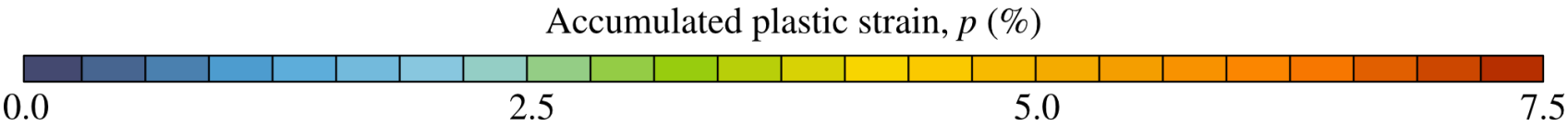

Displacement × 5

Indenter radius $R = 20\mu$m
Max plastic strain $p_{\max} \approx 7.5\%$

Displacement × 5

Indenter radius $R = 2\mu$m
Max plastic strain $p_{\max} \approx 11\%$

Accumulated plasticity

- Different plastic distribution

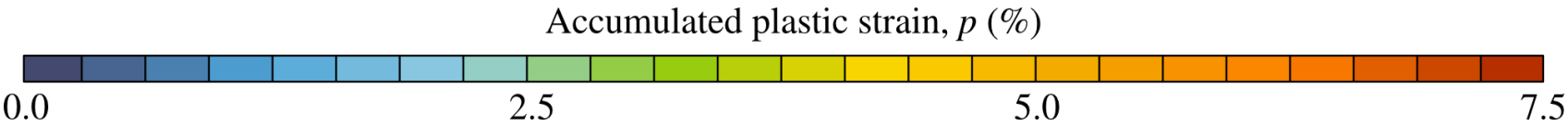

Displacement × 5

Indenter radius $R = 20\mu$m
Max plastic strain $p_{\max} \approx 7.5\%$

Displacement × 5

Indenter radius $R = 2\mu$m
Max plastic strain $p_{\max} \approx 11\%$

Accumulated plasticity

- Different plastic distribution

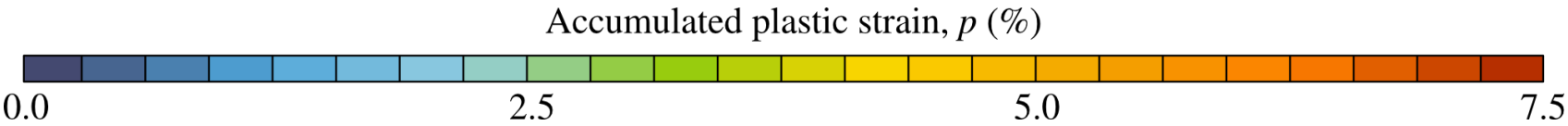

Displacement × 5

Indenter radius $R = 20\mu$m
Max plastic strain $p_{\max} \approx 7.5\%$

Displacement × 5

Indenter radius $R = 2\mu$m
Max plastic strain $p_{\max} \approx 11\%$

Accumulated plasticity

- Different plastic distribution

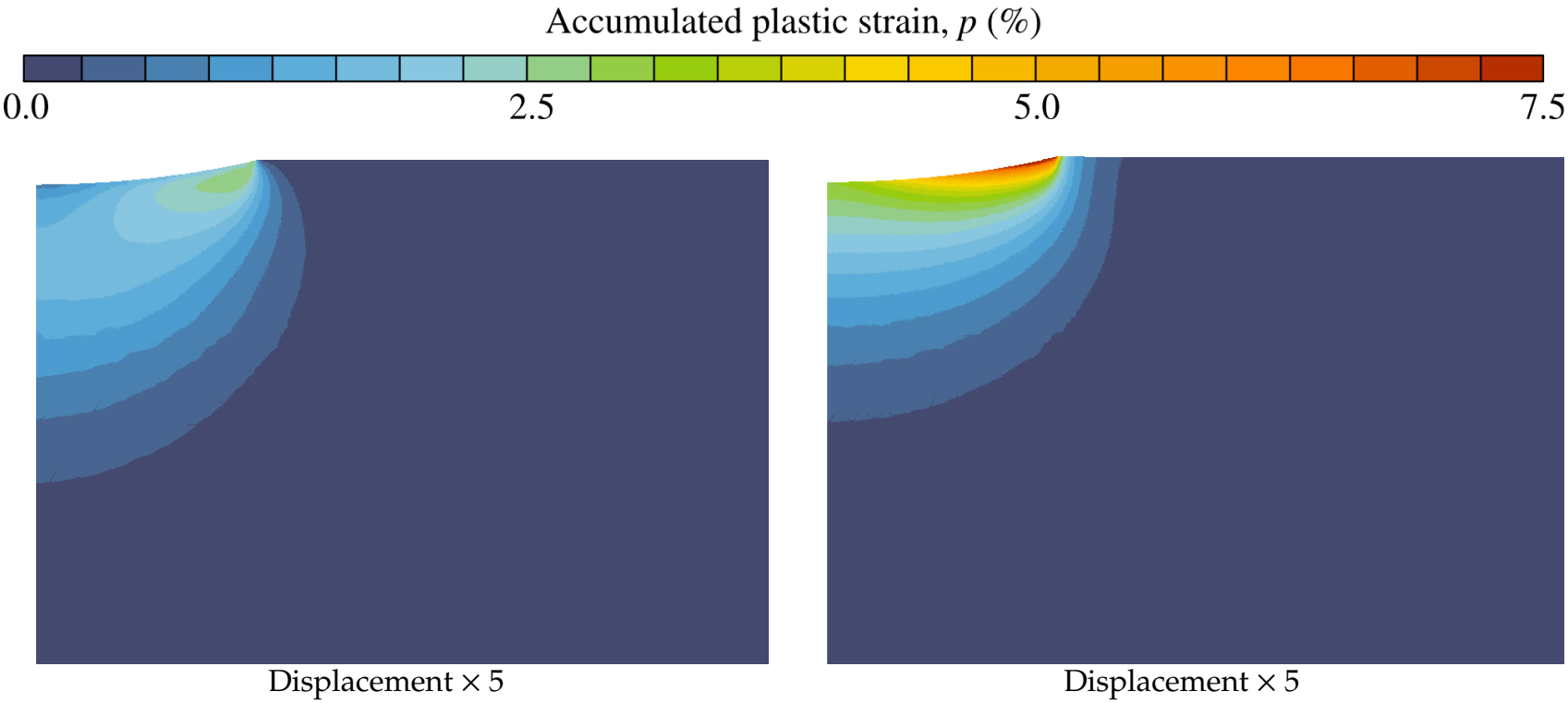

Indenter radius $R = 20\mu$m
Max plastic strain $p_{\max} \approx 7.5\%$

Indenter radius $R = 2\mu$m
Max plastic strain $p_{\max} \approx 11\%$

Accumulated plasticity

- Different plastic distribution

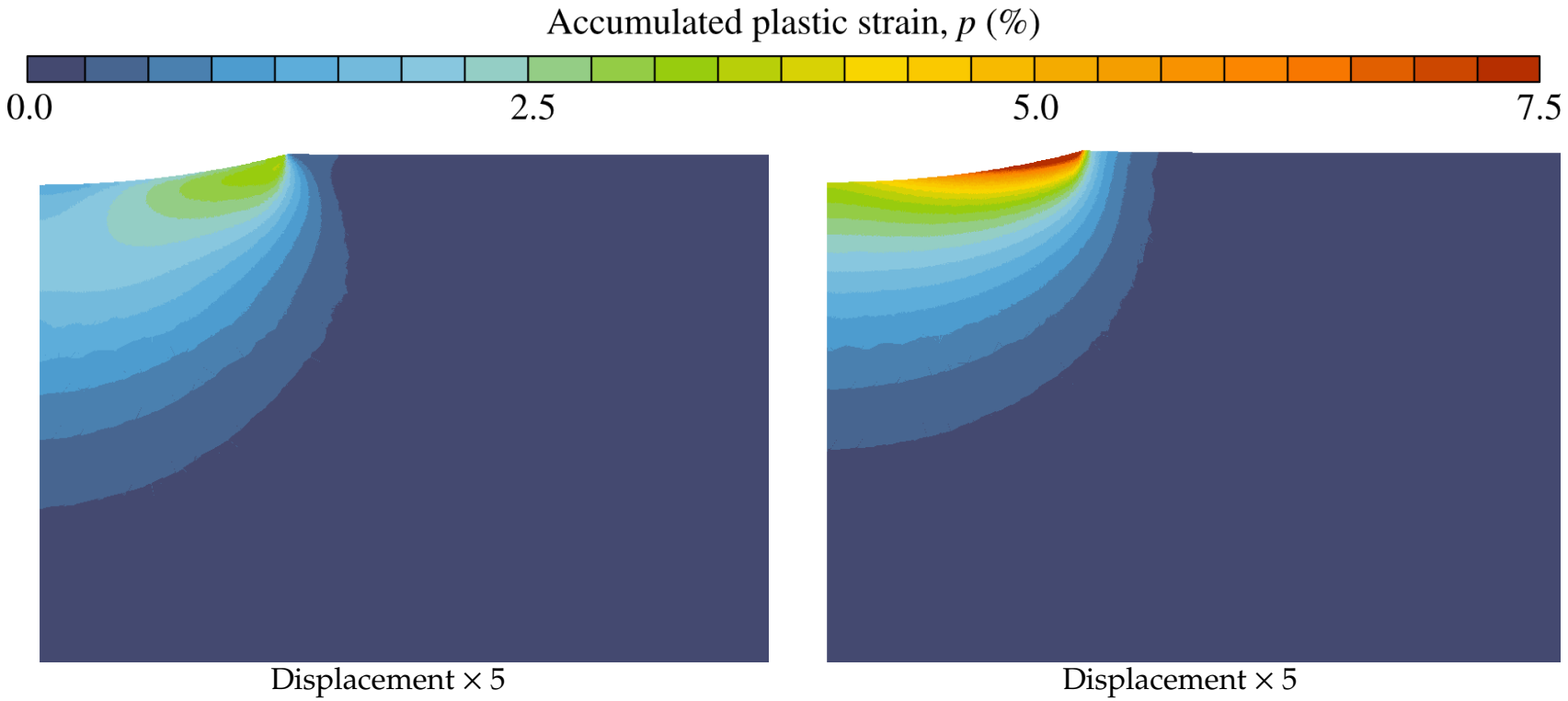

Indenter radius $R = 20\mu$m
Max plastic strain $p_{\max} \approx 7.5\%$

Indenter radius $R = 2\mu$m
Max plastic strain $p_{\max} \approx 11\%$

Accumulated plasticity

- Different plastic distribution

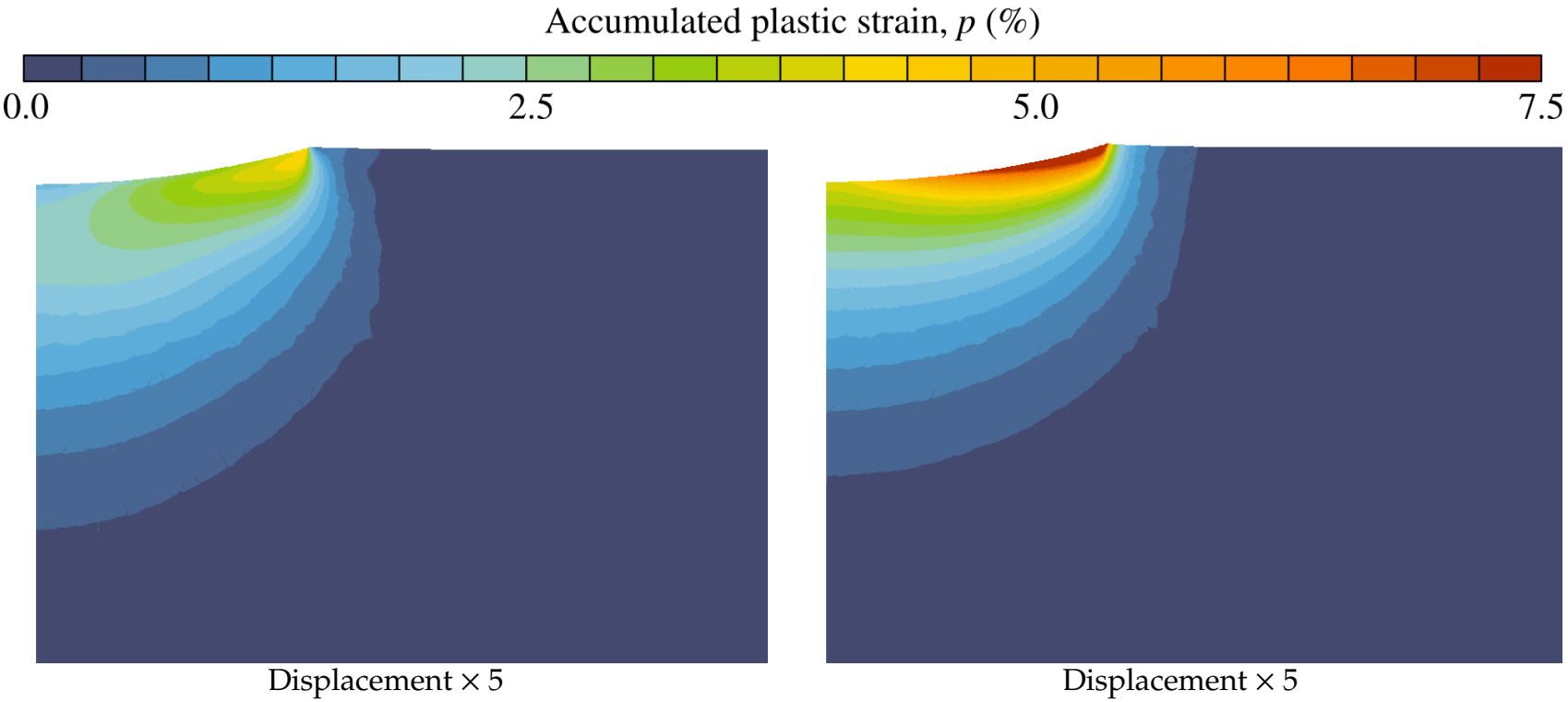

Indenter radius $R = 20\mu$m
Max plastic strain $p_{\max} \approx 7.5\%$

Indenter radius $R = 2\mu$m
Max plastic strain $p_{\max} \approx 11\%$

Displacement–force–contact radius

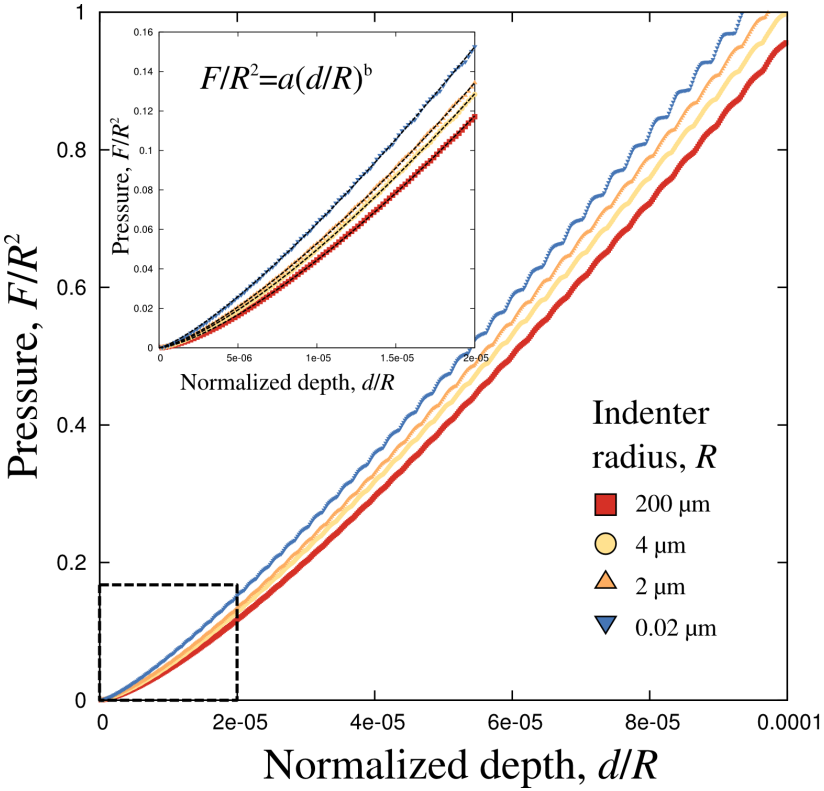

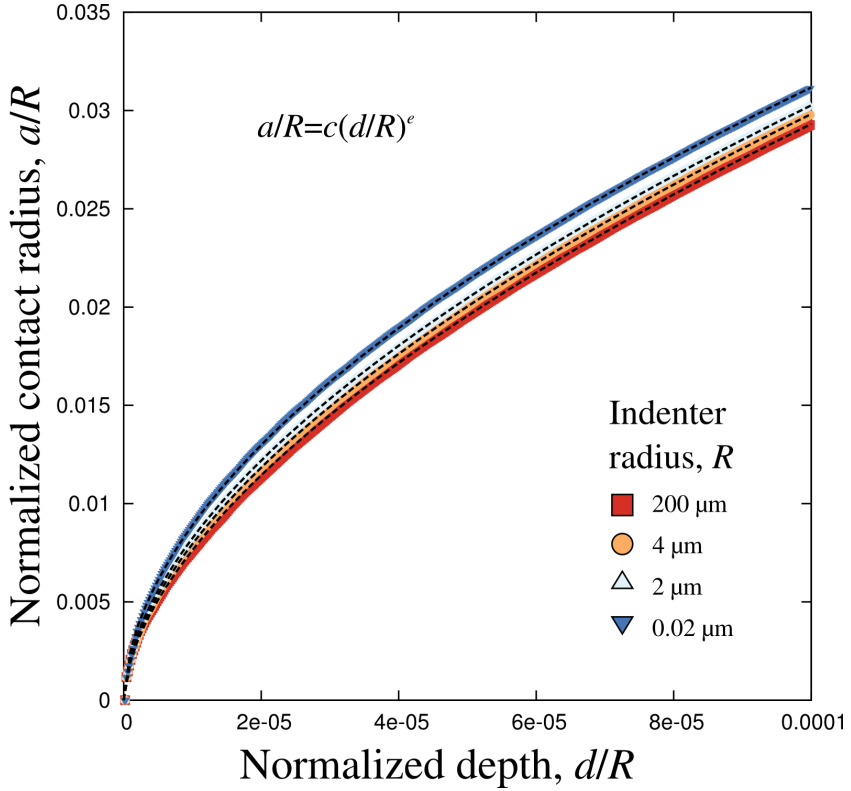

Parameters:
$a(R), b(R), c(R), e(R)$
`else:` using NURBS curve fit.

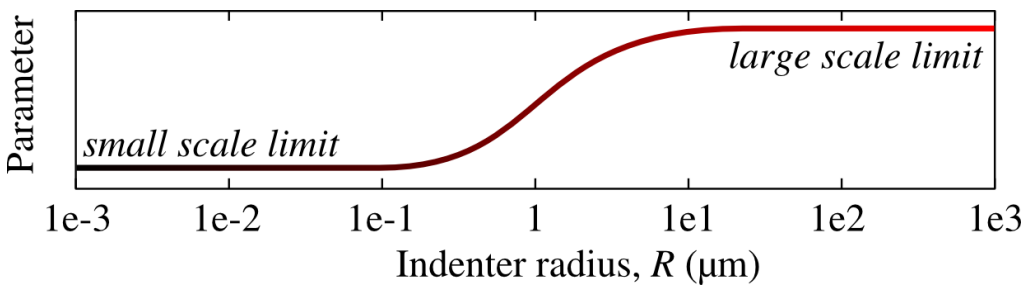

Working model

- Gradient-enhanced hardening with the Cosserat crystal plasticity theory[1]
- Cubic elasticity with C_{11}, C_{12}, C_{44} is to be taken into account

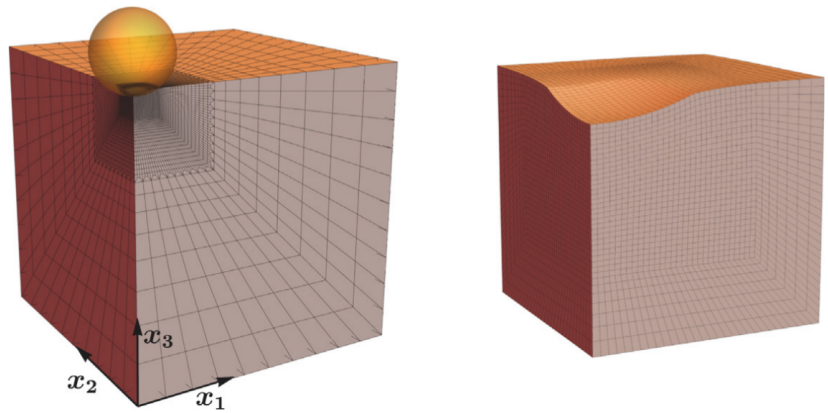

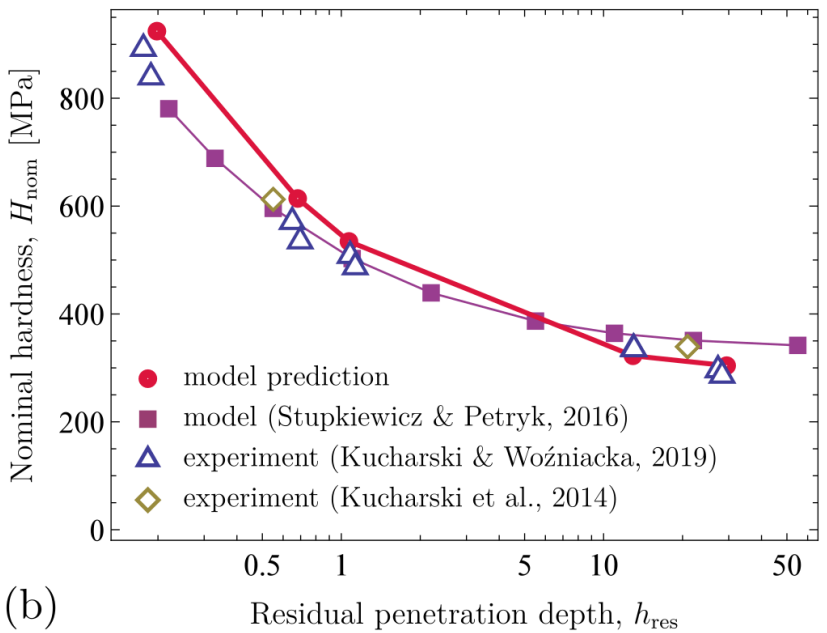

[1] Ryś, M., Stupkiewicz, S. and Petryk, H., 2022. Micropolar regularization of crystal plasticity with the gradient-enhanced incremental hardening law. International Journal of Plasticity, 156, p.103355.

Working model

- Gradient-enhanced hardening with the Cosserat crystal plasticity theory[1]
- Cubic elasticity with C_{11}, C_{12}, C_{44} is to be taken into account

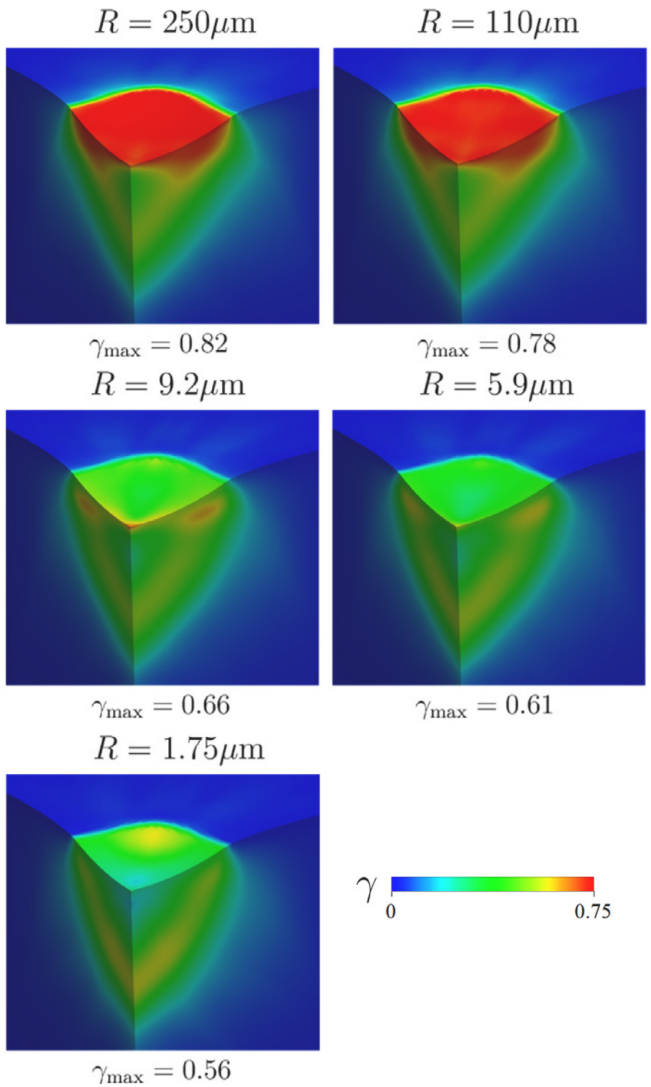

Residual plastic slip for different indenter radii R

[1] Ryś, M., Stupkiewicz, S. and Petryk, H., 2022. Micropolar regularization of crystal plasticity with the gradient-enhanced incremental hardening law. International Journal of Plasticity, 156, p.103355.

Viscoelasticity

Viscoelastic material

One-dimensional constitutive equations

- Applied stress σ
- In the left branch $\sigma_1 = E_\infty \varepsilon$
- In the dashpot $\sigma_2 = \eta \dot{\varepsilon}_d \quad (*)$
- In the right spring $\sigma_2 = E(\varepsilon - \varepsilon_d) \quad (**)$
- For the whole system $\sigma = \sigma_1 + \sigma_2$

$$\boxed{\sigma = (E_\infty + E)\varepsilon - E\varepsilon_d}$$

- From $(*)$ and $(**)$, and denoting $\tau = \eta/E$:

$$\boxed{\dot{\varepsilon}_d + \frac{\varepsilon_d}{\tau} = \frac{\varepsilon}{\tau},} \qquad \varepsilon_d \xrightarrow[t \to -\infty]{} 0$$

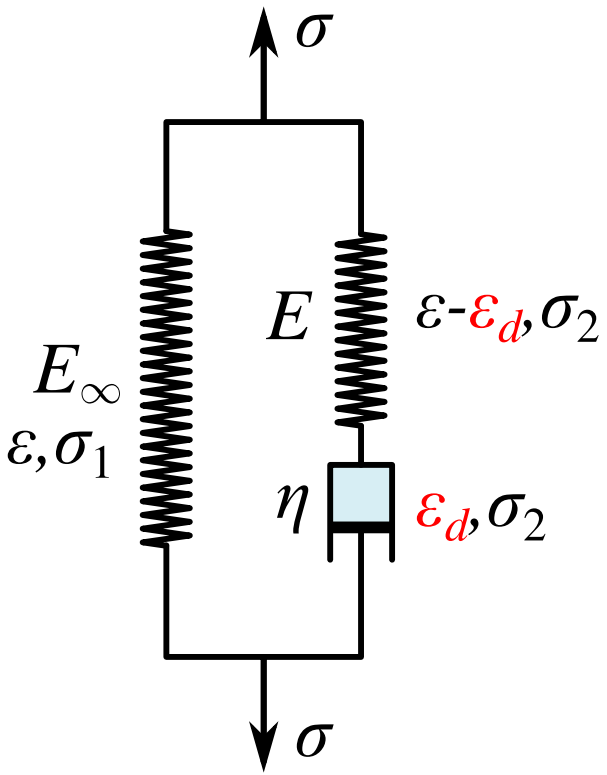

• One-dimensional viscoelastic model

- Recall: 1D model

$$\sigma = (E_\infty + E)\varepsilon - E\varepsilon_d, \quad \dot{\varepsilon}_d + \frac{\varepsilon_d}{\tau} = \frac{\varepsilon}{\tau}, \quad \varepsilon_d \xrightarrow[t\to-\infty]{} 0$$

- Multiple dashpots in parallel

$$\sigma = \underbrace{(E_\infty + \sum_i E_i)\varepsilon}_{\text{elastic stress } \sigma_0} - \sum_i E_i \varepsilon_d^i, \quad \dot{\varepsilon}_d^i + \frac{\varepsilon_d^i}{\tau_i} = \frac{\varepsilon}{\tau_i}, \quad \varepsilon_d^i \xrightarrow[t\to-\infty]{} 0, \quad \tau_i = \frac{\eta_i}{E_i}$$

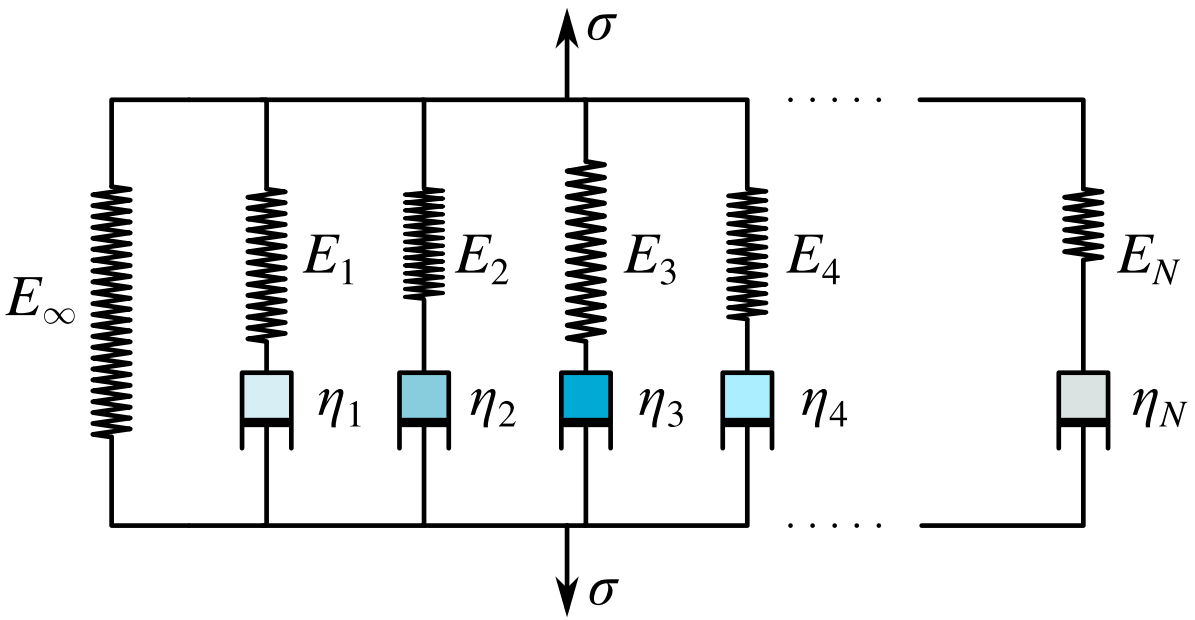

• One-dimensional viscoelastic model

- Recall: 1D model

$$\sigma = (E_\infty + E)\varepsilon - E\varepsilon_d, \quad \dot{\varepsilon}_d + \frac{\varepsilon_d}{\tau} = \frac{\varepsilon}{\tau}, \quad \varepsilon_d \xrightarrow[t\to-\infty]{} 0$$

- Multiple dashpots in parallel

$$\sigma = \underbrace{(E_\infty + \sum_i E_i)\varepsilon}_{\text{elastic stress } \sigma_0} - \sum_i E_i \varepsilon_d^i, \quad \dot{\varepsilon}_d^i + \frac{\varepsilon_d^i}{\tau_i} = \frac{\varepsilon}{\tau_i}, \quad \varepsilon_d^i \xrightarrow[t\to-\infty]{} 0, \quad \tau_i = \frac{\eta_i}{E_i}$$

- Denote $E_0 = E_\infty + \sum_i E_i$, $\psi_i = E_i/E_0$, and $q_i = E_i\varepsilon_d^i$ we obtain

$$\sigma = E_0\varepsilon - \sum_i q_i, \quad \dot{q}_i + \frac{q_i}{\tau_i} = \frac{\psi_i}{\tau_i}\sigma_0, \quad \varepsilon_d^i \xrightarrow[t\to-\infty]{} 0$$

- By construction

$$\sum_i \psi_i + \frac{E_\infty}{E_0} = 1 \quad \Rightarrow \quad \sum_i \psi_i = 1 - \frac{E_\infty}{E_0}$$

• Three-dimensional viscoelastic model

Linear viscoelastic (generalized Maxwell model, standard solid)

- Stress-strain relation:

$$\underline{\underline{\sigma}}(t) = K\theta\underline{\underline{I}} + \int_{-\infty}^{t} G(t-\tau)\dot{\underline{\underline{e}}}(\tau)d\tau,$$

- Kernel $G(\tau)$ is given by:

$$G(\tau) = 2G_\infty + 2(G_0 - G_\infty)\Psi(\tau) \text{ with } \Psi(\tau) = \sum_{i=1}^{n} \psi_i \exp(-\tau/\tau_i)$$

  - G_∞, G_0 are the slow/fast loading shear moduli, respectively, such that $G_\infty \leq G_0$;
  - K is the bulk modulus, and for elastomers/polymers $K/G_0 \gg 1$;
  - ψ_i are the influence coefficients, such that $\sum_{i=1}^{n} \psi_i = 1$;
  - τ_i are the respective relaxation times.

• Material model: *storage* and loss moduli

- Consider a harmonic (rigid) loading: $\underline{e}(t) = \underline{e}_0 \exp(i\omega t)$
- Split the kernel: $G(t) = 2G_\infty + \tilde{G}(t)$
- Then, the storage modulus (general case):

$$G'(\omega) = 2G_\infty + \omega \int_0^\infty \tilde{G}(\tau) \sin(\omega\tau)\, d\tau$$

- The storage modulus in the framework of the generalized Maxwell model:

$$G'(\omega) = 2G_\infty + 2\omega(G_0 - G_\infty) \sum_{i=1}^{n} \psi_i \int_0^\infty \exp(-\tau/\tau_i) \sin(\omega\tau)\, d\tau$$

$$G'(\omega) = 2G_\infty + 2(G_0 - G_\infty) \sum_{i=1}^{n} \frac{\psi_i \omega^2 \tau_i^2}{1 + \omega^2 \tau_i^2}$$

- Remark:

$$\int \exp(cx) \sin(bx)\, dx = \frac{\exp(cx)}{c^2 + b^2} [c \sin(bx) - b \cos(bx)]$$

• Material model: storage and *loss* moduli

- The loss modulus (general case):

$$G''(\omega) = \omega \int_0^\infty \tilde{G}(\tau) \cos(\omega\tau)\, d\tau$$

- The loss modulus in the framework of the generalized Maxwell model:

$$G''(\omega) = 2\omega(G_0 - G_\infty) \sum_{i=1}^{n} \psi_i \int_0^\infty \exp(-\tau/\tau_i) \cos(\omega\tau)\, d\tau$$

$$G''(\omega) = 2(G_0 - G_\infty) \sum_{i=1}^{n} \frac{\psi_i \omega\tau_i}{1 + \omega^2\tau_i^2}.$$

- Remark:

$$\int \exp(cx) \cos(bx)\, dx = \frac{\exp(cx)}{c^2 + b^2} [c \cos(bx) + b \sin(bx)]$$

• Material model: example

- Material parameters: $G_0 = 1.1$ MPa, $G_\infty = 50$ kPa
- Single relaxation time: $\tau_0 = 10^{-7}$ s
- Quasi-incompressible material: $K/G_0 = 10^6 \gg 1$
- Uniaxial (rigid) loading: $\varepsilon_{xx} = A\sin(\omega t)$, $\sigma_{yy} = \sigma_{zz} = 0$, $\varepsilon_{yy} = \varepsilon_{zz} \approx -0.5\varepsilon_{xx}$
- Spherical and deviatoric parts: $\underline{\boldsymbol{\epsilon}} \approx A(1-2\nu)\sin(\omega t)\underline{\boldsymbol{I}}$, $\underline{\boldsymbol{e}} \approx \underline{\boldsymbol{\varepsilon}}$
- Stress-strain relation:

$$\underline{\boldsymbol{\sigma}}(t) = \int_{-\infty}^{t} 2(G_0 - G_\infty)\exp[-(t-\tau)/\tau_0]\underline{\dot{\boldsymbol{e}}}(\tau)d\tau + 2G_\infty\underline{\boldsymbol{e}} + K\underline{\boldsymbol{\epsilon}},$$

- Axial and radial stress components:

$$\sigma_{xx} = 2G_\infty\varepsilon_{xx} + K(\varepsilon_{xx} + 2\varepsilon_{yy}) + \int_{-\infty}^{t} 2(G_0 - G_\infty)\exp[-(t-\tau)/\tau_0]\dot{\varepsilon}_{xx}(\tau)d\tau$$

• Material model: example

- Material parameters: $G_0 = 1.1$ MPa, $G_\infty = 50$ kPa
- Single relaxation time: $\tau_0 = 10^{-7}$ s
- Quasi-incompressible material: $K/G_0 = 10^6 \gg 1$
- Uniaxial (rigid) loading: $\varepsilon_{xx} = A\sin(\omega t)$, $\sigma_{yy} = \sigma_{zz} = 0$, $\varepsilon_{yy} = \varepsilon_{zz} \approx -0.5\varepsilon_{xx}$
- Spherical and deviatoric parts: $\underline{\boldsymbol{\epsilon}} \approx A(1-2\nu)\sin(\omega t)\underline{\boldsymbol{I}}$, $\underline{\boldsymbol{e}} \approx \underline{\boldsymbol{\varepsilon}}$
- Stress-strain relation:

$$\underline{\boldsymbol{\sigma}}(t) = \int_{-\infty}^{t} 2(G_0 - G_\infty)\exp[-(t-\tau)/\tau_0]\underline{\dot{\boldsymbol{e}}}(\tau)d\tau + 2G_\infty\underline{\boldsymbol{e}} + K\underline{\boldsymbol{\epsilon}},$$

- Axial and radial stress components:

$$\sigma_{xx} = 2G_\infty\varepsilon_{xx} + K(\varepsilon_{xx} + 2\varepsilon_{yy}) + \int_{-\infty}^{t} 2(G_0 - G_\infty)\exp[-(t-\tau)/\tau_0]\dot{\varepsilon}_{xx}(\tau)d\tau$$

$$\sigma_{yy} = 0$$

• Material model: example

- Material parameters: $G_0 = 1.1$ MPa, $G_\infty = 50$ kPa
- Single relaxation time: $\tau_0 = 10^{-7}$ s
- Quasi-incompressible material: $K/G_0 = 10^6 \gg 1$
- Uniaxial (rigid) loading: $\varepsilon_{xx} = A\sin(\omega t)$, $\sigma_{yy} = \sigma_{zz} = 0$, $\varepsilon_{yy} = \varepsilon_{zz} \approx -0.5\varepsilon_{xx}$
- Spherical and deviatoric parts: $\underline{\boldsymbol{\epsilon}} \approx A(1-2\nu)\sin(\omega t)\underline{\boldsymbol{I}}$, $\underline{\boldsymbol{e}} \approx \underline{\boldsymbol{\varepsilon}}$
- Stress-strain relation:

$$\underline{\boldsymbol{\sigma}}(t) = \int_{-\infty}^{t} 2(G_0 - G_\infty)\exp[-(t-\tau)/\tau_0]\underline{\dot{\boldsymbol{e}}}(\tau)d\tau + 2G_\infty\underline{\boldsymbol{e}} + K\underline{\boldsymbol{\epsilon}},$$

- Axial and radial stress components:

$$\sigma_{xx} = 2G_\infty\varepsilon_{xx} + K(\varepsilon_{xx} + 2\varepsilon_{yy}) + \int_{-\infty}^{t} 2(G_0 - G_\infty)\exp[-(t-\tau)/\tau_0]\dot{\varepsilon}_{xx}(\tau)d\tau$$

$$\sigma_{yy} = 0 = 2G_\infty\varepsilon_{yy} + K(\varepsilon_{xx} + 2\varepsilon_{yy}) + \int_{-\infty}^{t} 2(G_0 - G_\infty)\exp[-(t-\tau)/\tau_0]\dot{\varepsilon}_{yy}(\tau)d\tau$$

• Material model: example

- Material parameters: $G_0 = 1.1$ MPa, $G_\infty = 50$ kPa
- Single relaxation time: $\tau_0 = 10^{-7}$ s
- Quasi-incompressible material: $K/G_0 = 10^6 \gg 1$
- Uniaxial (rigid) loading: $\varepsilon_{xx} = A\sin(\omega t)$, $\sigma_{yy} = \sigma_{zz} = 0$, $\varepsilon_{yy} = \varepsilon_{zz} \approx -0.5\varepsilon_{xx}$
- Spherical and deviatoric parts: $\underline{\boldsymbol{\epsilon}} \approx A(1-2\nu)\sin(\omega t)\underline{\boldsymbol{I}}$, $\underline{\boldsymbol{e}} \approx \underline{\boldsymbol{\varepsilon}}$
- Stress-strain relation:

$$\underline{\boldsymbol{\sigma}}(t) = \int_{-\infty}^{t} 2(G_0 - G_\infty)\exp[-(t-\tau)/\tau_0]\underline{\dot{\boldsymbol{e}}}(\tau)d\tau + 2G_\infty\underline{\boldsymbol{e}} + K\underline{\boldsymbol{\epsilon}},$$

- Axial and radial stress components:

$$\sigma_{xx} = 2G_\infty\varepsilon_{xx} + K(\varepsilon_{xx} + 2\varepsilon_{yy}) + \int_{-\infty}^{t} 2(G_0 - G_\infty)\exp[-(t-\tau)/\tau_0]\dot{\varepsilon}_{xx}(\tau)d\tau$$

$$\sigma_{yy} = 0 = 2G_\infty\varepsilon_{yy} + K(\varepsilon_{xx} + 2\varepsilon_{yy}) + \int_{-\infty}^{t} 2(G_0 - G_\infty)\exp[-(t-\tau)/\tau_0]\dot{\varepsilon}_{yy}(\tau)d\tau$$

$$\boxed{\sigma_{xx} = 3G_\infty\varepsilon_{xx} + \int_{-\infty}^{t} 3(G_0 - G_\infty)\exp[-(t-\tau)/\tau_0]\dot{\varepsilon}_{xx}(\tau)d\tau}$$

• Material model: example II

- Uniaxial storage modulus:

$$E'(\omega) = 3G_\infty + 3(G_0 - G_\infty)\frac{\omega^2\tau_0^2}{1+\omega^2\tau_0^2}$$

- Uniaxial loss modulus:

$$E''(\omega) = 3(G_0 - G_\infty)\frac{\omega\tau}{1+\omega^2\tau_0^2}$$

• Material model: example (FEA vs Analytics)

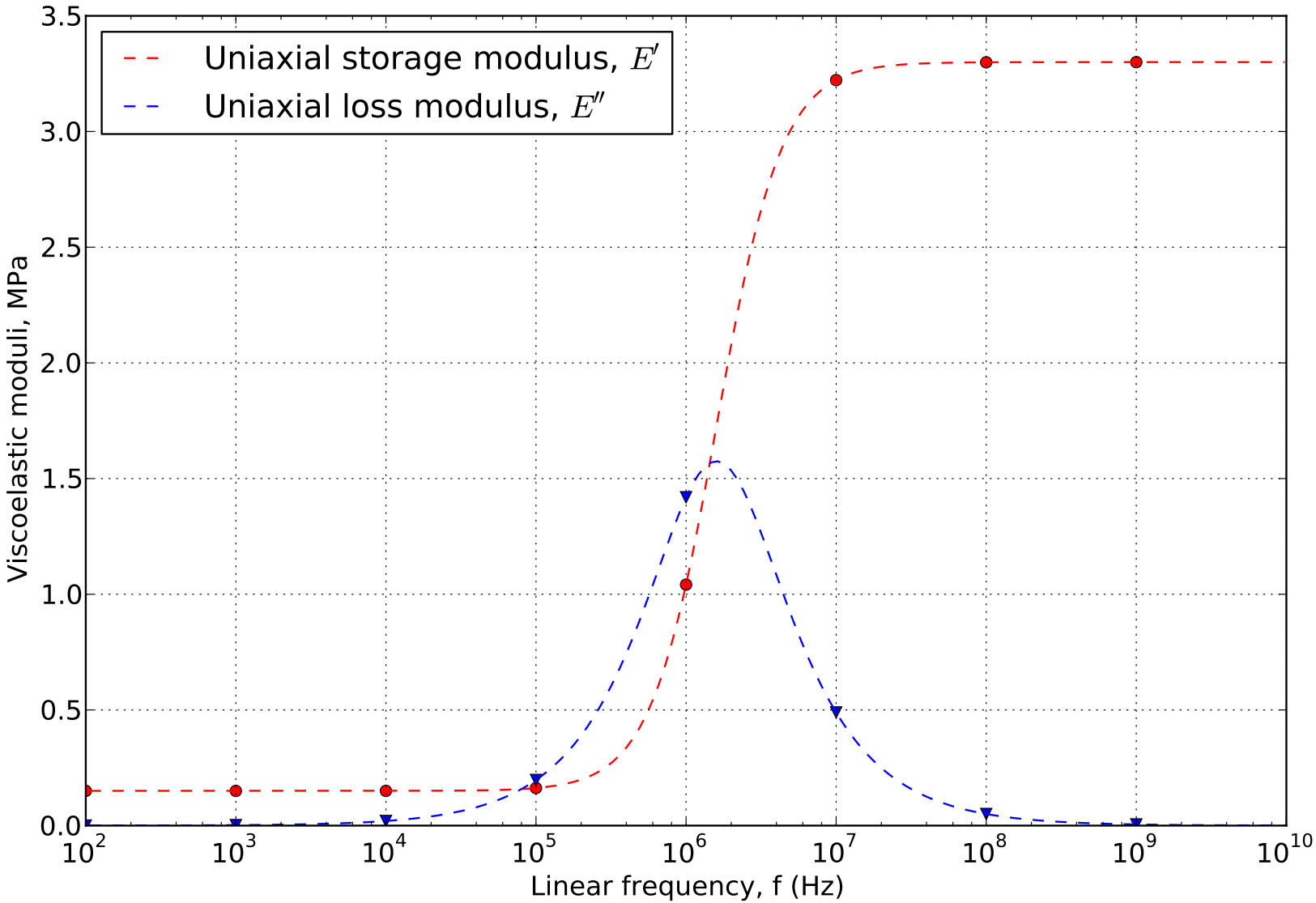

• Material model: example (FEA vs Analytics)

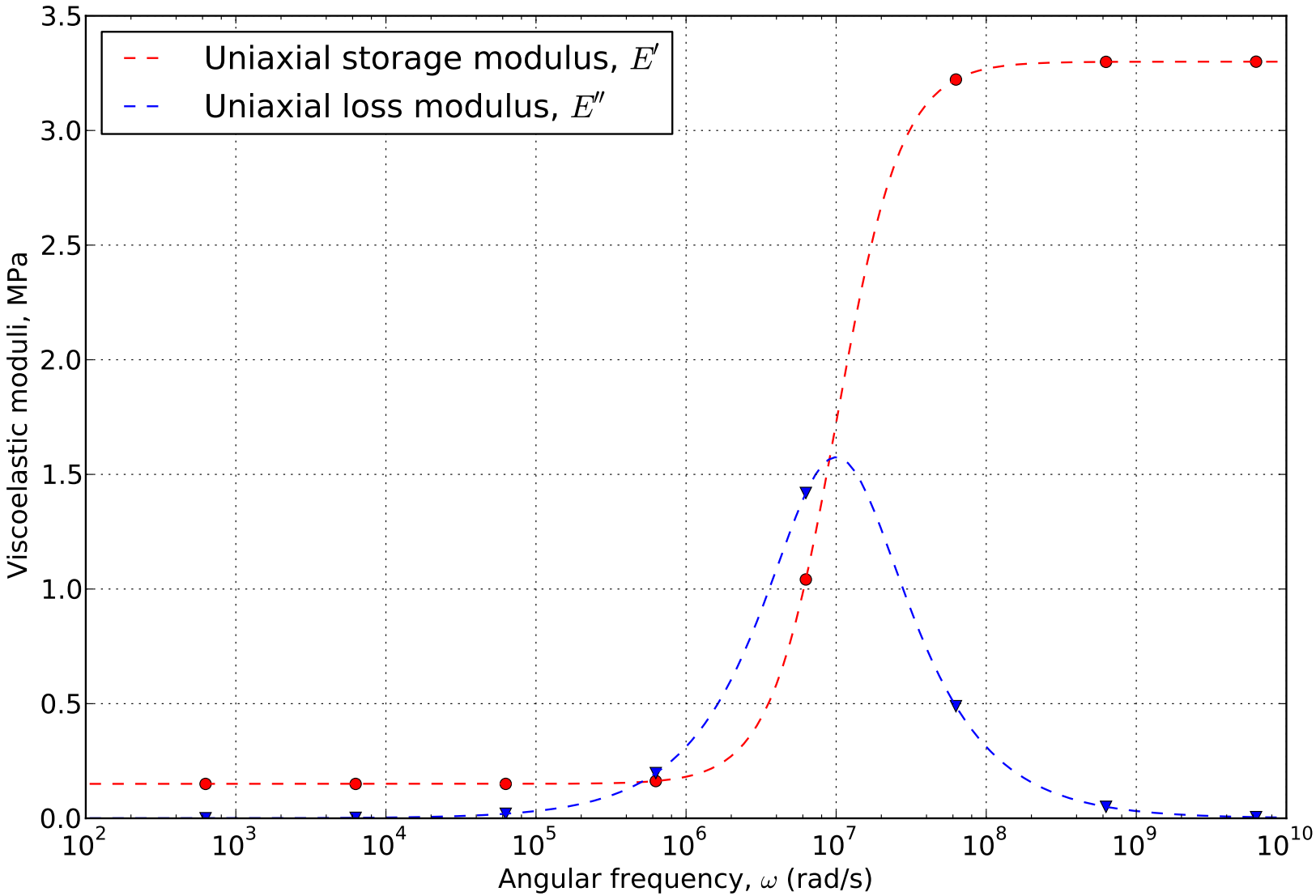

• Material model: example (FEA vs Analytics)

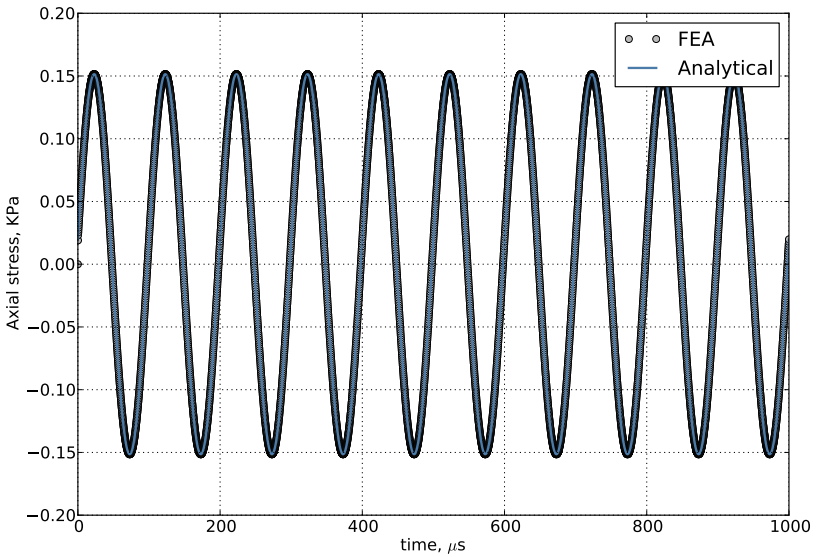

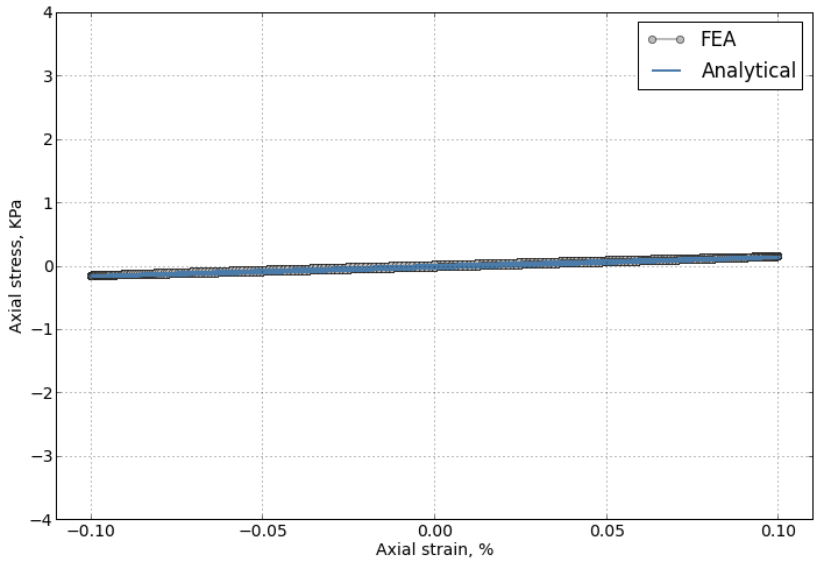

Linear frequency $f = 10^4$ Hz

• Material model: example (FEA vs Analytics)

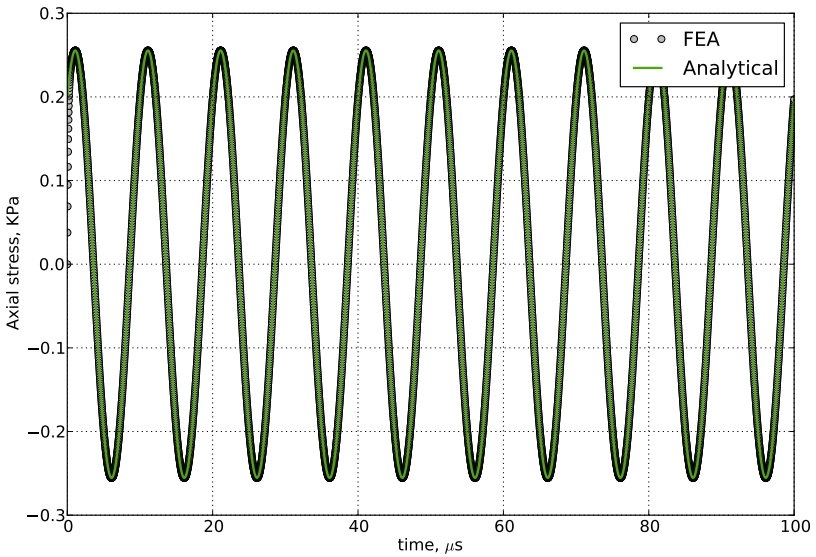

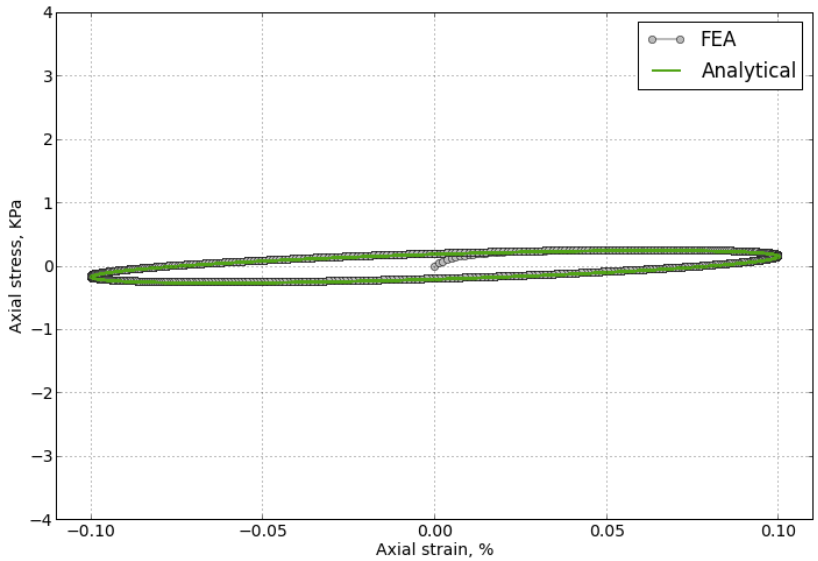

Linear frequency $f = 10^5$ Hz

• Material model: example (FEA vs Analytics)

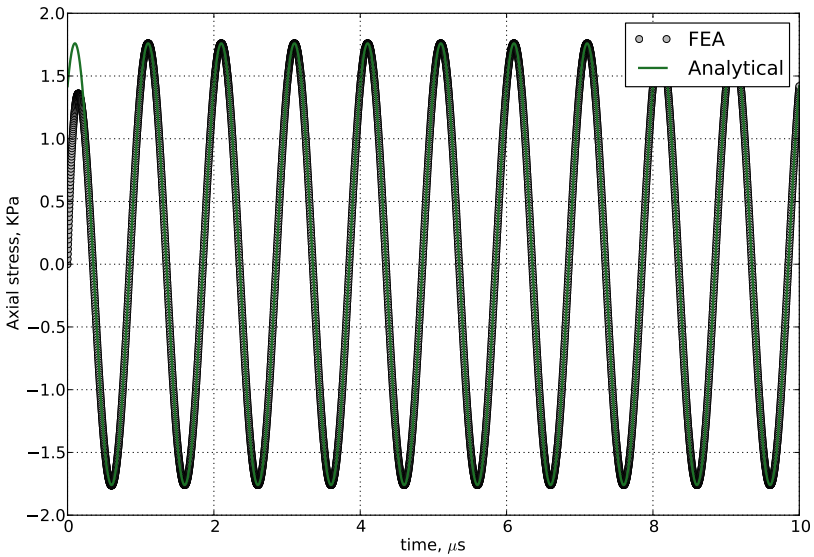

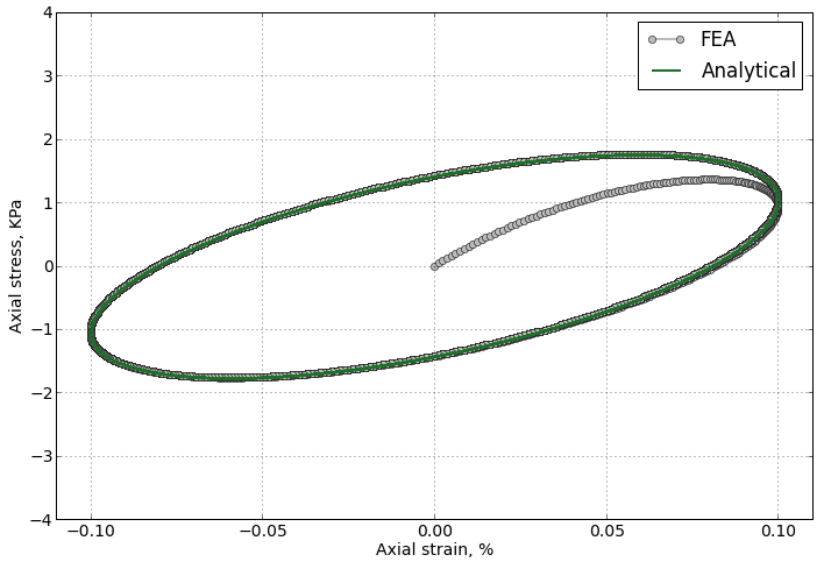

Linear frequency $f = 10^6$ Hz

• Material model: example (FEA vs Analytics)

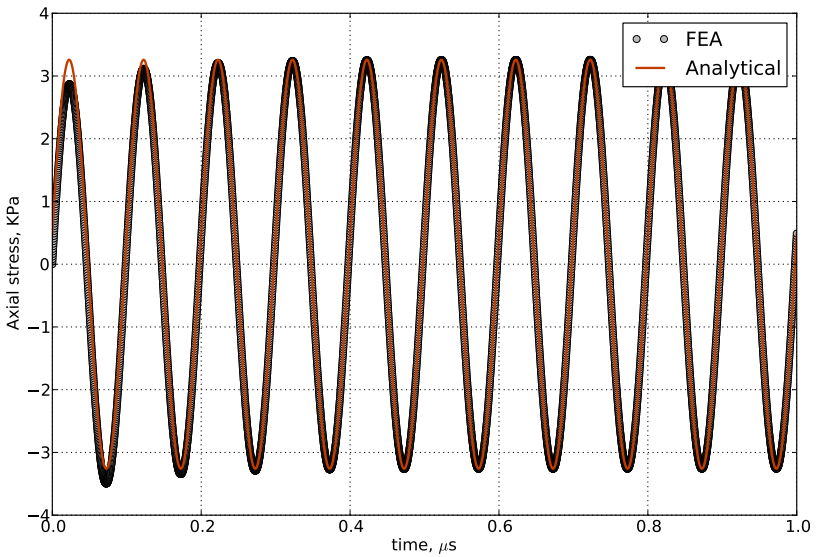

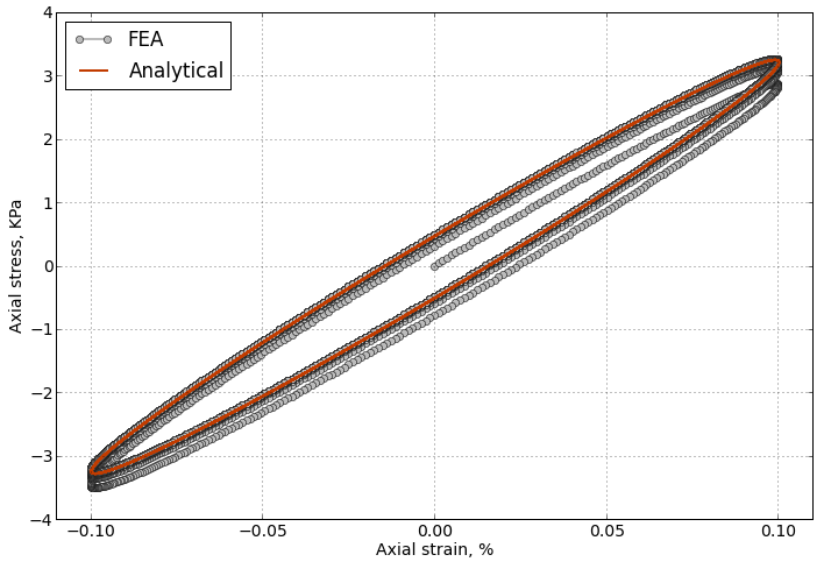

Linear frequency $f = 10^7$ Hz

• Material model: example (FEA vs Analytics)

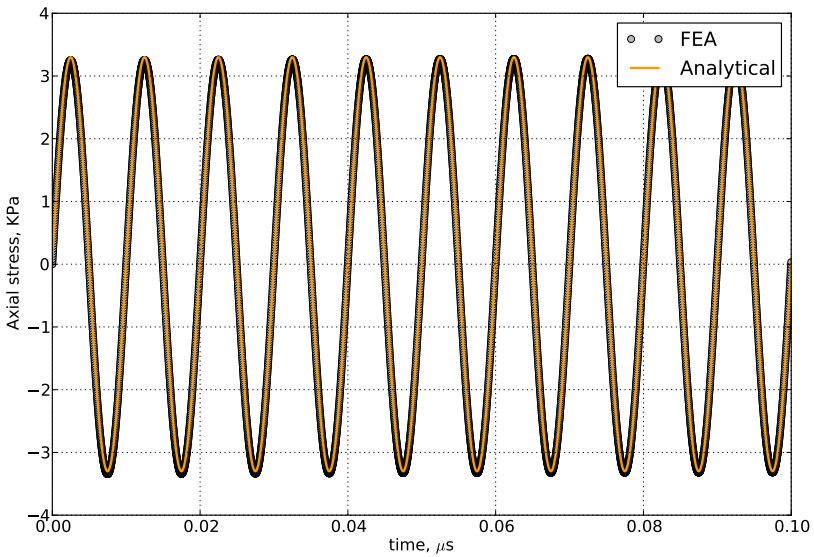

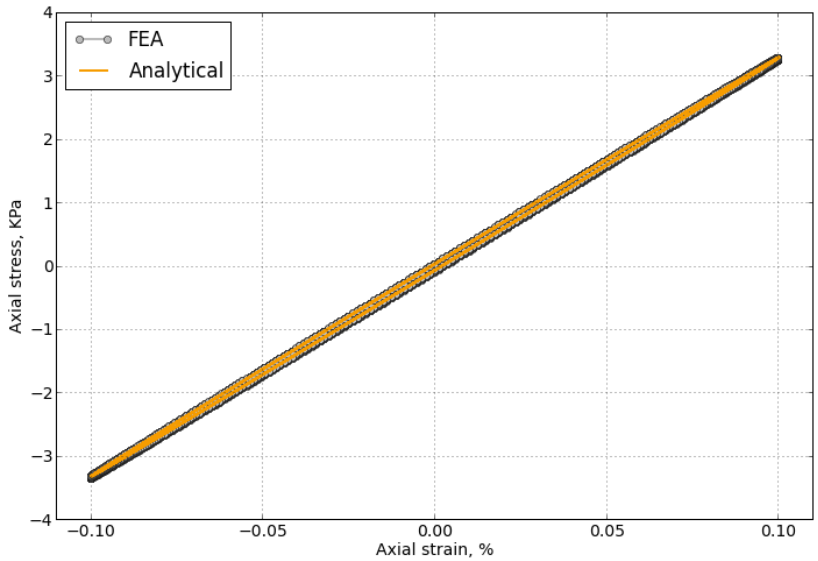

Linear frequency $f = 10^8$ Hz

Viscoelastic sliding: bulk friction

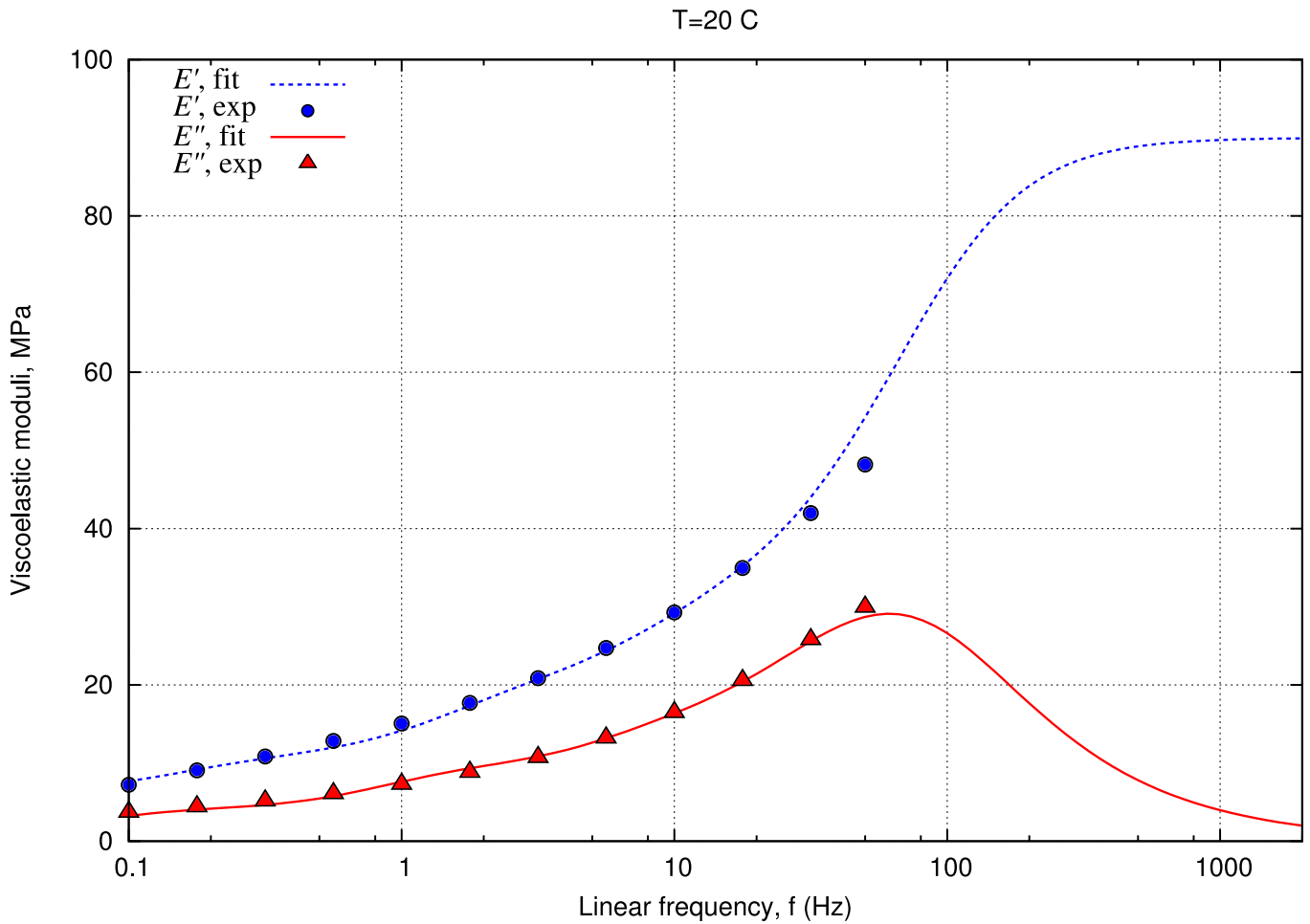

Fitting generalized Maxwell model for rubber to experimental data at $T = 20\ ^{o}C$

Viscoelastic sliding: bulk friction

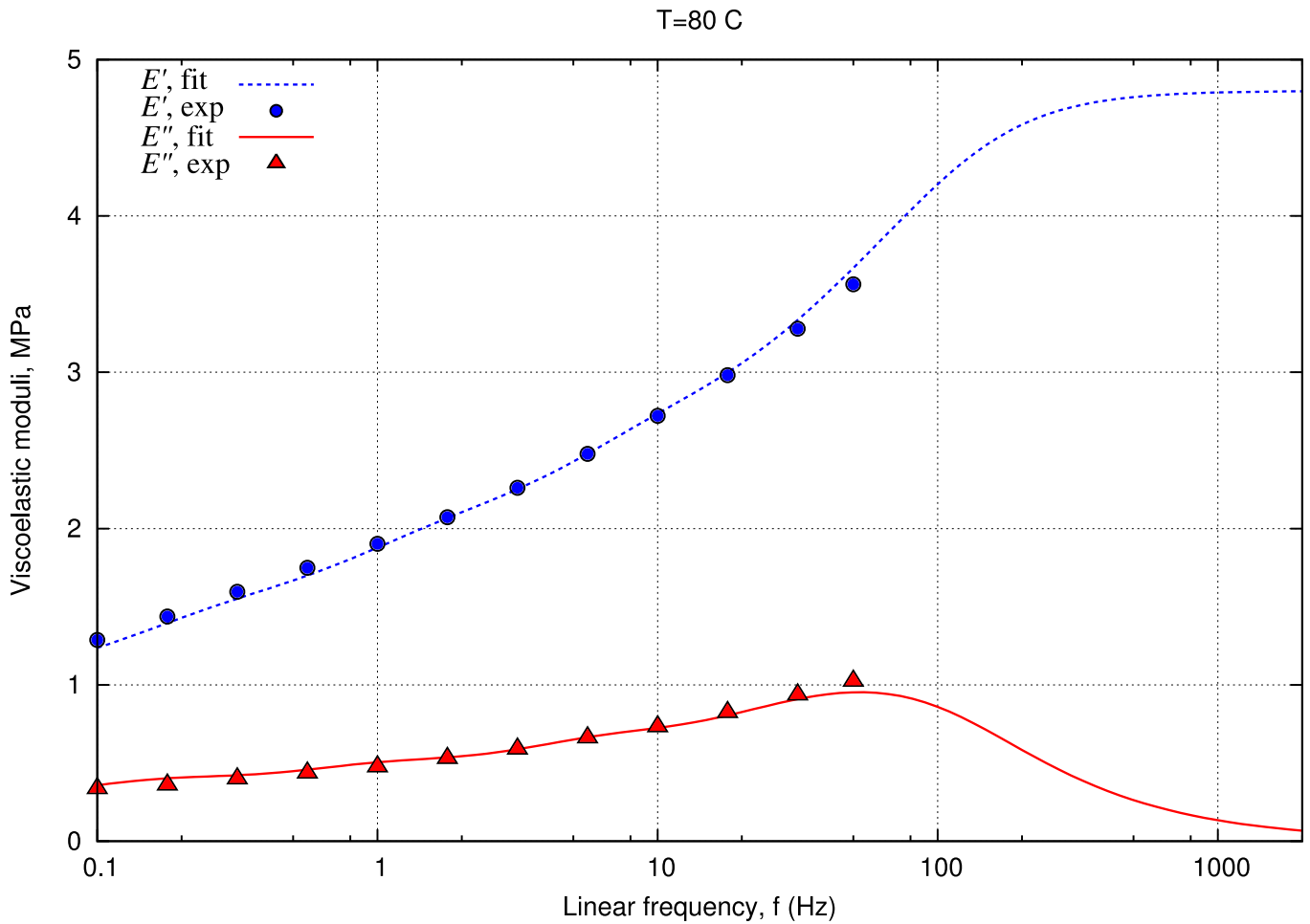

Fitting generalized Maxwell model for rubber to experimental data at $T = 80\ ^{o}C$

Viscoelastic sliding: bulk friction

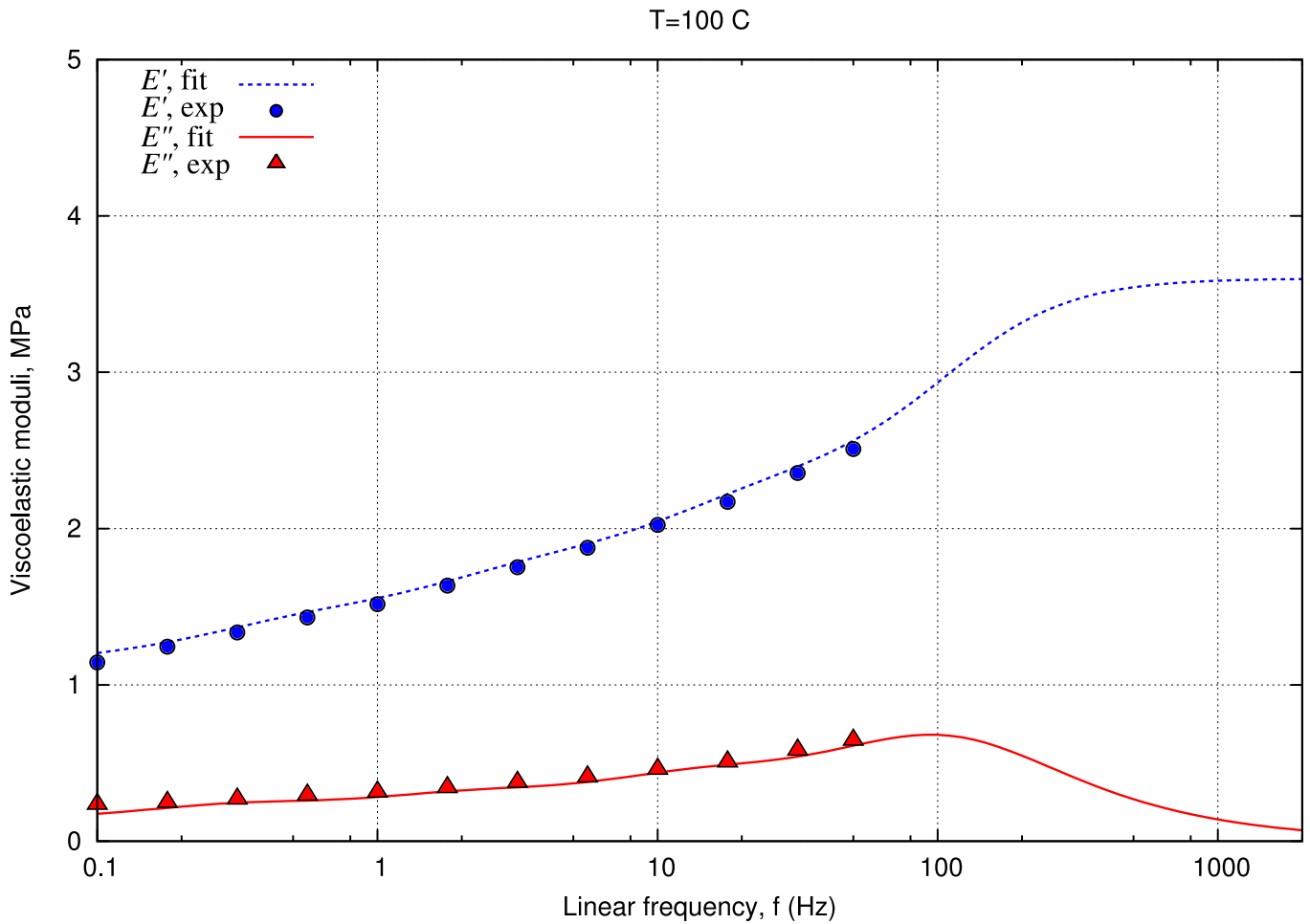

Fitting generalized Maxwell model for rubber to experimental data at $T = 100\ ^{o}C$

Viscoelastic sliding: bulk friction

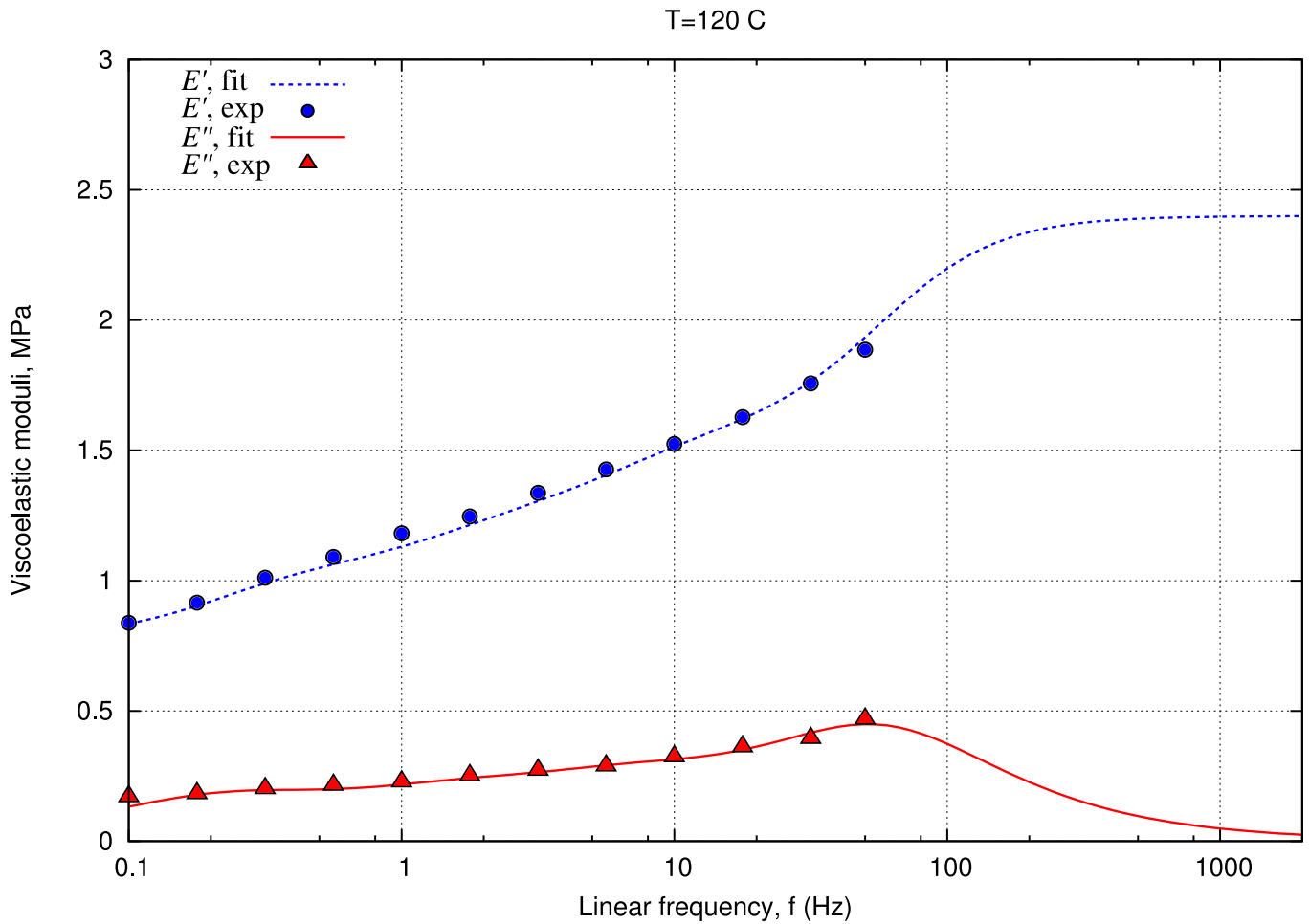

Fitting generalized Maxwell model for rubber to experimental data at $T = 120\ ^{o}C$

Viscoelastic sliding: bulk friction

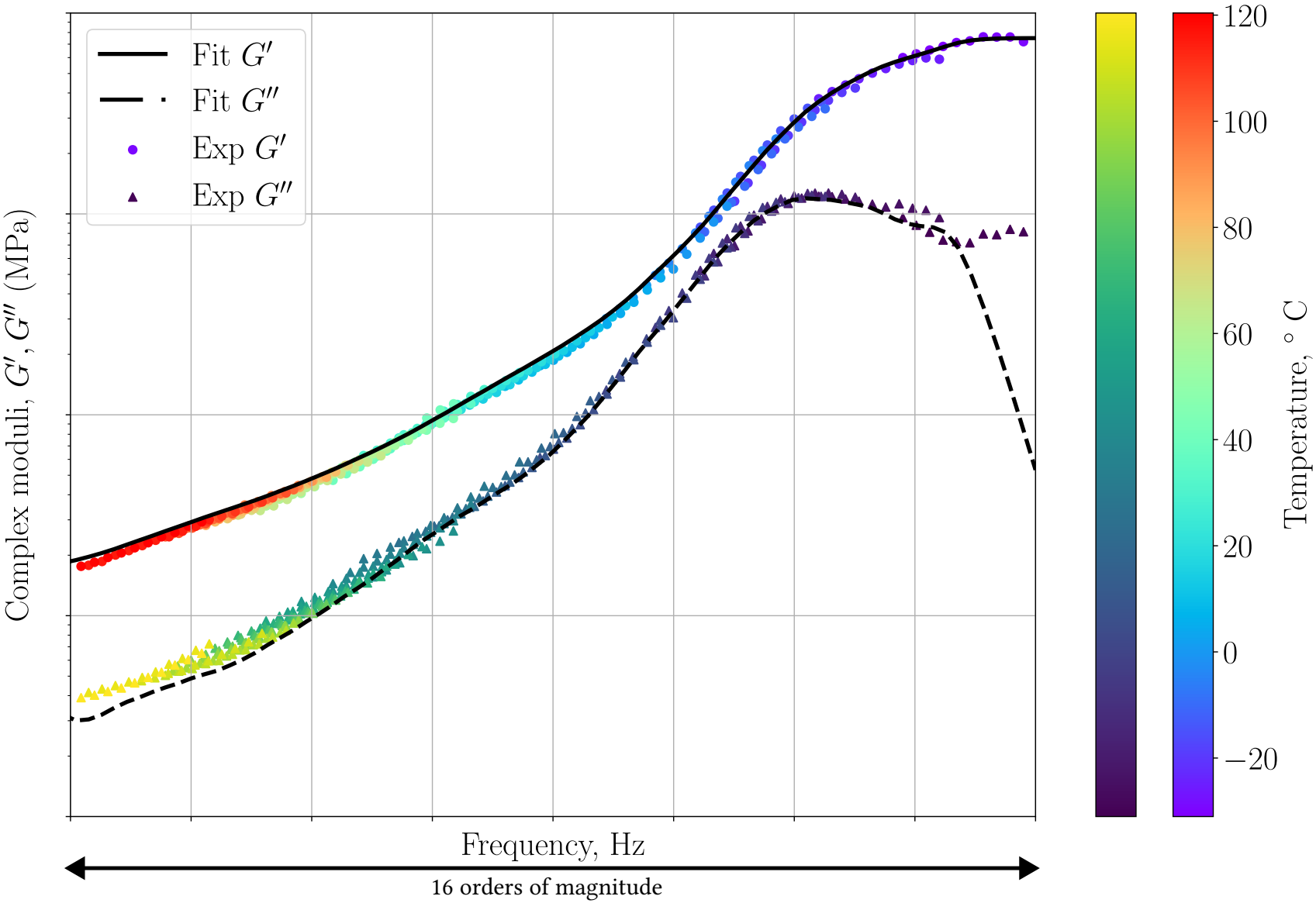

Full data on complex moduli of a sample charged rubber

Viscoelastic sliding: bulk friction

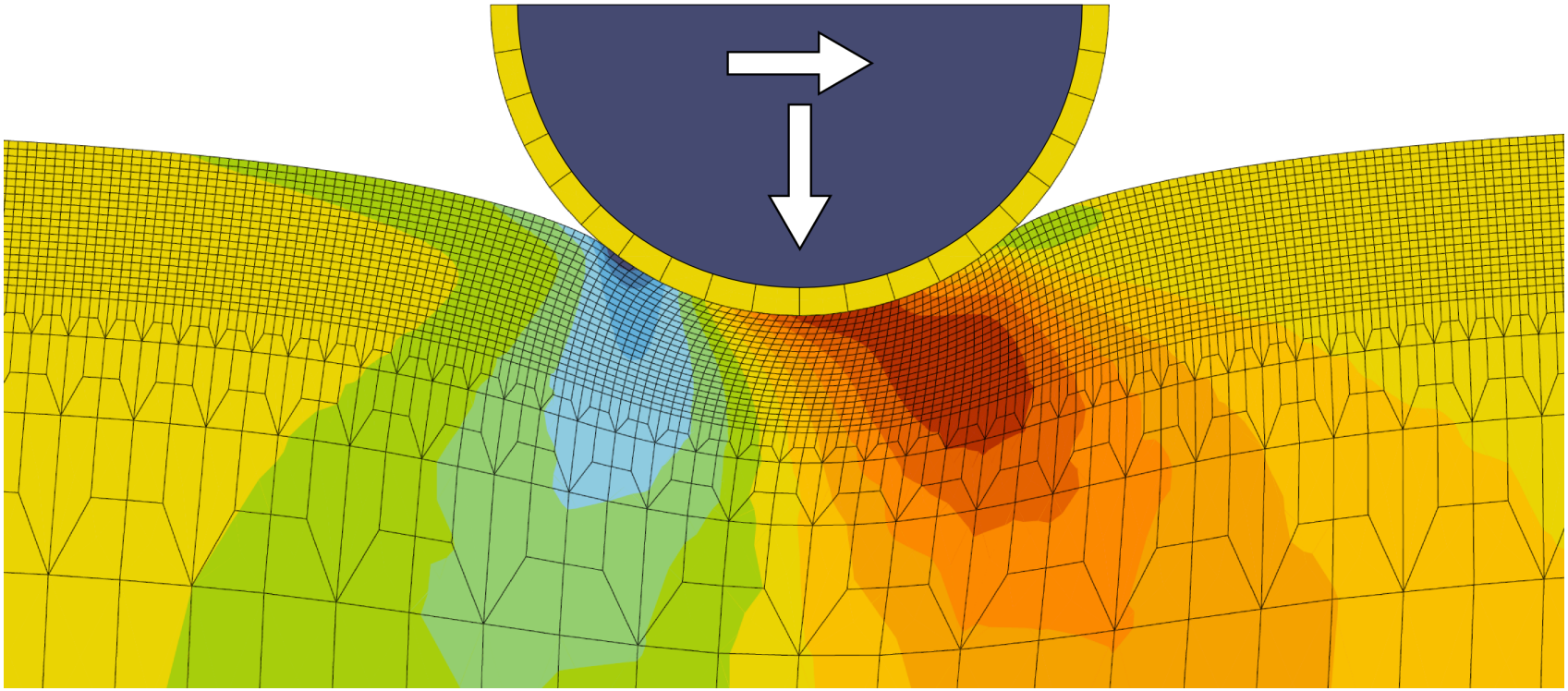

Simulation sketch

Viscoelastic sliding: bulk friction

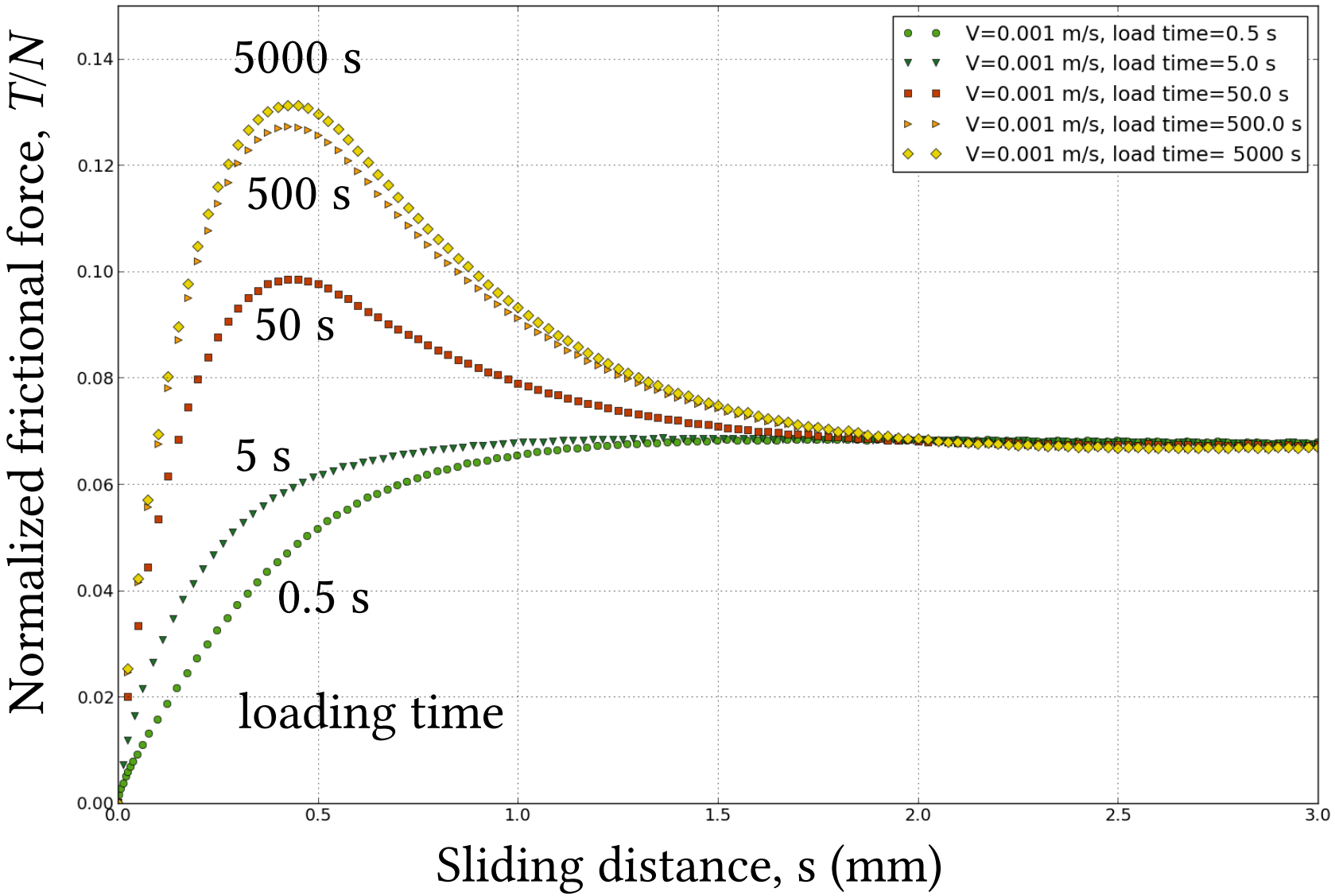

Effect of normal-loading rate on the frictional force evolution

Viscoelastic sliding: bulk friction

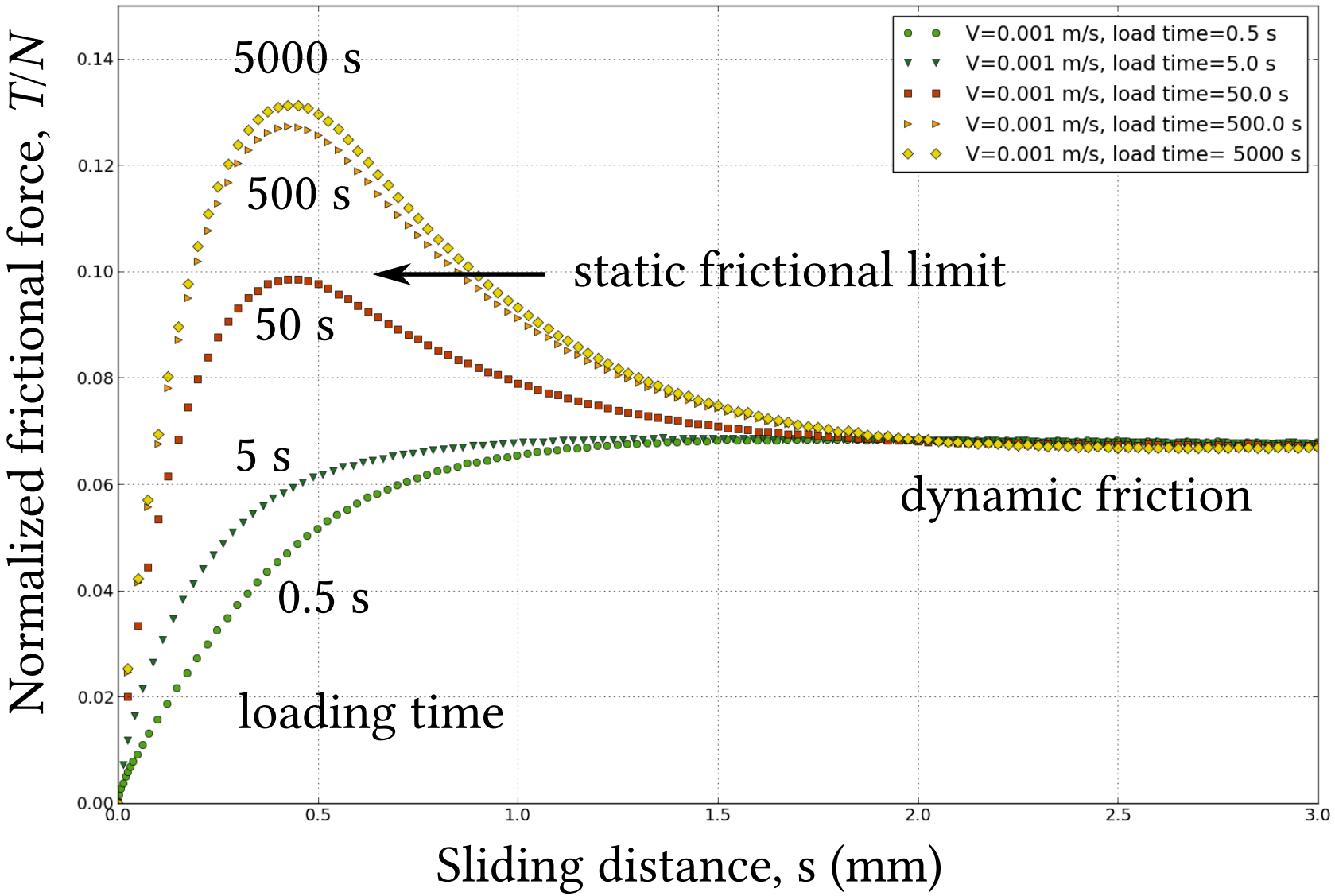

Effect of normal-loading rate on the frictional force evolution

Viscoelastic sliding: bulk friction

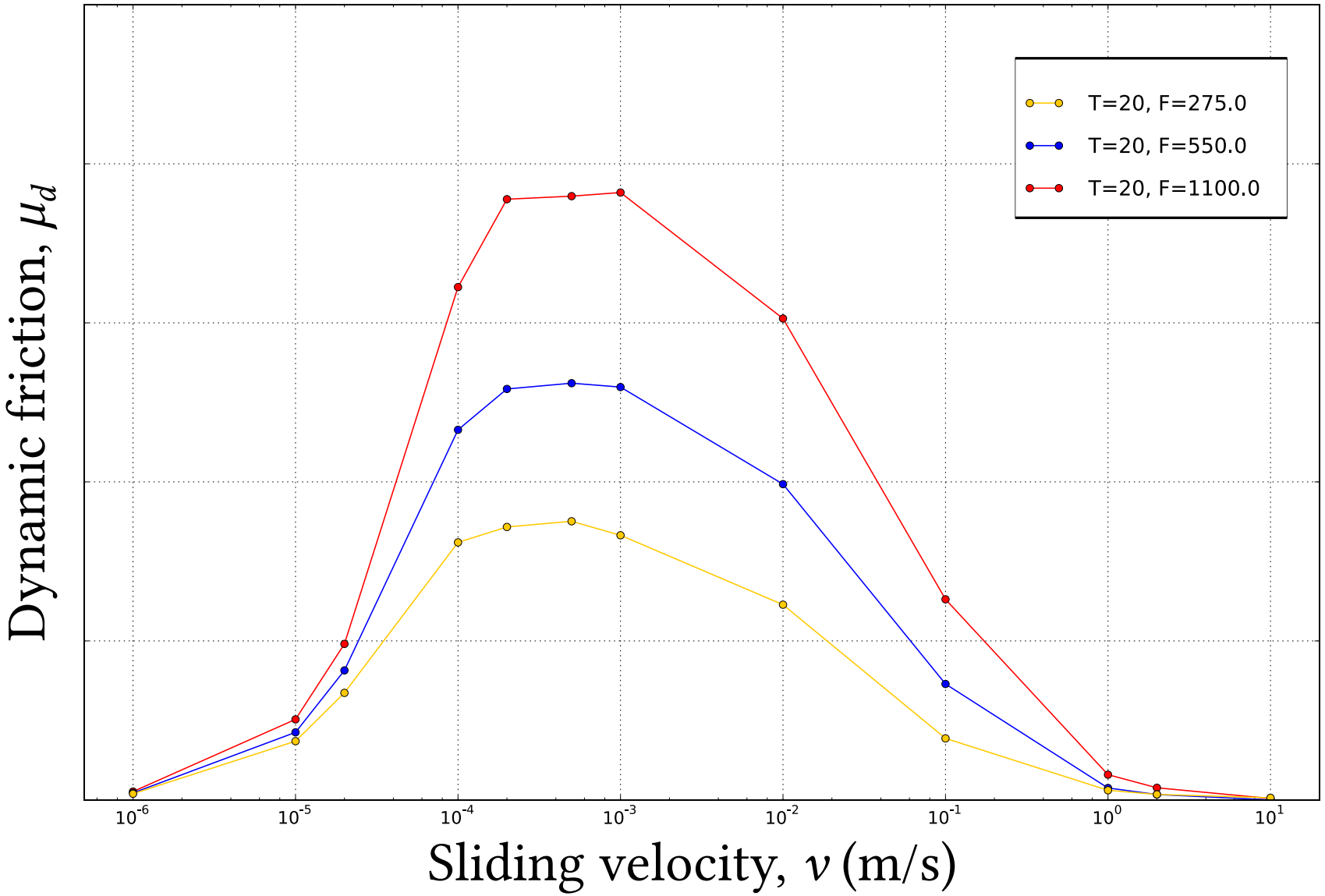

Frictional force at different slip velocity (effect of force)

Viscoelastic sliding: bulk friction

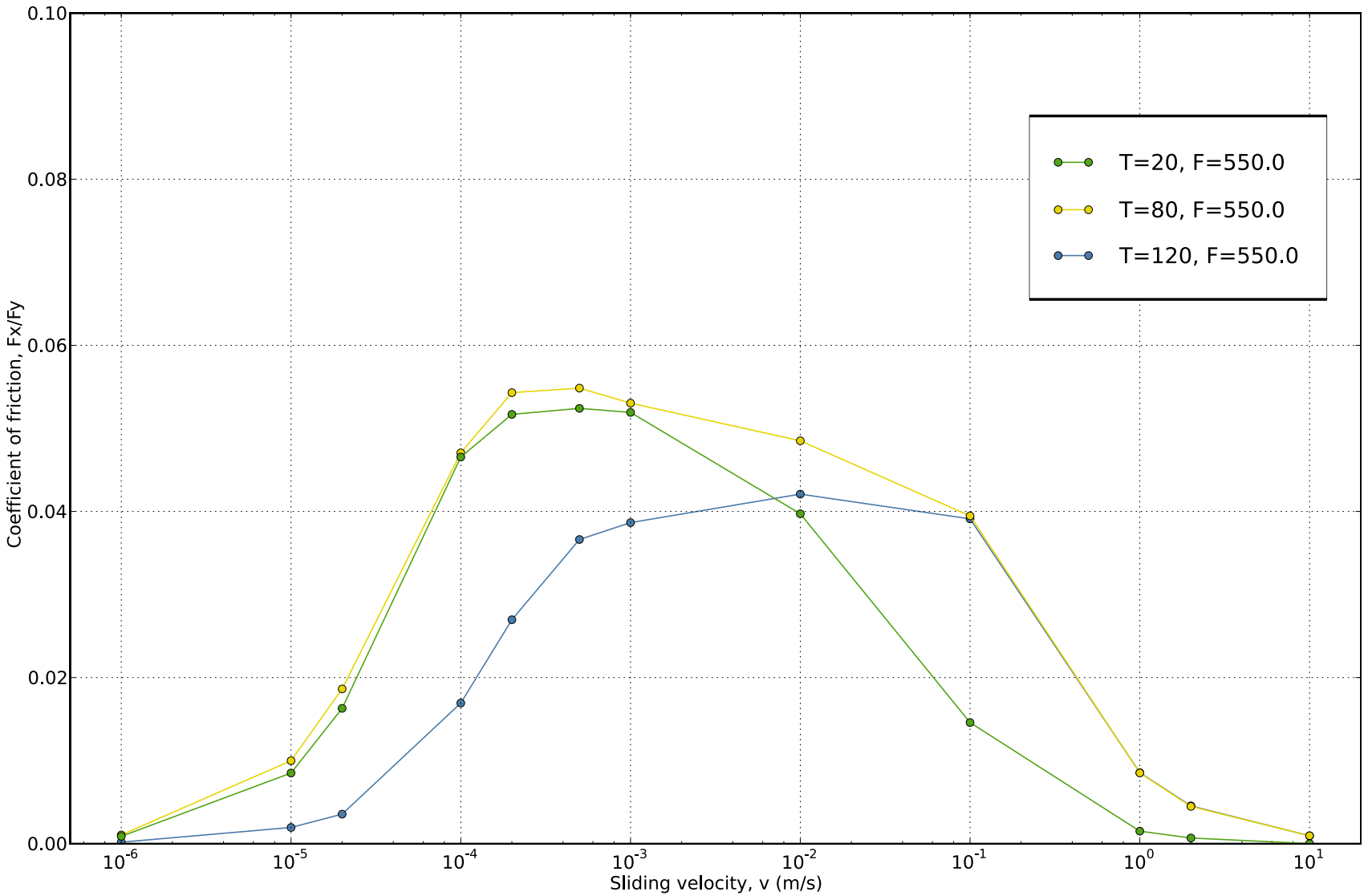

Frictional force at different slip velocity (effect of temperature)

Viscoelastic friction: recent progress

- Account for multiscales[1,2]
- Account for adhesion[1,2]
- Account for large deformations[3]

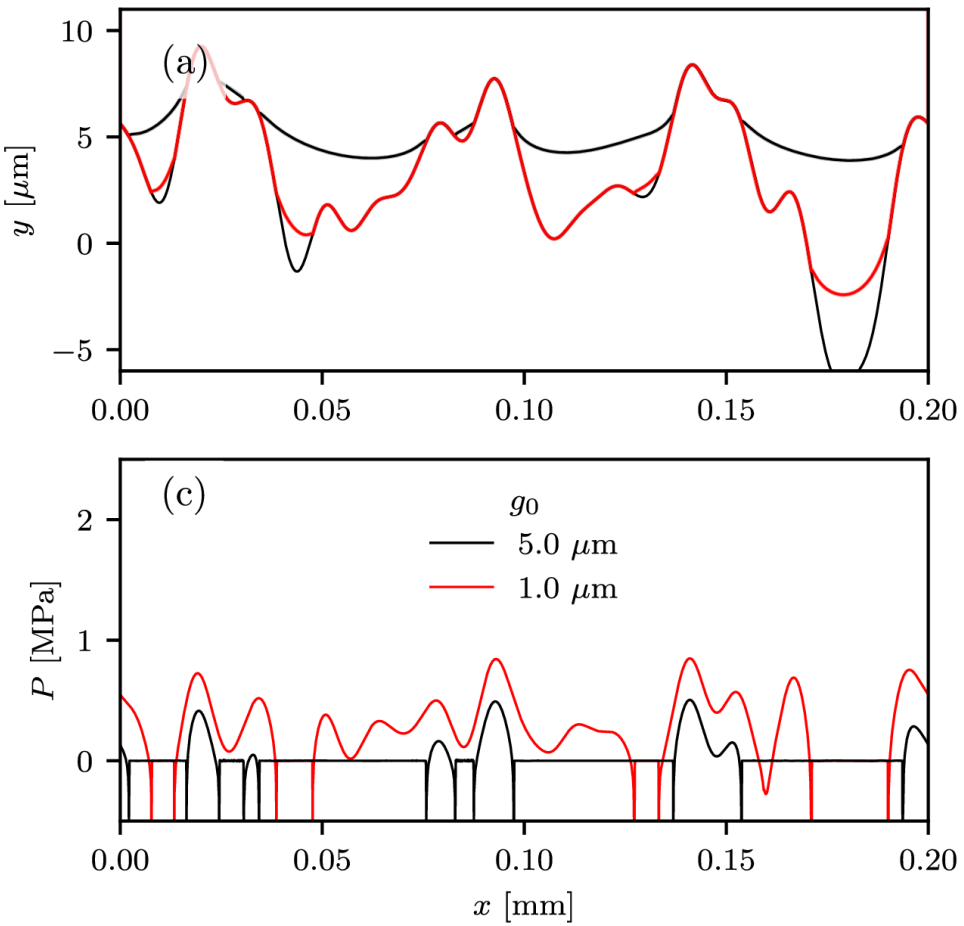

Simulation results[1]

[1] Plagge, J. and Hentschke, R., (2022) Numerical solution of the adhesive rubber-solid contact problem and friction coefficients using a scale-splitting approach. Tribology International, 173:107622.

[2] Carbone, G., Mandriota, C. and Menga, N., (2022) Theory of viscoelastic adhesion and friction. Extreme Mechanics Letters, 56:101877.

[3] Lengiewicz, J., de Souza, M., Lahmar, M.A., Courbon, C., Dalmas, D., Stupkiewicz, S. and Scheibert, J., (2020)

Viscoelastic friction: recent progress

- Account for multiscales[1,2]
- Account for adhesion[1,2]
- Account for large deformations[3]

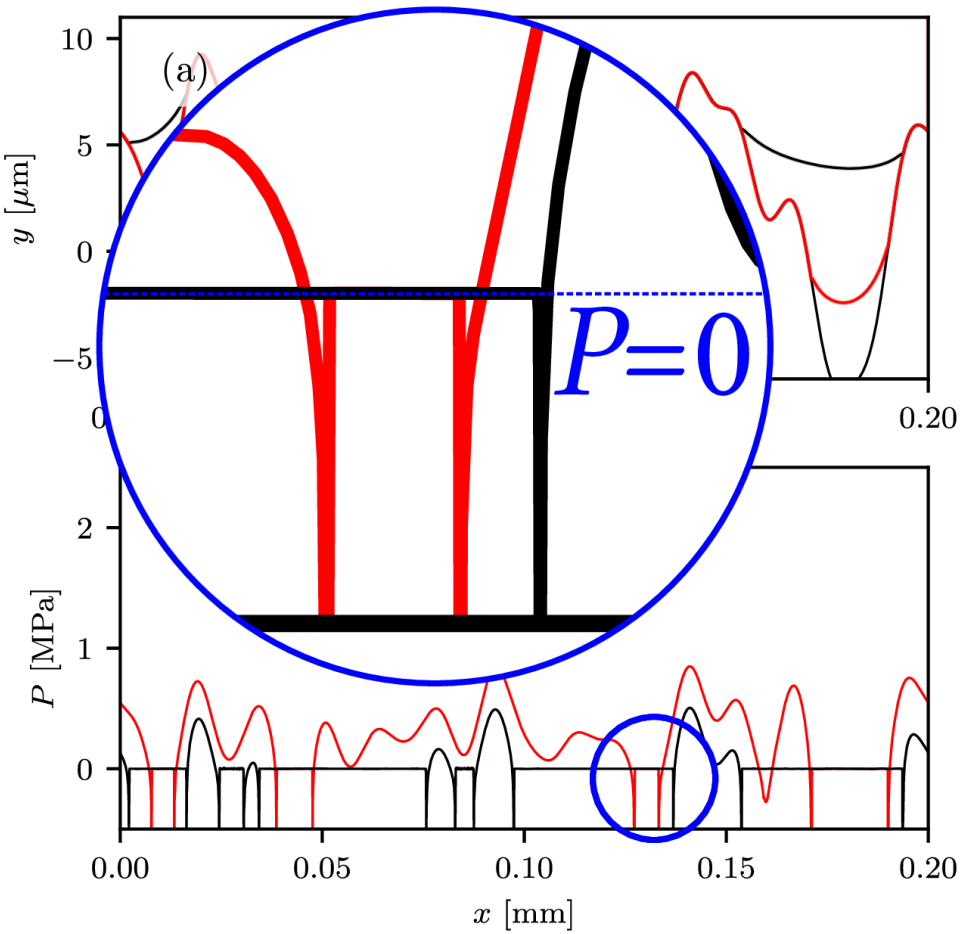

Simulation results[1]

[1] Plagge, J. and Hentschke, R., (2022) Numerical solution of the adhesive rubber-solid contact problem and friction coefficients using a scale-splitting approach. Tribology International, 173:107622.

[2] Carbone, G., Mandriota, C. and Menga, N., (2022) Theory of viscoelastic adhesion and friction. Extreme Mechanics Letters, 56:101877.

[3] Lengiewicz, J., de Souza, M., Lahmar, M.A., Courbon, C., Dalmas, D., Stupkiewicz, S. and Scheibert, J., (2020)

Viscoelastic friction: recent progress

- Account for multiscales[1,2]
- Account for adhesion[1,2]
- Account for large deformations[3]

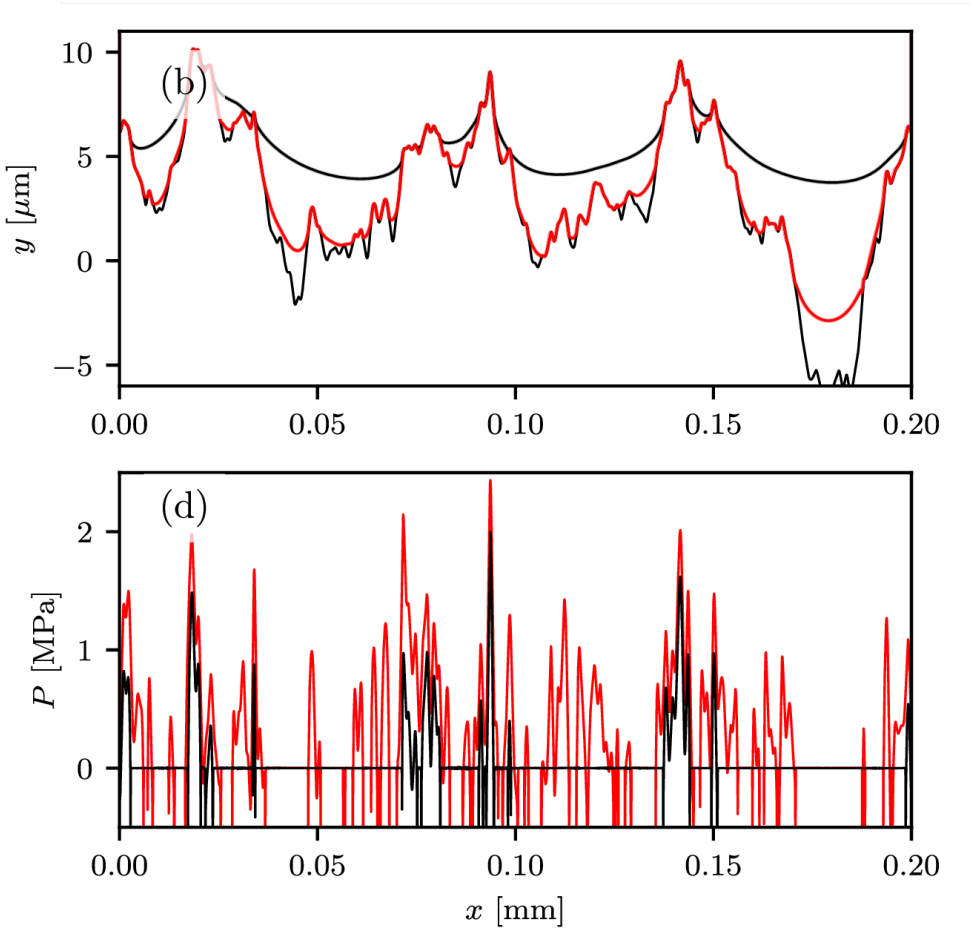

Simulation results[1]

[1] Plagge, J. and Hentschke, R., (2022) Numerical solution of the adhesive rubber-solid contact problem and friction coefficients using a scale-splitting approach. Tribology International, 173:107622.

[2] Carbone, G., Mandriota, C. and Menga, N., (2022) Theory of viscoelastic adhesion and friction. Extreme Mechanics Letters, 56:101877.

[3] Lengiewicz, J., de Souza, M., Lahmar, M.A., Courbon, C., Dalmas, D., Stupkiewicz, S. and Scheibert, J., (2020) Finite deforma- tions govern the anisotropic shear-induced area reduction of soft elastic 2contacts. Journal of the

Viscoelastic friction: recent progress

- Account for multiscales[1,2]
- Account for adhesion[1,2]
- Account for large deformations[3]

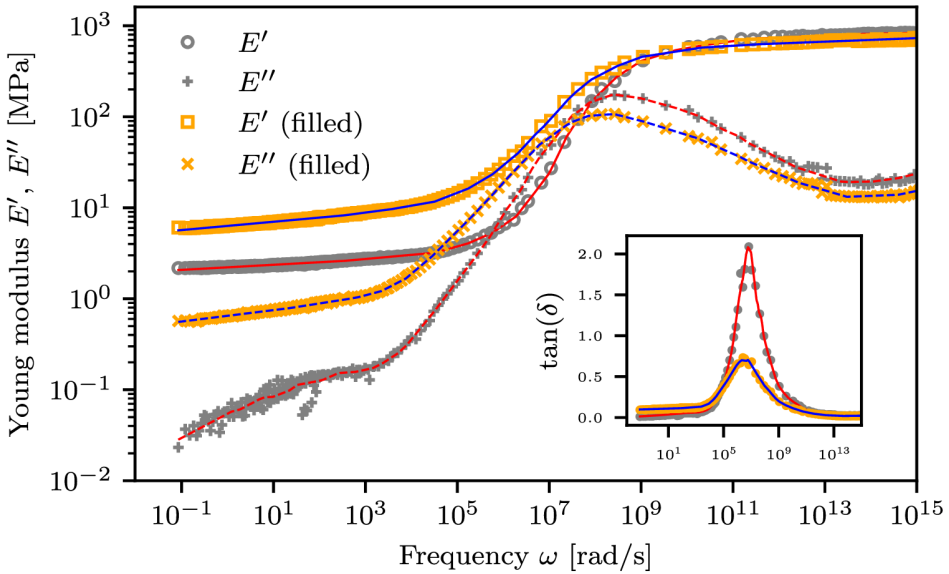

Simulation results[1]

[1] Plagge, J. and Hentschke, R., (2022) Numerical solution of the adhesive rubber-solid contact problem and friction coefficients using a scale-splitting approach. Tribology International, 173:107622.

[2] Carbone, G., Mandriota, C. and Menga, N., (2022) Theory of viscoelastic adhesion and friction. Extreme Mechanics Letters, 56:101877.

[3] Lengiewicz, J., de Souza, M., Lahmar, M.A., Courbon, C., Dalmas, D., Stupkiewicz, S. and Scheibert, J., (2020) Finite deforma- tions govern the anisotropic shear-induced area reduction of soft elastic 2contacts. Journal of the Mechanics and Physics of Solids, 143:104056

Viscoelastic friction: recent progress

- Account for multiscales[1,2]
- Account for adhesion[1,2]
- Account for large deformations[3]

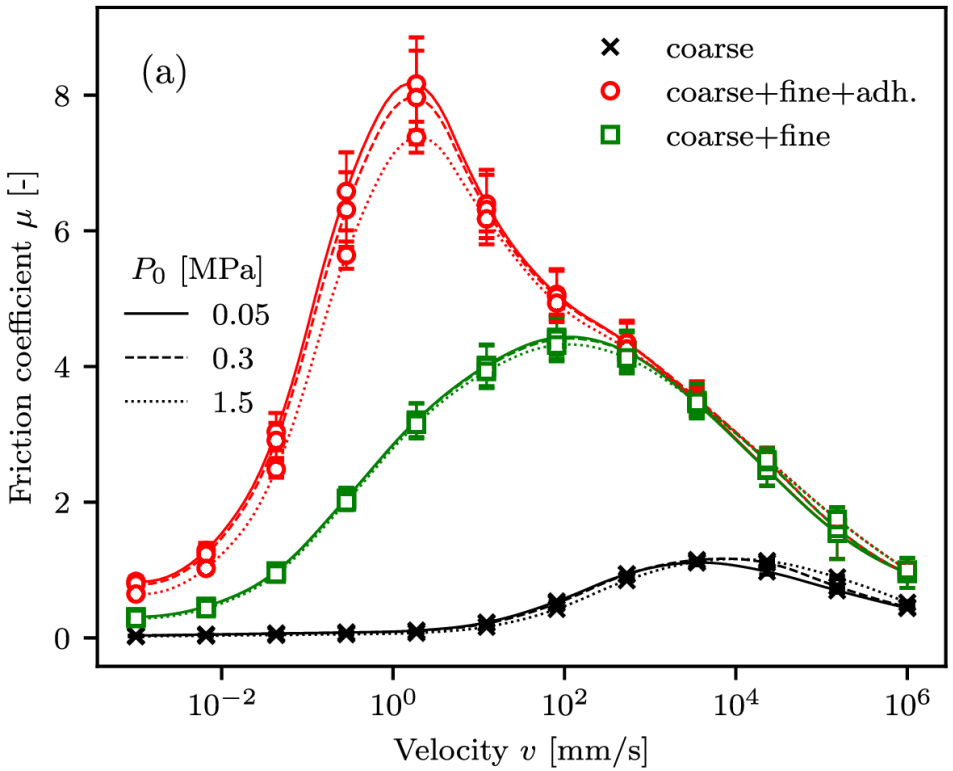

Simulation results[1]

[1] Plagge, J. and Hentschke, R., (2022) Numerical solution of the adhesive rubber-solid contact problem and friction coefficients using a scale-splitting approach. Tribology International, 173:107622.

[2] Carbone, G., Mandriota, C. and Menga, N., (2022) Theory of viscoelastic adhesion and friction. Extreme Mechanics Letters, 56:101877.

[3] Lengiewicz, J., de Souza, M., Lahmar, M.A., Courbon, C., Dalmas, D., Stupkiewicz, S. and Scheibert, J., (2020) Finite deforma- tions govern the anisotropic shear-induced area reduction of soft elastic 2contacts. Journal of the Mechanics and Physics of Solids, 143:104056

Material and tribological properties

Material properties interdependence

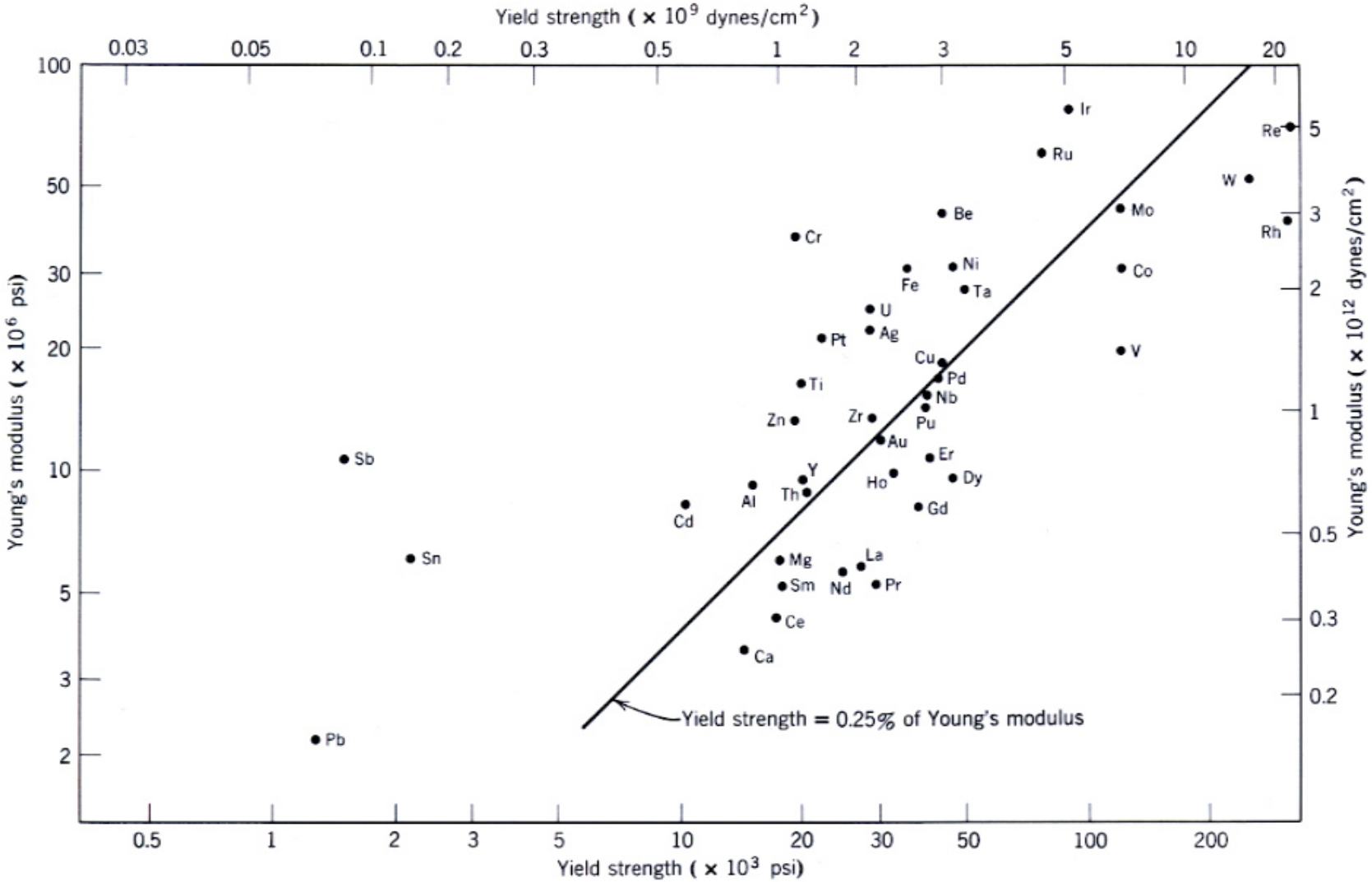

Young's modulus and yield strength interdependence

Rabinowicz, Friction and wear of materials, Wiley (1965)

Material properties interdependence

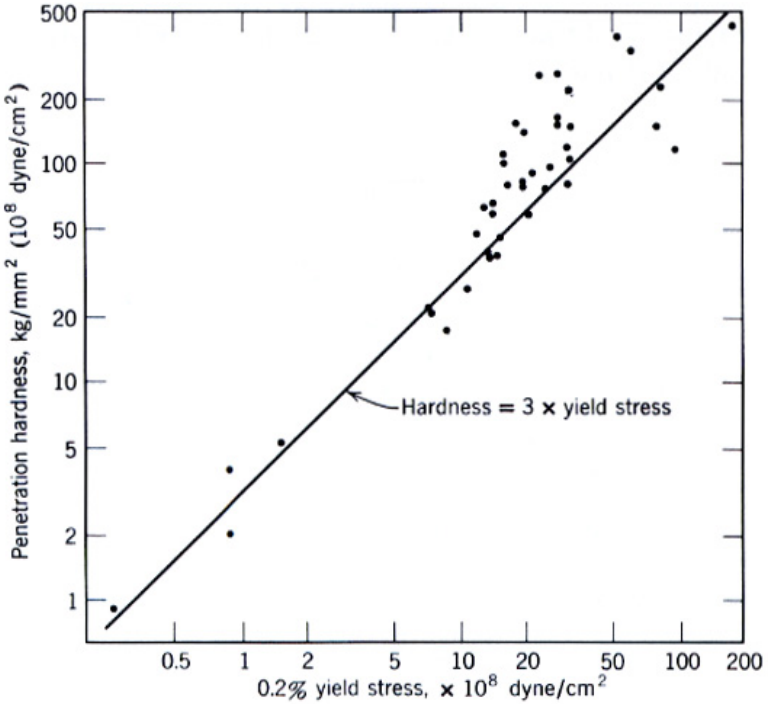

Penetration hardness and yield stress interdependence

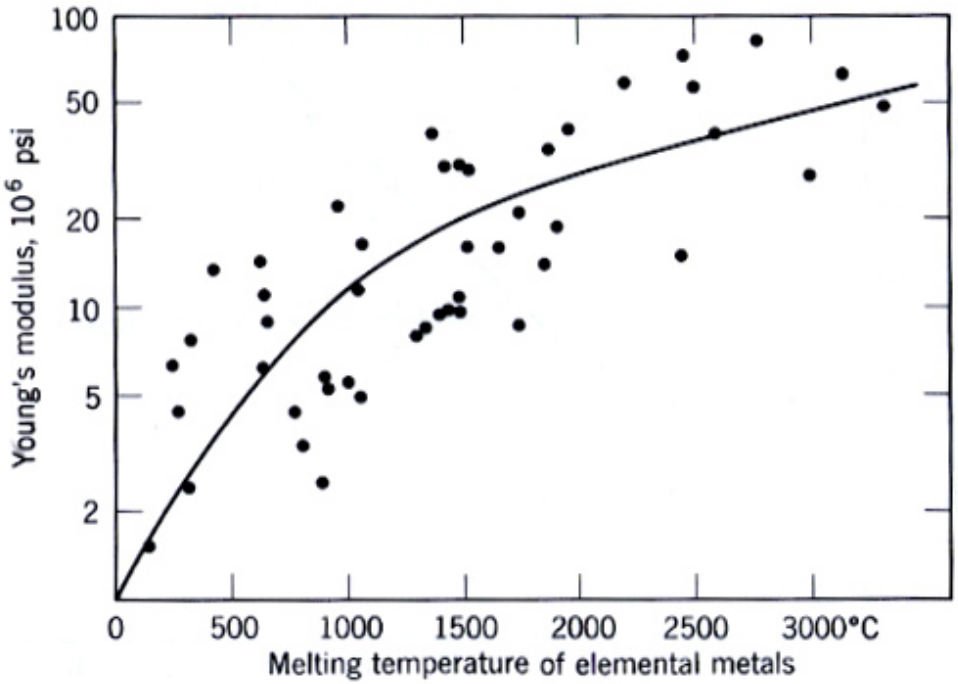

Young's modulus and melting temperature interdependence

Rabinowicz, Friction and wear of materials, Wiley (1965)

Material properties interdependence

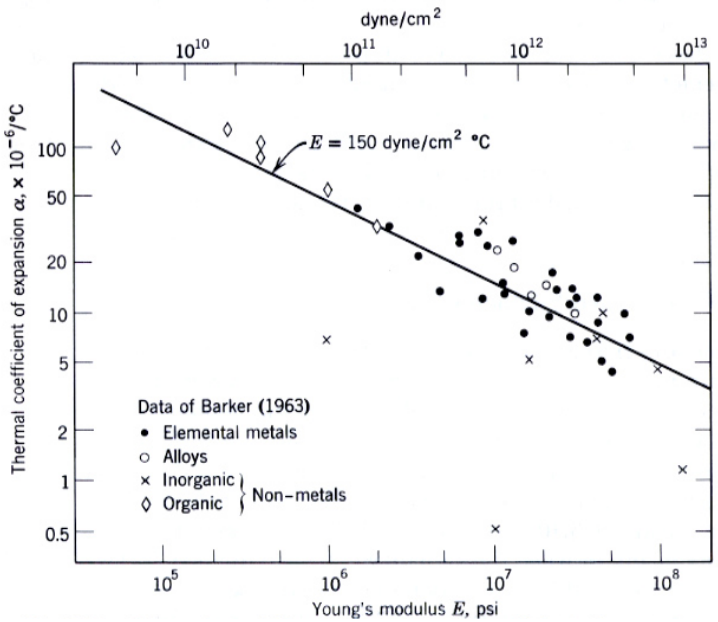

Thermal coefficient of expansion and Young's modulus interdependence

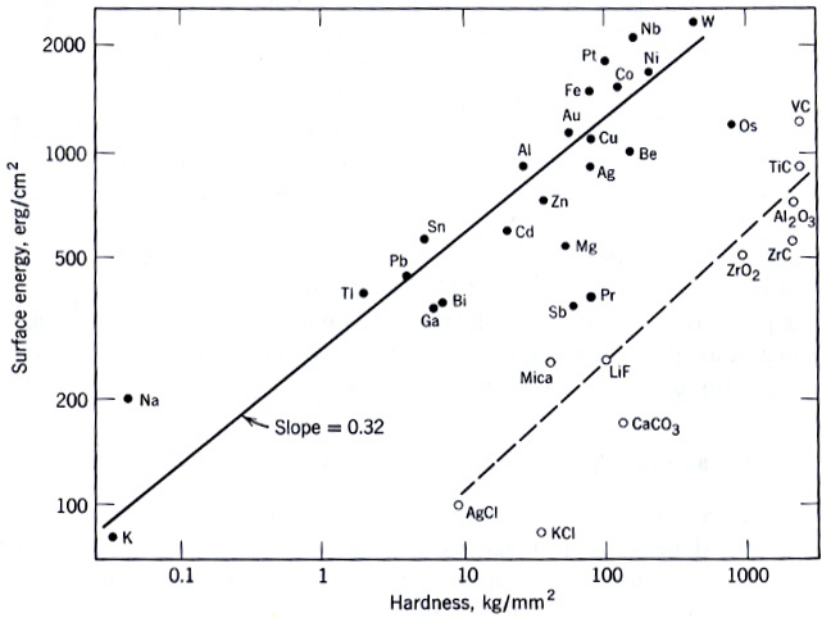

Surface energy and hardness interdependence

Rabinowicz, Friction and wear of materials, Wiley (1965)

Real area of contact

Real area of contact depends on

Real area of contact

Real area of contact depends on

- **normal load**:
  real area of contact is proportional to the normal load and inversely proportional to the hardness H

$$A_r \sim p_0$$

A_r - real contact area, p_0 - applied pressure

Real area of contact

Real area of contact depends on

- **normal load**:
  real area of contact is proportional to the normal load and inversely proportional to the hardness H

$$A_r = A_0 \frac{p_0}{H}$$

A_r - real contact area, p_0 - applied pressure; H - hardness, A_0 - nominal contact area

Real area of contact

Real area of contact depends on

- **normal load**:
  real area of contact is proportional to the normal load and inversely proportional to the hardness H
- **sliding distance**:
  contact area might be significantly smaller than before shear forces were first applied

$$A_r = A_0 \frac{p_0}{H}$$

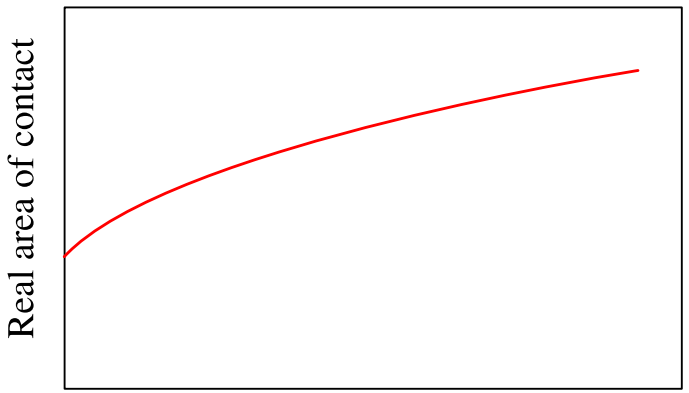

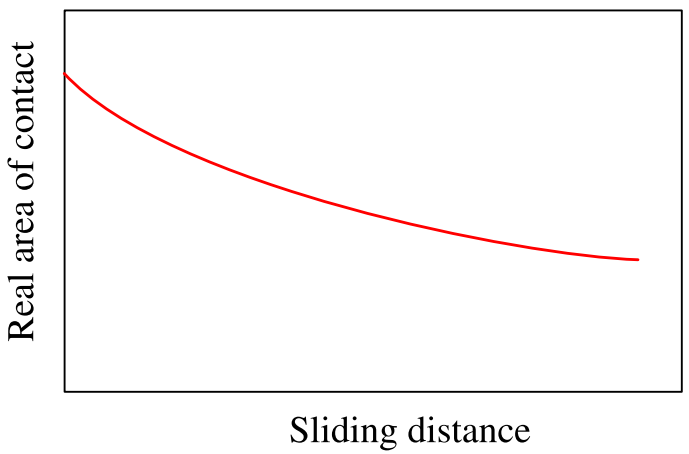

Real area of contact

Real area of contact depends on

- **normal load**:
  real area of contact is proportional to the normal load and inversely proportional to the hardness H
- **sliding distance**:
  contact area might be significantly smaller than before shear forces were first applied
- **time**:
  real area of contact increases with time (*for creeping materials*)

$$A_r = A_0 \frac{p_0}{H}$$

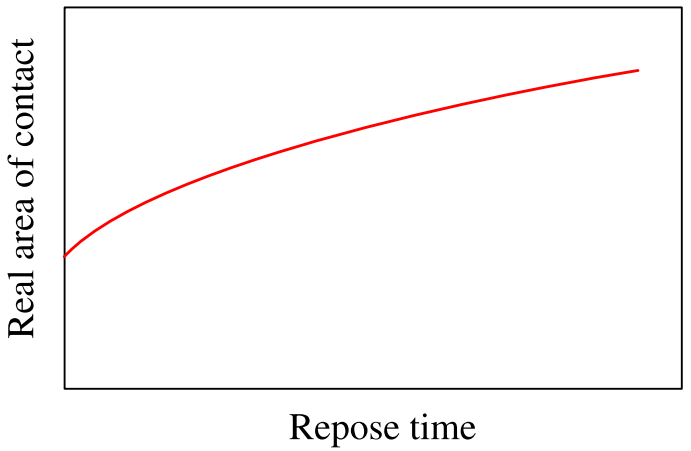

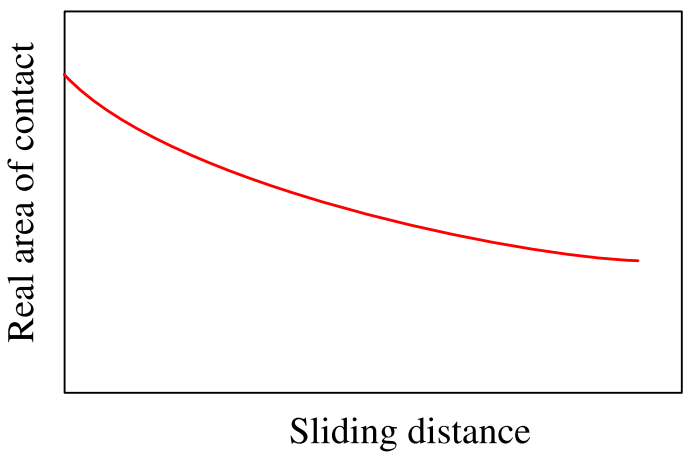

Real area of contact

Real area of contact depends on

- **normal load**:
  real area of contact is proportional to the normal load and inversely proportional to the hardness H
- **sliding distance**:
  contact area might be significantly smaller than before shear forces were first applied
- **time**:
  real area of contact increases with time (*for creeping materials*)
- **surface energy**:
  the higher the surface energy, the greater the area of contact

$$A_r = A_0 \frac{p_0}{H}$$

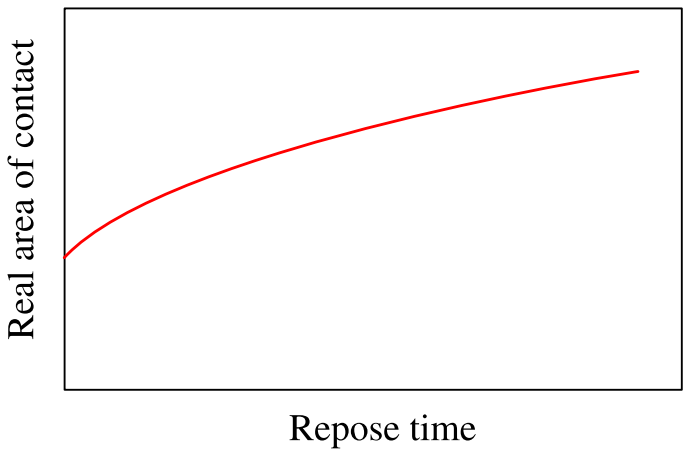

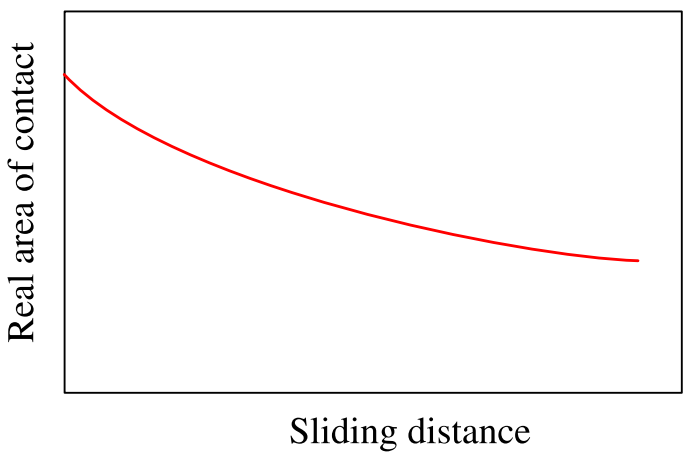

Engineering friction

First approximations: friction coefficient does not depend on

- normal load
- apparent area of contact
- velocity
- surface roughness
- repose time

- friction force direction is opposite to the sliding

Engineering friction

First approximations: friction coefficient does not depend on

- normal load ☺/☹
- apparent area of contact ☺
- velocity ☹
- surface roughness ☹/☺
- repose time ☹/☺

- friction force direction is opposite to the sliding ☺

Real friction :: normal load

First approximation:

- friction coefficient does not depend on normal load.

Exceptions:

Real friction :: normal load

First approximation:

- friction coefficient does not depend on normal load.

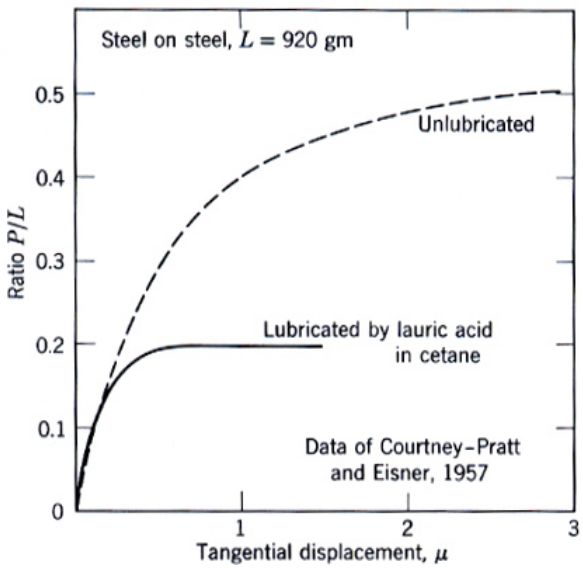

Fig. 1. For very small sliding, the force of friction is not proportional to the normal force[1]

[1] Rabinowicz, Friction and wear of materials, Wiley (1965)

Exceptions:

- at micro scale for small slidings

Real friction :: normal load

First approximation:

- friction coefficient does not depend on normal load.

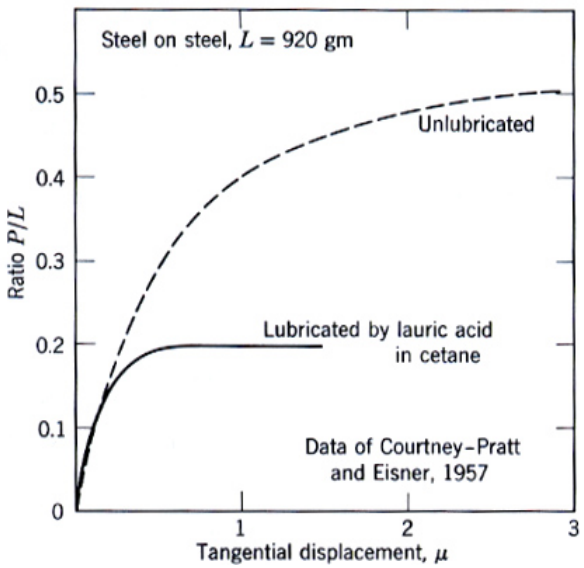

Fig. 1. For very small sliding, the force of friction is not proportional to the normal force[1]

[1] Rabinowicz, Friction and wear of materials, Wiley (1965)

Exceptions:

- at micro scale for small slidings
- for huge pressures (metal forming) friction force is limited

Real friction :: normal load

First approximation:

- friction coefficient does not depend on normal load.

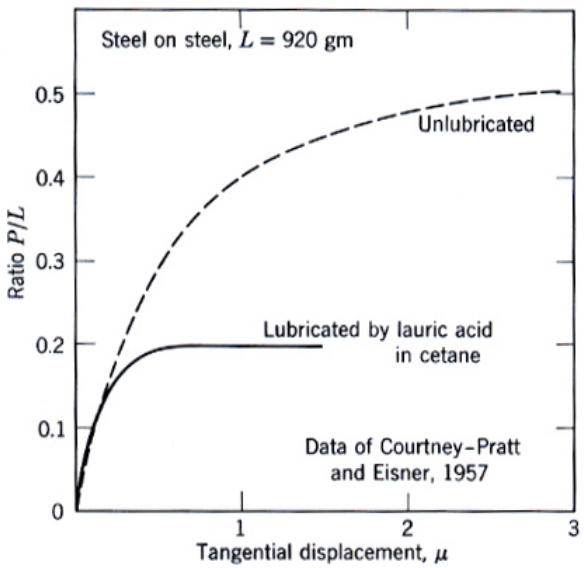

Fig. 1. For very small sliding, the force of friction is not proportional to the normal force[1]

[1] Rabinowicz, Friction and wear of materials, Wiley (1965)

Exceptions:

- at micro scale for small slidings
- for huge pressures (metal forming) friction force is limited
- for too hard (diamond) or too soft (teflon) materials:
  - generally $T = cF^{\alpha}, \alpha \in \left[\frac{2}{3}; 1\right]$;

Real friction :: normal load

First approximation:

- friction coefficient does not depend on normal load.

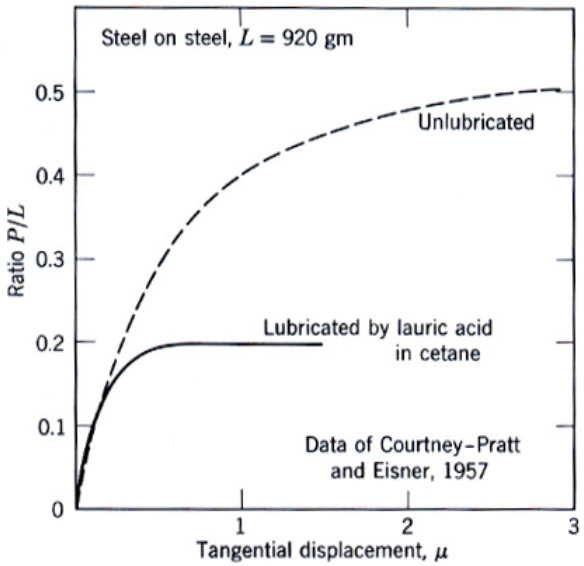

Fig. 1. For very small sliding, the force of friction is not proportional to the normal force[1]

[1] Rabinowicz, Friction and wear of materials, Wiley (1965)

Exceptions:

- at micro scale for small slidings
- for huge pressures (metal forming) friction force is limited
- for too hard (diamond) or too soft (teflon) materials:
  - generally $T = cF^{\alpha}, \alpha \in \left[\frac{2}{3}; 1\right]$;
- hard coating (film) and a softer substrate

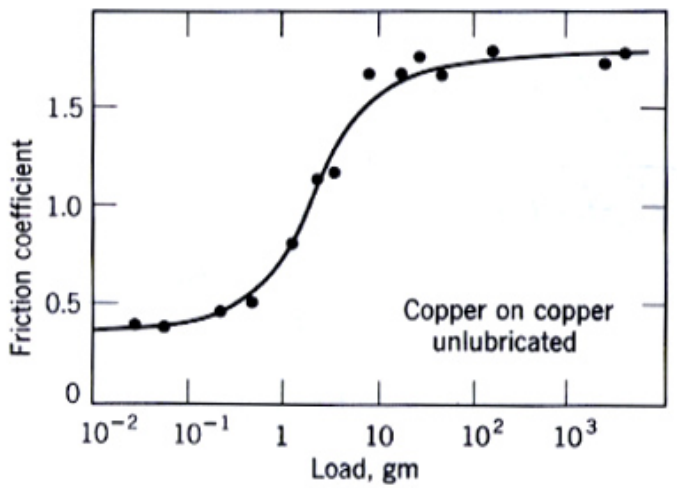

Fig. 2. Hard film on a softer substrate, at moderate loads friction is determined by the film friction, at higher loads, the coating brakes and softer material determines the frictional properties[1]

Real friction :: normal force

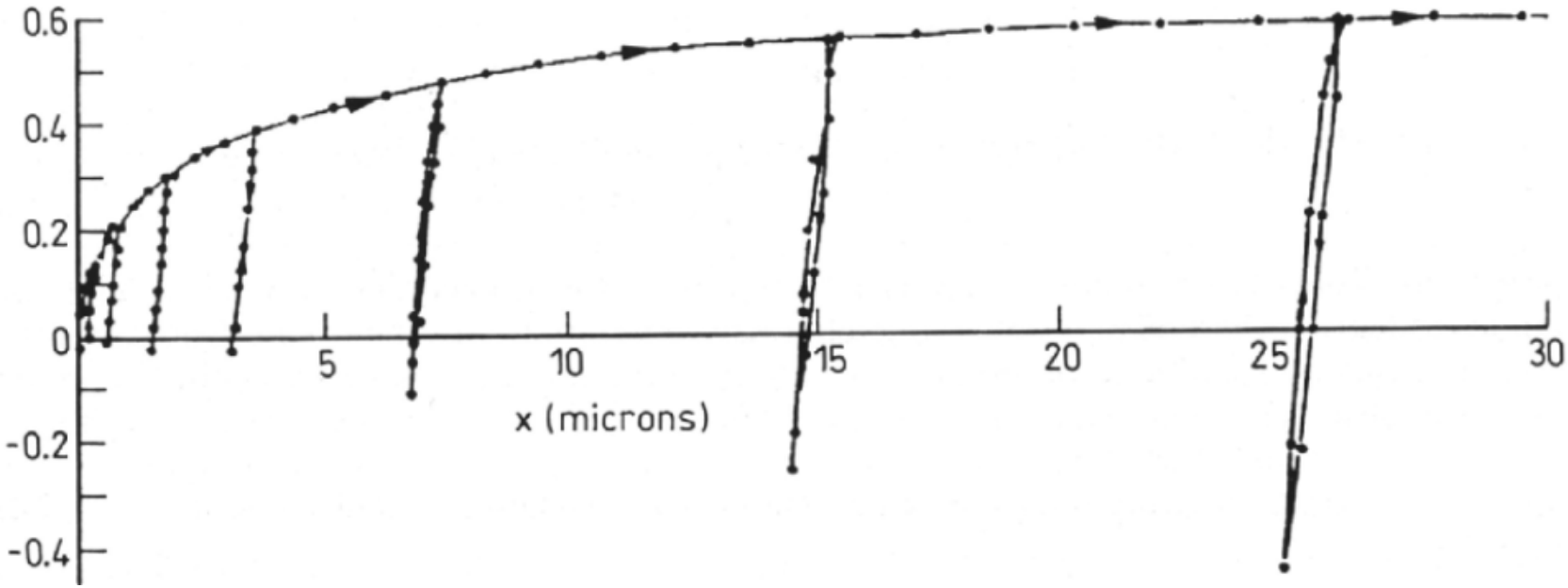

Friction coefficient versus tangential movement

Courtney-Pratt J. S., and E. Eisner. The effect of a tangential force on the contact of metallic bodies. Proc R Soc A 238 (1957)

Real friction :: normal force

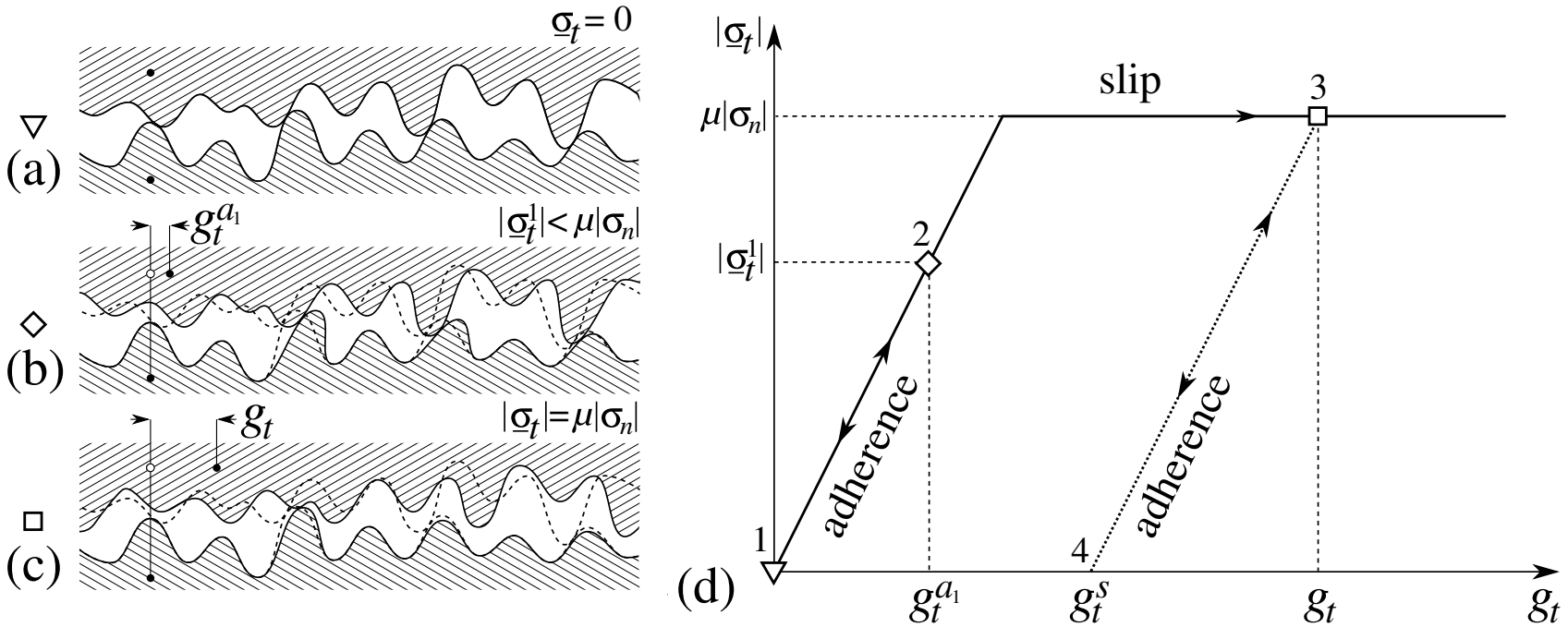

Asperity deformations in the contact interface

Real friction :: friction direction

First approximation:

- friction force direction is opposite to the sliding.

Real friction :: friction direction

First approximation:

- friction force direction is opposite to the sliding.

Exceptions:

- the direction of the friction force remains within [178; 182] degrees to sliding direction (fig. 1);

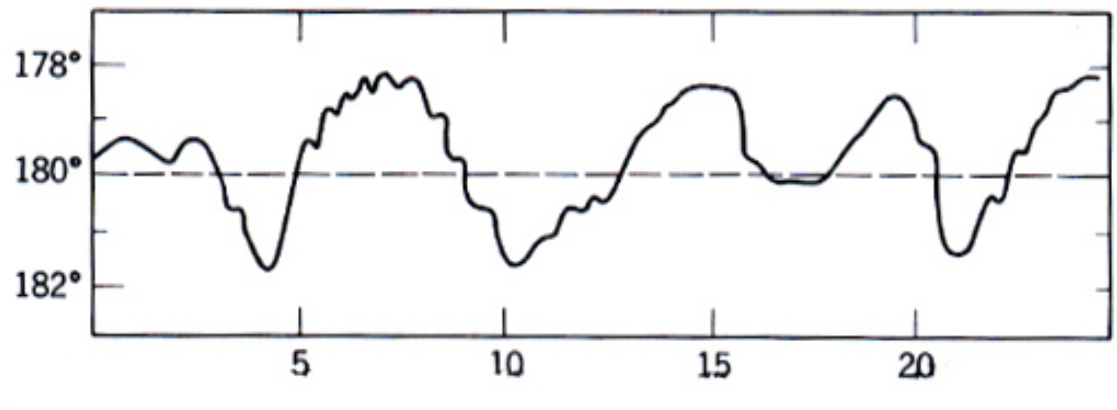

Direction of friction force in sliding

[1] Rabinowicz, Friction and wear of materials, Wiley (1965)

Real friction :: friction direction

First approximation:

- friction force direction is opposite to the sliding.

Exceptions:

- the direction of the friction force remains within [178; 182] degrees to sliding direction (fig. 1);
- the difference is higher for anisotropic surface roughness

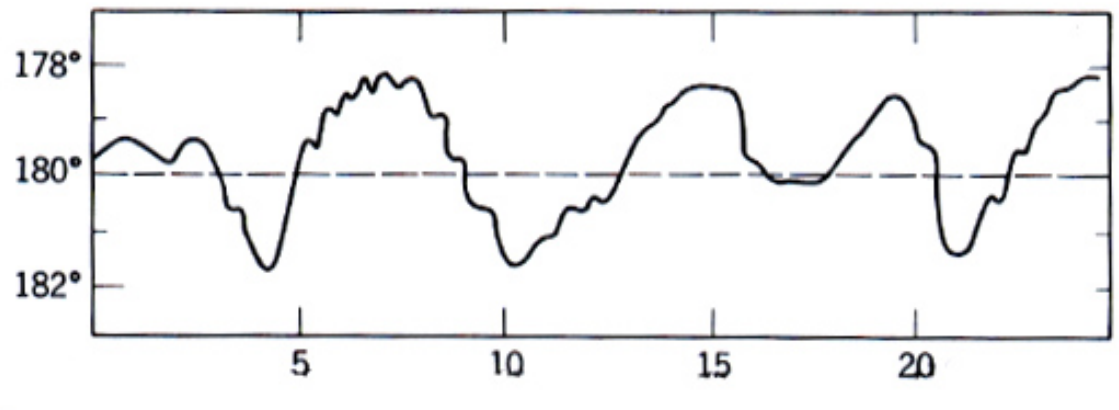

Direction of friction force in sliding

[1] Rabinowicz, Friction and wear of materials, Wiley (1965)

Real friction :: friction direction

First approximation:

- friction force direction is opposite to the sliding.

Exceptions:

- the direction of the friction force remains within [178; 182] degrees to sliding direction (fig. 1);
- the difference is higher for anisotropic surface roughness
- asymmetry of roughness and friction

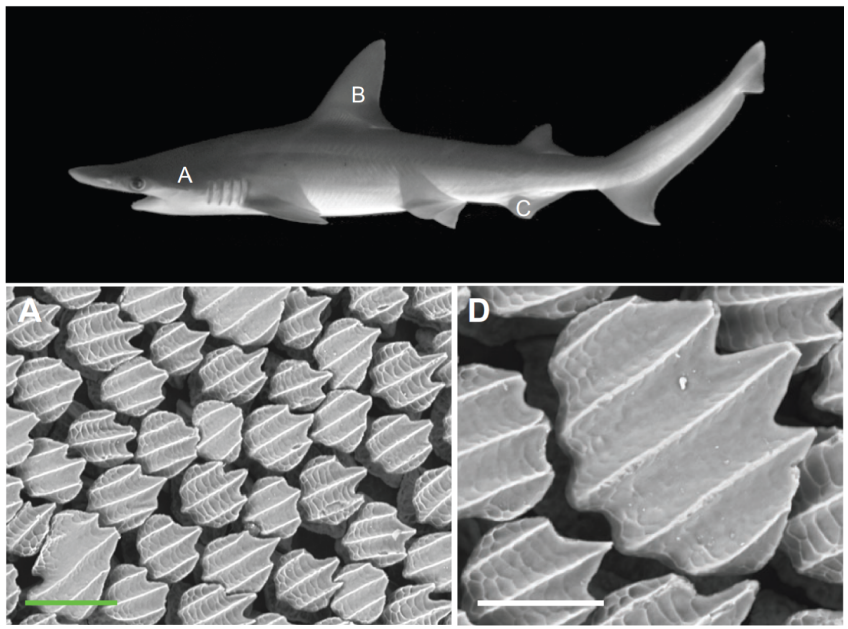

Examples of asymmetric friction

Real friction :: apparent area and roughness

First approximation:

- Friction coefficient does not depend on the apparent area of contact

Exceptions:

First approximation:

- Friction coefficient does not depend on surface roughness

Exceptions:

Real friction :: apparent area and roughness

First approximation:

- Friction coefficient does not depend on the apparent area of contact

Exceptions:

- very smooth and clean surfaces

First approximation:

- Friction coefficient does not depend on surface roughness

Exceptions:

Real friction :: apparent area and roughness

First approximation:

- Friction coefficient does not depend on the apparent area of contact

Exceptions:

- very smooth and clean surfaces

First approximation:

- Friction coefficient does not depend on surface roughness

Exceptions:

- too smooth or too rough surfaces

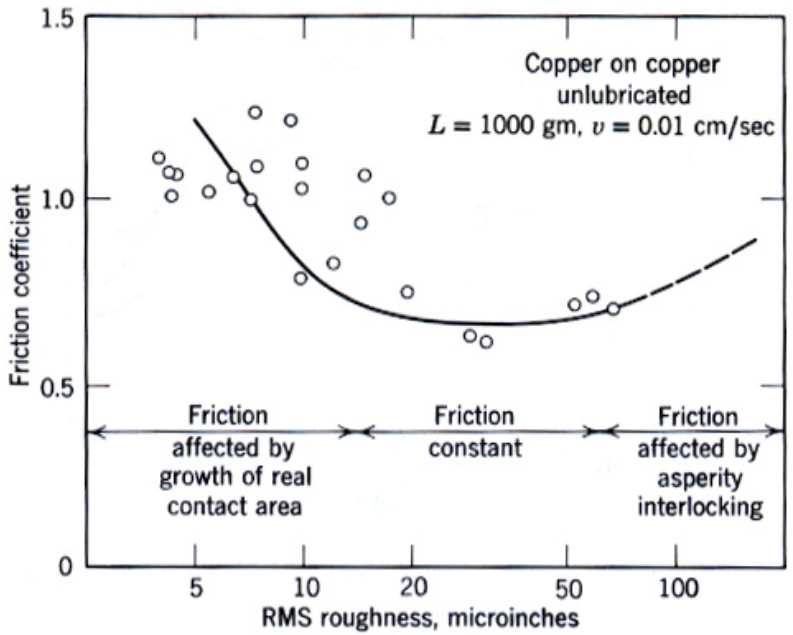

Effect of roughness on the coefficient of friction

[1] Rabinowicz, Friction and wear of materials, Wiley (1965)

Real friction :: time and velocity

First approximation:

- Friction coefficient does not depend on time

Exceptions:

First approximation:

- Friction coefficient does not depend on sliding velocity

Exceptions:

Real friction :: time and velocity

First approximation:

- Friction coefficient does not depend on time

Exceptions:

- creeping materials

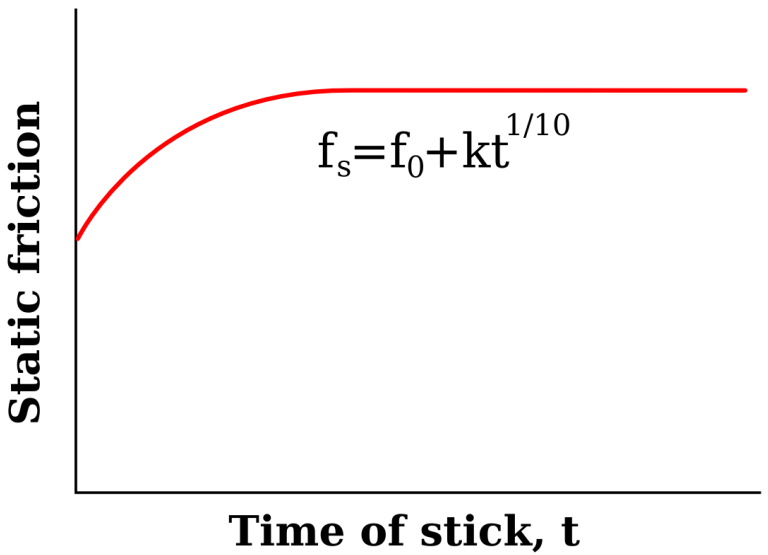

Evolution of the static coefficient of friction with the time of repose

First approximation:

- Friction coefficient does not depend on sliding velocity

Exceptions:

Real friction :: time and velocity

First approximation:

- Friction coefficient does not depend on time

Exceptions:

- creeping materials

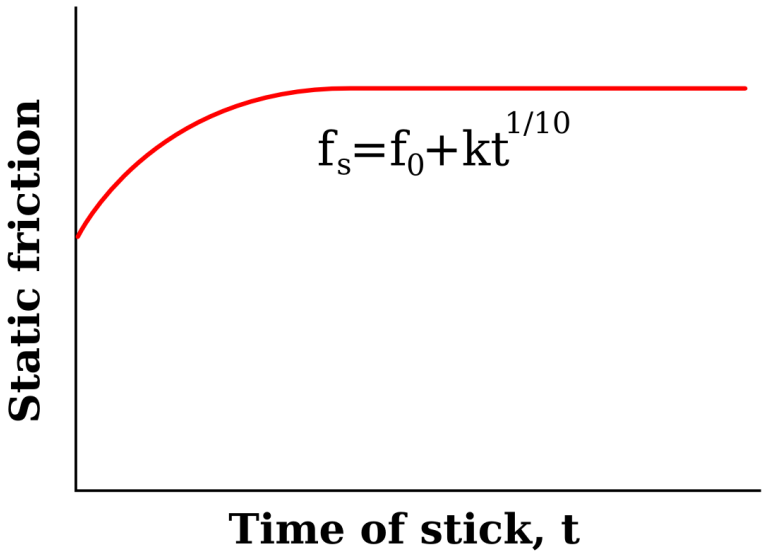

Evolution of the static coefficient of friction with the time of repose

First approximation:

- Friction coefficient does not depend on sliding velocity

Exceptions:

- if material behaves differently at different loading rate, then the friction depends on the sliding velocity

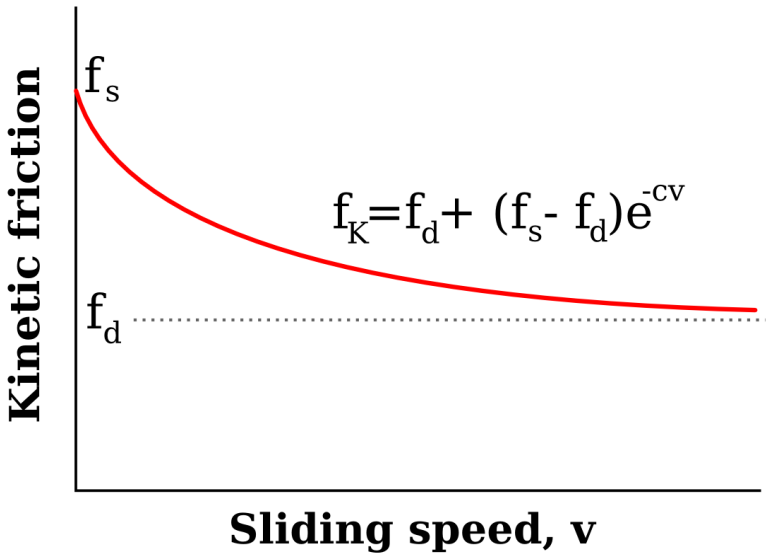

Kinetic friction decreases with increasing sliding velosity

Real friction :: velocity

First approximation:

- Friction coefficient does not depend on sliding velocity

Exceptions:

- if material behaves differently at different loading rate (polymers)
- considerable rise in temperature (thermo-mechanical coupling)

Real friction :: velocity

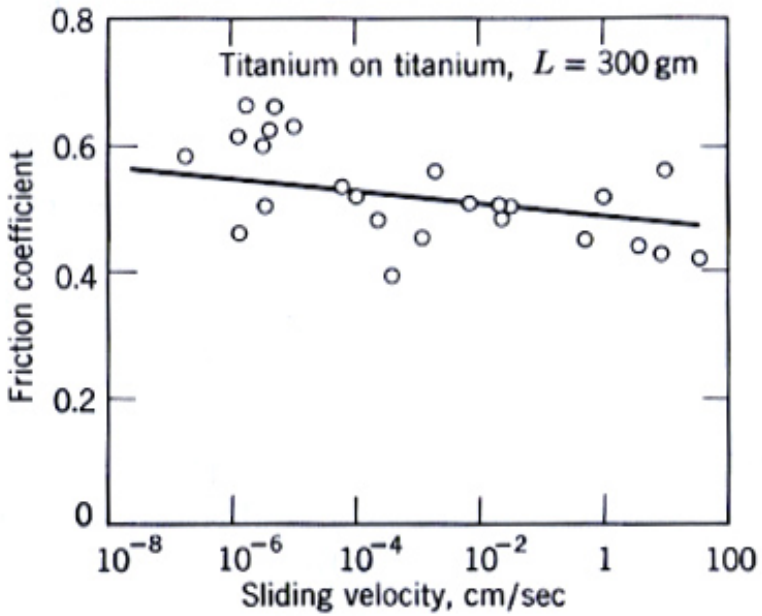

Friction coefficient slightly decreses with increasing velocity of sliding, titanium on titanium

First approximation:

- Friction coefficient does not depend on sliding velocity

Exceptions:

- if material behaves differently at different loading rate (polymers)
- considerable rise in temperature (thermo-mechanical coupling)

Real friction :: velocity

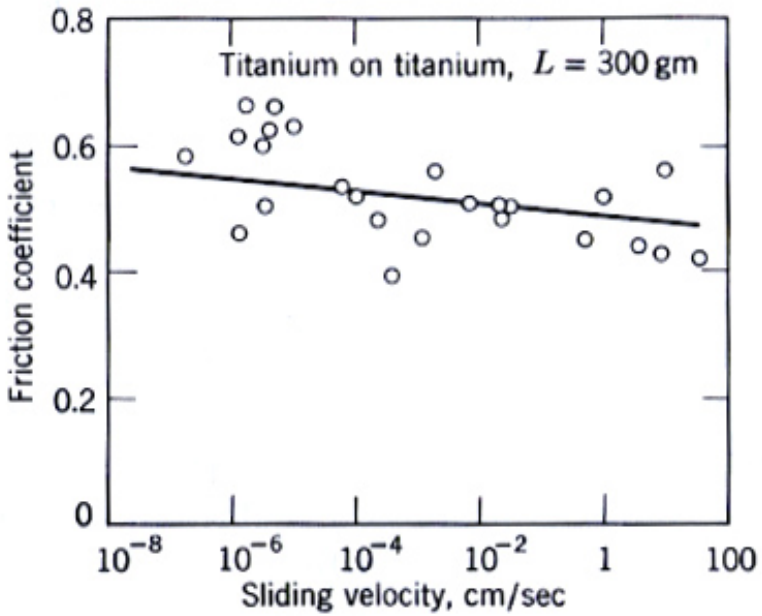

Friction coefficient slightly decreses with increasing velocity of sliding, titanium on titanium

First approximation:

- Friction coefficient does not depend on sliding velocity

Exceptions:

- if material behaves differently at different loading rate (polymers)
- considerable rise in temperature (thermo-mechanical coupling)

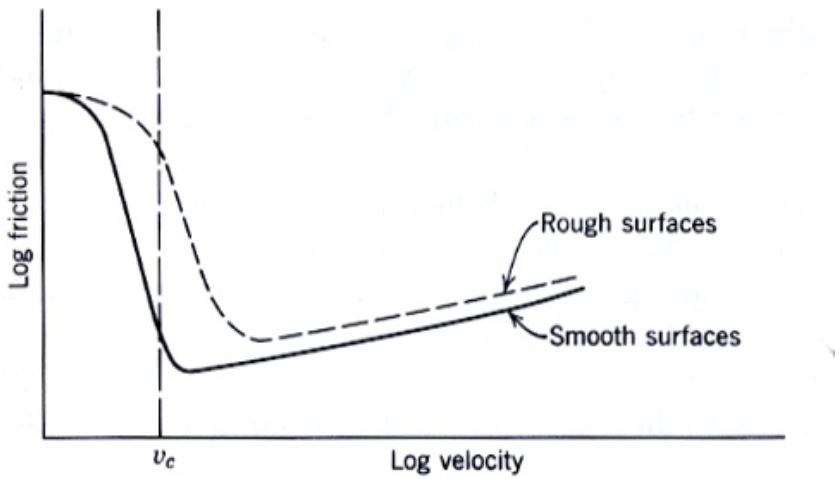

Friction coefficient dependence on velocity of sliding for lubricated surfaces

Real friction :: velocity

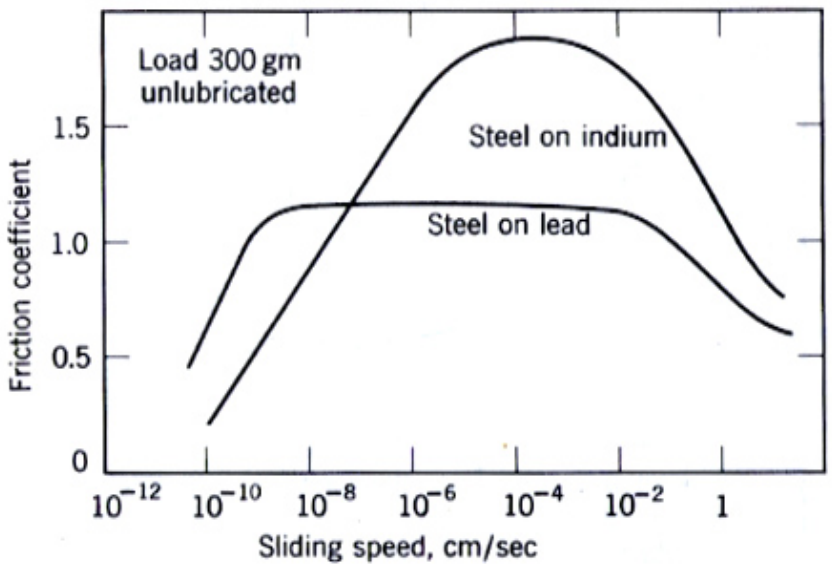

Friction coefficient increases and decreases with increasing velocity of sliding, hard on soft (steel on lead, steel on indium)

First approximation:

- Friction coefficient does not depend on sliding velocity

Exceptions:

- if material behaves differently at different loading rate (polymers)
- considerable rise in temperature (thermo-mechanical coupling)

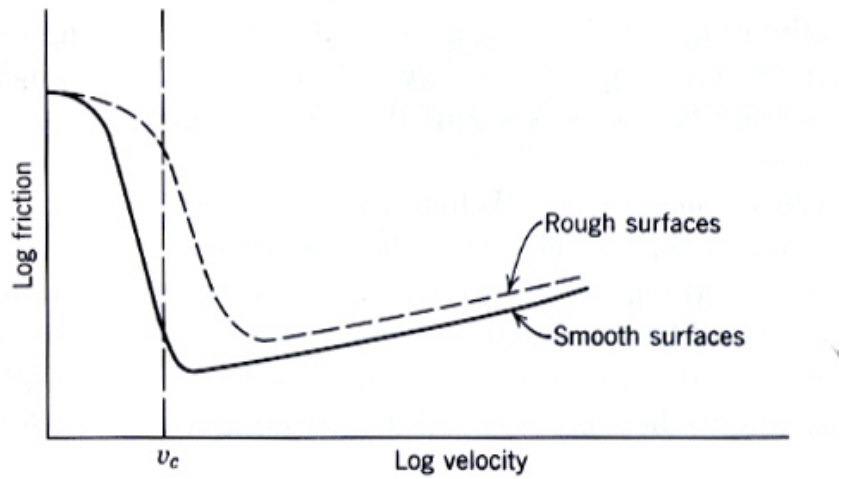

Friction coefficient dependence on velocity of sliding for lubricated surfaces

Thank you for your attention!